Drivers, challenges, and emerging technologies for desalination of high-salinity brines: A critical review

Kinnari M. Shah [a,1], Ian H. Billinge [a,1], Xi Chen [a], Hanqing Fan [a], Yuxuan Huang [a], Robert K. Winton [a], Ngai Yin Yip [a,b,*]

[a] Department of Earth and Environmental Engineering, Columbia University, New York, NY 10027-6623, United States
[b] Columbia Water Center, Columbia University, New York, NY 10027-6623, United States

HIGHLIGHTS

- Ten emerging technologies for high-salinity desalination are critically reviewed.
- ED and OMRO show most promise in achieving high energy efficiencies.
- SED, HDH, FO, MD, and STD can be driven by low-grade heat.
- SED, SCWD, and HDH can potentially sidestep scaling issues.
- High-salinity brines are diverse and will require different desalination approaches.

GRAPHICAL ABSTRACT
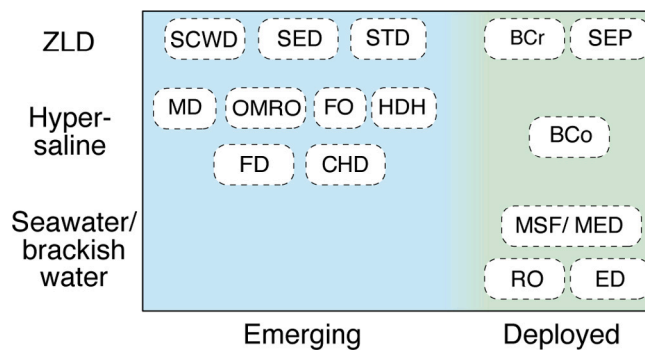
ABSTRACT

Hypersaline brines are of growing environmental concern. While high-salinity desalination and zero liquid discharge (ZLD) are increasingly attractive treatment options, the high salt and scalant contents pose considerable technical difficulties to existing desalination techniques. In this review, we introduce sources of hypersaline brines, examine factors driving high-salinity desalination, and present the thermodynamic minimum energy of hypersaline desalination and ZLD, highlighting effects of mineral precipitation and imperfect salt rejection. We then critically examine prospects and challenges of 10 alternative technologies for hypersaline desalination: electrodialysis, osmotically-mediated reverse osmosis, forward osmosis, membrane distillation, humidification-dehumidification, solvent extraction desalination, supercritical water desalination, freeze desalination, clathrate hydrate desalination, and solar thermal desalination. Although electrodialysis and osmotically-mediated reverse osmosis show promise of having competitive energy efficiencies, these membrane-based techniques are still constrained by concentrate salinity limits. Recovery and reuse of heat will be vital for competitiveness of thermally-driven approaches. Technologies that intrinsically precipitate salts in bulk solution, namely solvent extraction desalination, supercritical water desalination, and humidification-dehumidification, can advantageously avoid mineral scaling. Due to the highly heterogeneous nature of hypersaline streams and

the wide array of end-use goals, the high-salinity desalination market will ultimately be best served by a range of different technologies with distinctive capabilities.

1. Introduction

The management of hypersaline streams is a topic of growing environmental concern [1–4]. Prominent sources of such high-salinity streams include produced water from oil and gas extraction, inland desalination concentrate, landfill leachate, and wastewaters from coal-to-chemical, textile, mining, and leather tanning industries. Because of the very high total dissolved solids (TDS) content and co-presence of other pollutants, the brines cannot be discharged to the environment [1,5,6]. Desalinating these high-salinity streams can facilitate brine management by reducing the volume of the dewatered brine while producing freshwater to alleviate supply stress [7,8]. These potential benefits have, in recent years, spurred the research and development of better hypersaline desalination technologies [9–18].

The growing interest in hypersaline desalination is reflected in the number of review papers on the subject [2,19–23]. However, almost all of these articles are centered on a specific brine source (such as produced water) and most constrained the range of techniques (e.g., membrane-based only). Critical reviews that are both comprehensive in scope and rigorous in technical assessment can offer broad and harmonized perspectives on the current state of high-salinity desalination technologies; however, such analyses are conspicuously absent. Additionally, a primer covering the key aspects of brine characteristics, desalination energy consumption, and existing desalination methods can serve as an informative guide for the scientific community.

In this review, we critically examine the prospects and challenges of emerging technologies for hypersaline desalination. First, sources and primary characteristics of hypersaline streams are introduced. The inadequacies of current brine management practices are detailed, and the motivations for desalination as a preferred treatment option are underscored. Next, we present a primer on the energy requirements of high-salinity desalination and zero liquid discharge. In particular, the impacts of mineral precipitation and fit-for-purpose desalination on energy consumption are analyzed. The implications of different energy inputs, namely, electricity, steam, and low-grade heat, are examined. Conventional desalination techniques are introduced and their limitations in desalinating hypersaline brines are highlighted. We then provide a critical review of alternative and emerging technologies for hypersaline desalination. The appraised technologies are: electrodialysis, osmotically-mediated reverse osmosis, forward osmosis, membrane distillation, humidification-dehumidification, solvent extraction desalination, supercritical water desalination, freeze desalination, clathrate hydrate desalination, and solar thermal desalination. For each innovation, the working principles are briefly explained, state-of-the-art research and recent developments are discussed, and the prospects, challenges, and research priorities are assessed. Lastly, we share our outlook on high-salinity desalination.

2. High-salinity streams

2.1. Sources and primary characteristics of high-salinity streams

There is no universal definition of hypersaline, or high-salinity, streams. Here, we define hypersalinity as concentrations of total dissolved solids, TDS, greater than 70,000 ppm (approximately twice the salinity of seawater, corresponding to typical effluent TDS from seawater desalination) [24]. Brines can be inherently hypersaline to begin with, such as produced water from oil and gas extraction, or arise from the dewatering of low-salinity sources, as with concentrate from brackish water desalination. Environmentally relevant hypersaline streams are presented in Table 1, along with key characteristics (yearly volumetric production, TDS, hardness, and other constituents of concern).

Produced water emitted from oil and gas wells during operation is an example of an inherently hypersaline brine that is particularly prominent in the United States. Produced water has extremely varied composition but typically contains high TDS and hardness together with other contaminants, including heavy metals, biocides, microbes, surfactants, and naturally-occurring radioactive materials [2,26,50–52]. The production of potassium, lithium, magnesium, and boron involves the crystallization of salts from mineral-rich flows, resulting in high TDS effluents [53–56]. Textile manufacturing and leather tanning use high TDS salt solutions to set dyes in fabrics and to pickle hides, respectively [32,37,57]. Geological carbon sequestration is an emerging source of inherently hypersaline brines [58]. Roughly 40% of candidate aquifers for carbon sequestration have TDS greater than 85,000 ppm [38]. Like produced water, these brines consist of a complex mixture of ions and often have high hardness [38].

Besides brines with inherently high TDS, hypersalinity can also result from the dewatering and concentration of low-salinity streams. These streams will be referred to as hypersaline concentrates. The desalination of brackish water with 1,000–15,000 ppm TDS is a significant source of such concentrates, contributing ≈10,700 × 10^6 m^3 per year [24]. Not all inland desalination concentrates exceed 70,000 ppm TDS (our definition of hypersalinity) since desalination may be halted at low recovery yields, primarily due to membrane fouling constraints [59,60]. However, there is a growing push to operate brackish water desalination at higher recovery yields to lower the cost of concentrate disposal, which currently accounts for as much as one-third of total inland desalination expenditures [61–63]; as such, the volume of hypersaline concentrate is expected to increase in the coming years. Coal-to-chemicals plants are another emerging source of hypersaline concentrates. While wastewaters from these facilities are seldom initially hypersaline, they contain substantial levels of contaminants, including organic molecules, ammoniacal nitrogen, chalcogens, and metals, prompting the use of high-recovery desalination to enable water recycling [44,64]. For example, coal-to-chemical plants in China are currently required to operate with >95% water recycling, thus producing waste effluents of hypersaline concentrates [42]. Likewise, flue gas desulfurization wastewater, the byproduct of flue gas scrubbing using slurries of limestone or lime, has TDS as high as 45,000 ppm, high hardness, and significant levels of selenium, arsenic, and lead [45,46]. Programs incentivizing power plants to install water recovery systems by 2023 are anticipated to drive the flue gas desulfurization wastewaters into hypersalinity [65]. Landfill leachates vary widely from low to high salinities (as much as 81,000 ppm TDS) and additionally have complex compositions that include heavy metals, bacteria, organic molecules, and other contaminants [48,66–69]. Even for low-salinity leachates, increasingly strict effluent regulations are compelling onsite dewatering, concentrating the streams into the hypersaline range [48].

The complex composition of hypersaline streams poses considerable technical difficulties for treatment. The high chloride content is corrosive for metals (the deleterious impact of corrosion is discussed later in Section 4) [70]. Many hypersaline streams also have high levels of hardness (sum of divalent cation concentrations, which are predominantly Mg^{2+} and Ca^{2+}) or other sparingly soluble minerals; dewatering the brines causes oversaturation and precipitation of solid minerals [71]. We show in a later analysis that scaling can occur at relatively low recovery yields, well before the predominant salt (i.e., NaCl) reaches saturation. Even though the sparingly soluble solids are typically minority dissolved species, precipitation of the minerals can impair and even stall treatment processes. The occurrence and impacts of scaling will be discussed for the

Table 1

Sources, annual volumes generated (where reported in literature), total dissolved solids range, hardness range, and other constituents of concern for prominent hypersaline streams. Bolded streams are inherently hypersaline, whereas non-bolded streams are low-salinity sources dewatered into hypersaline concentrates. "NDA" denotes "no data available".

Stream	Volumetric production $\times 10^6$ m^3/y	Total dissolved solids typical (low/high) parts per million	Hardness typical (low/high) parts per million	Other constituents of concern
Oil and gas produced water	USA: 3,300 [25]	190,000 (5,000/400,000) [2]	2,200 (NDA/162,000) [26]	Organic carbon [2], heavy metals [27], microbes [2], biocides [2], radioisotopes [27], surfactants [2]
Brine and solution mining flows	NDA	243,000 (223,000/270,000) [28]	6,600 (1,990/24,200) [28]	Radioisotopes [29], acids [30], metals [31]
Textile wastewater	NDA	60,000 (50,000/125,000) [32]	NDA	Organic carbon [33], dyes [34], acids and bases [33], metals [33]
Leather tanning wastewater	India: 18.2 [35]	67,000 (22,000/100,000) [36]	NDA	Microbes [36], acids [37], organic carbon [36]
Geological carbon sequestration formation water	NDA	85,000 (10,000/300,000) [38]	40,000 (10,000/80,000) [38]	Radioisotopes [39]
Inland desalination concentrate	World: 10,700 [24]	19,000 (10,000/35,000) [40]	2,100 (1,300/3,400) [40]	Colloidal silica [3], antiscalants [41]
Coal-to-chemicals wastewater	China: 475 [42]	2,000 (NDA/NDA) [43]	1,100 (NDA/NDA) [43]	Organic carbon [43,44], heavy metals [43], ammonia [44]
Flue-gas desulfurization wastewater	NDA	NDA (4,740/44,600) [45]	NDA (1,025/8,580) [45]	Heavy metals [46]
Landfill leachate	Ireland: 1.1 [47,68]	7,000[a] (2,600/12,500) [48] 52,000[b] (21,000/81,000) [48]	NDA	Organic carbon [48], heavy metals [48,49]

[a] Landfills without ash from municipal solid waste incineration.

[b] Landfills that accept ash from municipal solid waste incineration.

different desalination technologies evaluated here.

The presence of microorganisms can lead to biofouling on surfaces, such as membranes [72]. Similarly, organic molecules in hypersaline streams can complicate treatment and may need to be removed or degraded [26]. Other constituents of concern include toxic metals and metalloids (e.g., arsenic, selenium, lead, mercury, and chromium), acids or bases, and other foulants (e.g., colloidal silica, humic acids, proteins, and alginates) [65,73]. As water is removed from the recalcitrant brines during desalination, concentration of these problematic contaminants rises and the technical difficulties are amplified. Further compounding to the challenge is the highly diverse types and concentrations of foulants and pollutants found in hypersaline streams (for instance, impurities in brines from the same source, such as those listed in Table 1, can be dramatically heterogeneous). As different desalination approaches are affected by the disparate foulants to various extents and have dissimilar removals for different pollutants, the high-salinity market will likely be best served by a range of technologies.

2.2. Drivers for hypersaline desalination

Hypersaline stream management is increasingly shifting toward desalination, which offers both environmental and economic benefits compared to current approaches [74,75]. Due to the very high salt concentration and the almost ubiquitous presence of contaminants, direct discharge of high-salinity streams to surface waters will severely damage ecosystems and pollute drinking and agricultural water sources [1,6,65,76]. As such, proper management of hypersaline streams is mandated by state and federal regulations [2,4,6,77,78]. However, current management methods (Fig. 1) are inadequate, potentially deleterious to the environment, and costly [4,8,24,74]. Although hypersaline streams are often discharged into sewer systems, publicly-owned treatment works do not actually remediate the high TDS content, as they are designed to treat domestic sewage and have no desalination capabilities [1,4,75]. High-salinity streams can be injected into underground wells, but this practice is limited to specific geographic sites and can be costly, especially for deep wells [2,4,77]. Regulations around deep well injection are becoming increasingly strict due to concerns around seepage, contamination, and seismic activity [1,3,6]. High-salinity streams may be temporarily impounded in storage ponds prior to further treatment, though this is limited to small volumes and to

areas with inexpensive land. These impoundment ponds are often unlined and introduce environmental concerns associated with leakage [65,79,80]. Small amounts of hypersaline streams can be disposed of via land application, but this approach is restricted to streams with low contaminant levels and to very niche crops and soils [75,77]. When the brine or concentrate source and management option are not co-located, trucking the hypersaline streams can incur substantial transportation costs and increase the carbon footprint [75,81–83]. The tightening of regulations will further constrain the management options available and motivate alternative approaches to treat the hypersaline streams.

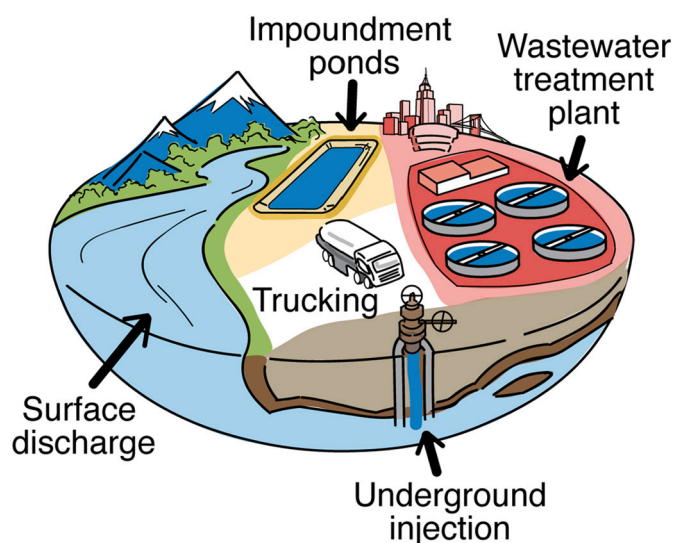Desalination is becoming an attractive treatment option for cost-

Fig. 1. Schematic showing the main management and disposal practices of high-salinity streams: direct discharge to surface waters, mixing with municipal wastewater and conveyance to wastewater treatment plants, injection into underground wells, and temporary impoundment in storage ponds. Where disposal or management facility is offsite, trucking is required to transport the hypersaline streams.

effective and environmentally sustainable management of high-salinity streams [2,8,74,75]. Dewatering hypersaline streams reduces the liquid volume, facilitating subsequent disposal. Additionally, the desalinated product water can be beneficially reused, alleviating water scarcity and stress to enhance water security [2,7,26,84]. As the overarching objective is brine management and not drinking water production, the desalinated product water generally does not need to meet potable water quality. End-uses permitting product waters with TDS concentrations above drinking water standards will allow for more affordable fit-for-purpose treatments [26,85].

2.3. Zero liquid discharge

Zero liquid discharge, ZLD, is the wastewater treatment outcome in which liquid waste is completely eliminated, i.e., all the water is recovered from the saline feed stream, leaving solids as the only waste product [84,86,87]. ZLD is of particular interest for high-salinity stream management: virtually all the water can be reclaimed for reuse, the environmental impacts and pollution risks associated with hypersaline brine management are diminished, and the small volume of remaining solids can be disposed of in leach-proof landfills [88]. Alternatively, the solids can be further processed to recover mineral byproducts of value, potentially enhancing the overall economic feasibility of implementing ZLD [84]. Increasingly strict environmental regulations are stimulating the growth of the ZLD market globally [84]. The approach is actively being pursued across a broad range of applications, such as in the treatment of wastewater from power plants [89], oil and gas produced water [90], and liquid waste from the chemical industry [87,88,91]. Several studies have highlighted that advancing ZLD technologies will be pivotal to greater realization of inland desalination [3,75,88,92].

3. Energy of high-salinity desalination

Desalination is inherently energy-intensive, and energy consumption is a significant contributor to overall cost and is also related to environmental impacts [5,93,94]. In this section, we examine the thermodynamic minimum energy to desalinate high-salinity streams up to zero liquid discharge and discuss the implications of different grades of energy input to provide a framework for assessing the energy intensity of existing and emerging desalination technologies.

3.1. Thermodynamic minimum energy of desalination

The Gibbs free energy of separation is the theoretical minimum energy required for desalination. To desalinate one mole of saline feed stream into the product of purified water and wastes of liquid concentrate and, where applicable, solid minerals (depicted in Fig. S1 of the Supplementary Material), the molar Gibbs free energy of separation, $\Delta \overline{G}_{sep}$, is the difference in total molar Gibbs free energies of the components before and after separation:

$$\Delta \overline{G}_{sep} = \phi_P \overline{G}_P + \phi_C \overline{G}_C + \phi_M \overline{G}_M - \overline{G}_F \tag{1}$$

where ϕ is the moles of product water, concentrate, and mineral solid normalized by the moles of feed. Gibbs free energy is represented by G, with subscripts "P", "C", "M", and "F" denoting the product water, concentrate, mineral solid, and saline feed streams, respectively. Note that when the concentrate is undersaturated in salt, there are no solid precipitates, and $\phi_M = 0$.

The Gibbs free energy of a real system is equivalent to the sum of the Gibbs free energy of an ideal system under the same conditions and the
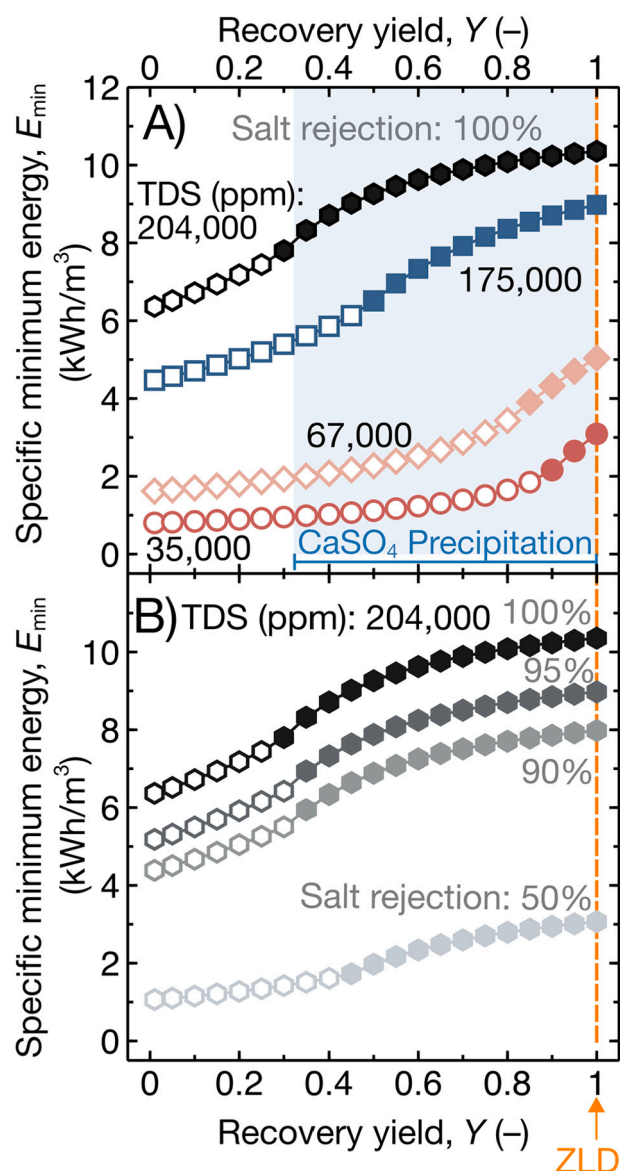

Fig. 2. A) Specific minimum energy, E_{min} as a function of water recovery yield, Y, to desalinate feed streams of 35,000, 65,000, 175,000, and 204,000 ppm TDS with 10 mM Ca^{2+} and SO_4^{2-}. Salt rejection of 100%, corresponding to pure water as product, is assumed. The shaded area indicates the precipitation of $CaSO_4$ mineral solids. B) E_{min} as a function of water recovery yield, Y, needed to desalinate a 204,000 ppm TDS feed with salt rejections of 50%, 90%, 95%, and 100% (i.e., 50%, 10%, 5%, and 0% of the salt in the initial feed ends up in the product stream, respectively). Y is defined as the ratio of water in the product stream to the saline feed; $Y = 1$ signifies zero liquid discharge (ZLD). Total dissolved solids are simulated by NaCl. Open and filled symbols denote undersaturated (i.e., no precipitation) and saturated (that is, with mineral precipitation) concentrate streams, respectively.

excess Gibbs free energy. The excess Gibbs free energy can be expressed using activity and osmotic coefficients of the electrolyte for aqueous solutions and the Gibbs free energy of formation for mineral solids and aqueous solutions (detailed in the Supplementary Material). In this analysis, NaCl is taken as the sole solute for representing the total dissolved solids in the saline feed, and Eq. 1 can be restated as:

$$\frac{\Delta \overline{G}_{\mathrm{sep}}}{RT} = \phi_{\mathrm{P}} \{\nu x_{\mathrm{s}}[ln(m\gamma_{\pm}) - \varphi]\}_{\mathrm{P}} + \phi_{\mathrm{C}}\{\nu x_{\mathrm{s}}[ln(m\gamma_{\pm}) - \varphi]\}_{\mathrm{C}} + \frac{\phi_{\mathrm{M}}}{RT}\left(\overline{G}_{\mathrm{NaCl_{(s)}}}^{\circ} - \overline{G}_{\mathrm{Na^+}}^{\circ} - \overline{G}_{\mathrm{Cl^-}}^{\circ}\right)_{\mathrm{M}} - \{\nu x_{\mathrm{s}}[ln(m\gamma_{\pm}) - \varphi]\}_{\mathrm{F}} \qquad (2)$$

where R is the ideal gas constant, T is the absolute temperature, ν is the number of ions each electrolyte molecule dissociates into (i.e., 2 for NaCl), x_{s} is the mole fraction of sodium chloride, and m is the molality. The molar standard Gibbs free energy of formation of mineral solid NaCl is $\overline{G}_{\mathrm{NaCl_{(s)}}}^{\circ}$, whereas $\overline{G}_{\mathrm{Na^+}}^{\circ}$ and $\overline{G}_{\mathrm{Cl^-}}^{\circ}$ are the molar standard Gibbs free energy of formation of sodium and chloride ions, respectively, in a one molal ideal aqueous solution. The activity and osmotic coefficients are $\gamma_{\pm}$ and φ, respectively, and account for nonideal behaviors arising from the interactions between solution components. In hypersaline streams, the coefficients deviate significantly from unity and need to be factored in for accuracy [95]. In this analysis, $\gamma_{\pm}$ and ϕ are calculated using the Pitzer model [96–98]. If the product water is pure water (i.e., $x_{\mathrm{s,P}} = 0$), then $\phi_{\mathrm{P}}\{\nu x_{\mathrm{s}}[ln(m\gamma_{\pm}) - \varphi]\}_{\mathrm{P}}$ in Eq. (2) vanishes. Further, for ZLD, there is no liquid concentrate stream and Eq. (2) simplifies to:

$$\Delta \overline{G}_{\mathrm{ZLD}} = x_{\mathrm{s,F}}\left(\overline{G}_{\mathrm{NaCl_{(s)}}}^{\circ} - \overline{G}_{\mathrm{Na^+}}^{\circ} - \overline{G}_{\mathrm{Cl^-}}^{\circ}\right) - \nu RT x_{\mathrm{s,F}}[ln(m\gamma_{\pm}) - \varphi]_{\mathrm{F}} \qquad (3)$$

where $x_{\mathrm{s,F}}$ is the mole fraction of dissolved salt in the feed stream.

3.2. Mineral Precipitation Increases Energy Intensity in Desalination of Ultrahigh-Salinity Brines

While $\Delta \overline{G}_{\mathrm{sep}}$ quantifies the thermodynamic minimum energy required to desalinate one mole of feed, it is often more practically useful to normalize the energy by product water volume, yielding the

specific minimum energy, E_{min}. E_{min} as a function of water recovery yield, Y, was determined using Eqs. (2) and (3) with molar volume conversions and shown in Fig. 2A (at temperature of 25 °C). Here, Y is defined as the ratio of water in the product stream to the saline feed. The analysis assumed complete salt removal, i.e., the product is pure water. Four characteristic feed salinities are presented: 35,000 ppm TDS signifies seawater and 67,000 ppm TDS simulates concentrates exiting seawater desalination facilities [99], whereas 157,000 and 204,000 ppm TDS represent high salinities found in some of the industrial brines and concentrates introduced above (Table 1). As expected, the desalination of higher feed salinities is more energy-intensive. With increasing Y, more product water is separated out, leaving a saltier concentrate stream, and E_{min} rises. Beyond a certain Y, the remaining concentrate reaches saturation, and solid minerals precipitate out from solution (indicated by filled symbols in Fig. 2). At these ultrahigh salinities where salt precipitation occurs, E_{min} increases more rapidly with Y. For example, for $Y = 0.5$, increasing feed salinity 5.8× from 35,000 to 204,000 ppm TDS disproportionally elevates E_{min} by a factor of 8.3, from 1.11 to 9.26 kWh/m^3 (NaCl precipitation occurs for $Y > 0.89$ and 0.20, respectively). This is because the change in Gibbs free energy associated with precipitation, $\overline{G}_{\mathrm{NaCl_{(s)}}}^{\circ} - \overline{G}_{\mathrm{Na^+}}^{\circ} - \overline{G}_{\mathrm{Cl^-}}^{\circ}$ (9.1 kJ/mol or 0.16 kWh/kg for NaCl at 25 °C), imposes an additional energy demand, primarily to overcome the entropic penalty of ordering free Na$^+$ and Cl$^-$ ions in aqueous solution into a solid crystal lattice. Since saltier feeds reach saturation with less water removal, the energy toll of precipitation
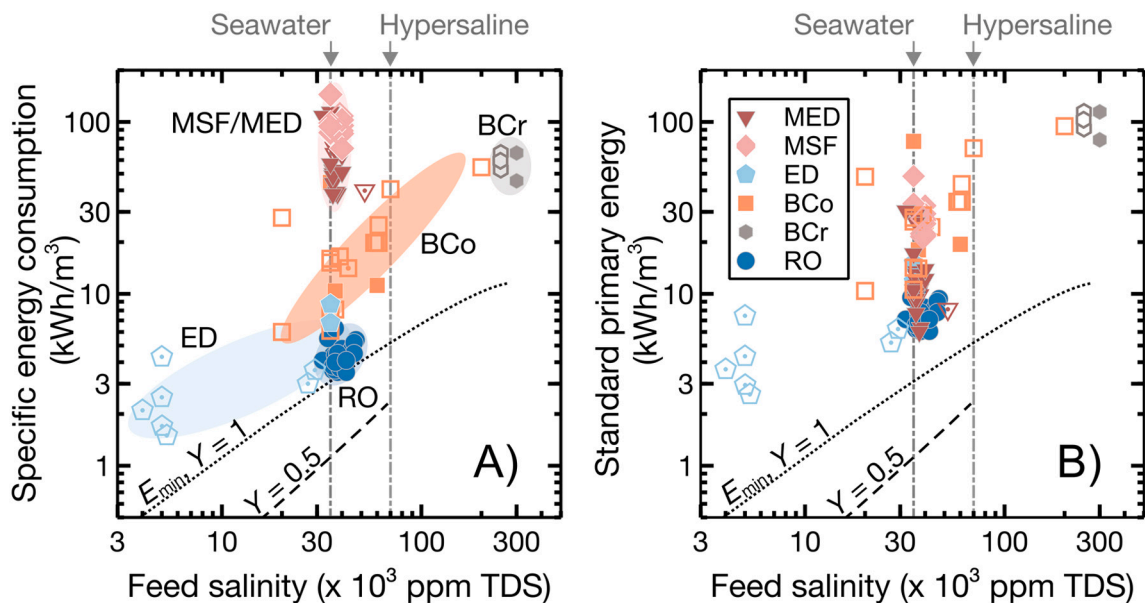

Fig. 3. A) Specific energy consumption of conventional membrane-based and evaporative methods in desalinating feed streams of different salinities. Electrodialysis (ED, light blue pentagons) and reverse osmosis (RO, dark blue circles) are membrane-based, whereas multi-stage flash (MSF, pink diamonds), multiple effect distillation (MED, maroon triangles), brine concentrators (BCo, orange squares), and brine crystallizers (BCr, gray hexagons) are evaporative techniques. Filled, dotted, and open symbols denote data from industrial operations, bench- and pilot-scale experiments, and modeling studies, respectively [8,74,99,107–134]. The specific minimum energy, E_{min}, for recovery yields, Y, of 0.5 and 1 are represented by dashed and dotted black lines, respectively. RO typically operates close to $Y = 0.5$, while BCo and BCr operate at high water recoveries that approach 0.9. Seawater salinity (35,000 ppm TDS) and our threshold for hypersalinity (70,000 ppm TDS) are marked by gray vertical dash-dot lines. Colored ellipses are intended as visual guides to indicate the general SEC and feed salinity ranges of each technology. B) Energy demand expressed as standard primary energy, SPE, one of the proposed methods to account for both quality and quantity of energy consumed [106], as the chief energy input for MSF and MED is heat in the form of steam, whereas the other technologies are mainly powered by electricity. Data on SECs, SPEs, feed and concentrate salinities, and the reference sources are detailed in Table S1 in the Supplementary Material.
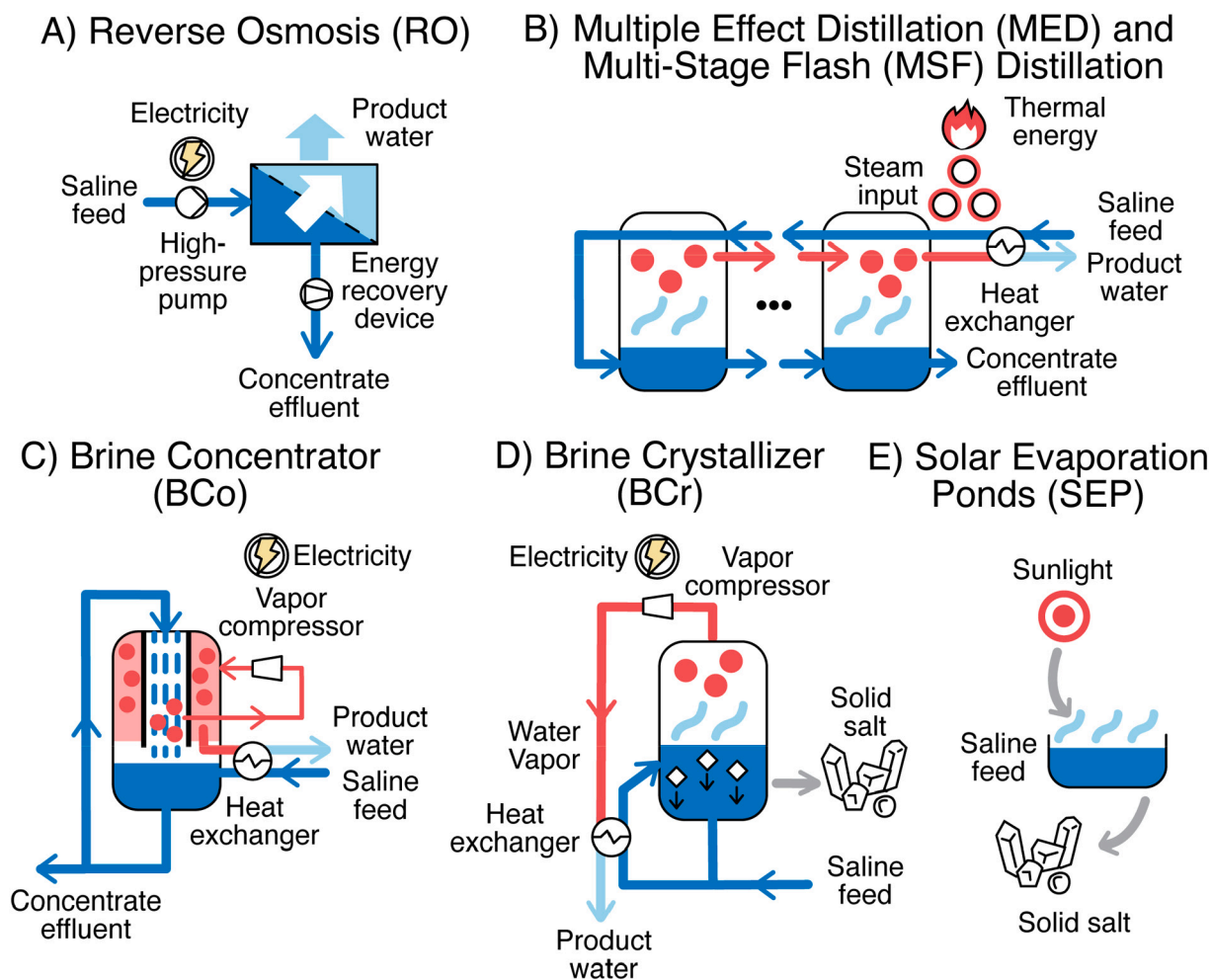
Fig. 4. Schematic illustrating working principles of conventional desalination technologies: A) reverse osmosis (RO), B) multiple effect distillation (MED) and multi-stage flash (MSF) distillation (ellipses represent repeating units), C) brine concentrator (BCo), D) brine crystallizer (BCr), and E) solar evaporation ponds (SEP). RO is a membrane-based technology with electricity as the energy input, whereas all the other technologies are thermally-driven for the evaporative phase-change of water, consuming heat from steam (MED and MSF), electrical energy (BCo and BCr), or solar energy (SEP).

impacts higher TDS feeds at lower Y.

The minimum energy of seawater desalination, which is considered one of the most costly methods to produce drinking water, is 1.11 kWh/m^3 (at a typical Y of 0.5) [100]. The desalination of hypersaline streams, especially at high recovery yields, is comparatively even more energy-intensive. The ZLD treatment of ultrahigh-salinity feeds is, therefore, an exceedingly energy-demanding operation; E_{min} for ZLD desalination of a 204,000 ppm TDS feed is 10.4 kWh/m^3, 9.3$\times$ seawater desalination. Depending on the end use, some applications can tolerate residual salinity in the product water, i.e., fit-for-purpose reuse [26,85]. If salt rejection is incomplete, i.e., product is not pure water, the thermodynamic minimum energy requirement decreases (Fig. 2B). For example, with a feed stream of 204,000 ppm TDS and $Y = 0.50$, lowering the salt rejection from 100% to 90% (i.e., 10% of the salt in the initial feed ends up in the product stream) lessens E_{min} from 9.26 to 6.88 kWh/m^3, a reduction of 26%. The lower E_{min} with imperfect salt rejection presents opportunities for desalination technologies to serve fit-for-purpose applications using slightly saline product water while requiring, in principle, reduced energy consumption.

In addition to Na$^+$ and Cl$^-$, precursor ions of sparingly soluble minerals, such as Ca^{2+}, Mg^{2+}, SO$_4^{2-}$, PO$_4^{3-}$, and CO$_3^{2-}$, are almost always present in hypersaline streams. Even though the concentrations of scalant precursor ions are much lower than NaCl, saline feeds often reach saturation with respect to these minerals at lower Y because of their order-of-magnitude lower solubilities. A representative analysis on the onset of scale formation is simulated using 10 mM each of Ca^{2+} and SO$_4^{2-}$ ions. Gypsum, CaSO$_{4(s)}$, has a solubility limit of 14.8 mM (1360 ppm), and precipitation is indicated by the shaded region in Fig. 2A [101]. Although the contribution of CaSO$_4$ to E_{min} is marginal (<2% for 204,000 ppm TDS), the formation of mineral scales at relatively low Y of 0.32 in this analysis has crucial practical implications for desalination operations: the formation of mineral scale on mass and heat transfer surfaces of current conventional technologies limits input feed salinities and achievable recovery yields (elaborated in Section 4). Mineral scaling is also anticipated to be a challenge for emerging high-salinity desalination methods. Approaches with working principles that inherently precipitate solids in bulk solution and away from liquid-solid interfaces can, hence, be advantageous for high-scaling propensity streams and also high recovery yield operations where NaCl precipitation occurs.

3.3. Electricity, steam, and low-grade heat

The specific minimum energy discussed thus far is for an ideal separation that is thermodynamically reversible. Real desalination processes inescapably produce excess entropy due to their irreversibility and, thus, demand additional heat or work input. Hence, the actual energy requirement is always greater than E_{min} [102–104]. Practical specific energy consumptions, SECs, reported for actual desalination processes are a more applied measure of the real energy demand [100,104]. Furthermore, SECs are often compared to evaluate the

relative energy intensity between different approaches. Fig. 3A shows SECs of conventional desalination techniques, reverse osmosis (RO), electrodialysis (ED), multi-stage flash (MSF), multiple effect distillation (MED), brine concentrator (BCo), and brine crystallizer (BCr), and the corresponding feed salinities (note that both axes are on logarithmic scales). Data used in Fig. 3A is detailed in Table S1 of the Supplementary Material, and Figs. S2 and S3 present the concentrate salinities (when reported) to illustrate the typical recovery yields attained by each technology. From Fig. 3A, it may appear that electricity-powered methods have lower SEC than MSF and MED, which use heat as input. However, the majority of U.S. electricity ($\approx$80%) is still generated from fossil fuel or nuclear plants that convert thermal energy into electricity, with actual efficiencies of 25.6–44.7% [105]. To illustrate the role of energy grade, SECs were converted to standard primary energy, SPE, one of the proposed methods to account for both quality and quantity of energy consumed by considering the equivalent work [106]. The converted SPEs are presented in Fig. 3B, and details for the conversion of SEC to SPE are included in the Supplementary Material. When the primary energy source is factored in, the gap between desalination technologies that use electricity and heat as energy input is considerably narrowed or even closed. As a case in point, the more energy-efficient MED processes have the same SPE as RO.

Processes that convert heat to work are inevitably bound by the Carnot efficiency ($1 - T_L/T_H$, where T_L and T_H are temperatures of the cold sink and hot source, respectively), whereas nonthermal methods are not constrained by this thermodynamic law. Therefore, thermal energy inherently has less utility than electricity and is considered to be of lower grade. To reflect this intrinsic inequality in achievable separation efficiencies, SECs discussed in this review will additionally report the energy source (kWh_e/m^3 and kWh_{th}/m^3 of product water for electrical and thermal, respectively). Further, because the Carnot efficiency is dependent on T_H, the grade of thermal energy is essentially determined by the heat source temperature, i.e., thermal sources <100 °C are of lower grade than steam. This trend is also generally represented in the economics: for the same amount of energy, electricity costs more than steam, whereas low-grade heat is often very cheap or even free. The nonequivalence of the energy types of electricity, steam, and low-grade heat is a significant, but often overlooked, aspect when evaluating different desalination technologies, as pointed out in recent studies [106,135,136]. Approaches that are seemingly less efficient, i.e., greater SECs, but are able to utilize lower grades of energy may still be overall cost-competitive.

4. Limitations of conventional desalination approaches for high-salinity streams

4.1. Reverse osmosis and thermal desalination

Desalination is a mature market, particularly for seawater and brackish water. In this section, we examine conventional desalination methods and specifically highlight the technical constraints in extending these approaches to higher salinities. Currently available technologies to desalinate feeds with a salinity of seawater and higher can be classified into two broad categories: membrane-based reverse osmosis (RO) and thermally-driven distillation. RO is presently the most widely used method for seawater and brackish water desalination, accounting for 69% of global capacity [100,137,138]. An electrically-powered pump pressurizes the saline feed above its osmotic pressure in RO to drive water permeation across a semipermeable polymeric membrane. Salts and other organic solutes are rejected by the membrane, yielding clean water as the product (Fig. 4A) [139]. Detailed reviews on the state-of-the-art of RO can be found in recent publications [99,140,141]. Electrodialysis, ED, is another conventional membrane technique, which utilizes an electrical voltage to drive the transport of charged species across ion-exchange membranes [142,143]. ED is primarily applied to desalinate brackish water; potential application of the technology for

hypersaline desalination will be discussed in Section 5.1.

Conventional thermal distillation technologies include multiple effect distillation (MED), multi-stage flash (MSF), brine concentrators (BCo), brine crystallizers (BCr), and solar evaporation ponds (SEP). These technologies use heat to vaporize water from the saline feed stream, leaving all nonvolatile solutes, including salts, in the concentrate [20,62]. Detailed descriptions of the working principles can be found in literature [20,84,92,144–147], and the key features differentiating each distillation method are highlighted here. Unlike evaporation ponds, which do not produce fresh water, MED, MSF, BCo, and BCr further condense the vapor to recover product water. MED and MSF are primarily employed for seawater desalination. Both methods take steam, usually from fossil fuel combustion, as the energy input to boil off the water in successively lower pressure effects/stages (Fig. 4B) [20,144,145,147,148], with the latent heat of vapor recovered for reuse in the next effect/stage (energy recovery is further elaborated in Subsection 4.3). A principal difference between the two techniques is the method of vaporization: saltwater is sprayed onto steam tubes in MED, whereas MSF flash boils the saline stream in chambers.

Brine concentrators are similar to single-effect evaporators. In the most common design, feedwater is mixed with a recirculating brine and is flowed down heat exchanger tubes, forming a thin liquid film on the inner tube surface (Fig. 4C). A portion of water vaporizes from the film. The vapor is removed, mechanically compressed, and fed to the outside of the heat exchanger tubes, where it condenses as product water and transfers latent heat to the cooler brine inside the tubes [4,20,84,146]. Electricity to power the mechanical vapor compressors is the primary energy input. BCo are able to treat feed salinities up to 250,000 ppm TDS [4,20,84,146]. The most prevalent type of brine crystallizer is the forced circulation crystallizer (Fig. 4D). Feedwater is combined with a recirculating brine to yield an almost saturated mixture, which is pressurized and flowed into submerged heat exchanger tubes. The heated stream is then depressurized in a crystallization vessel, and a fraction of the water is vaporized, causing precipitation of mineral solids. The water vapor is mechanically compressed and fed to the shell side of the heat exchanger to condense into product water, transferring the latent heat to warm up the brine. Most of the brine slurry is recirculated, with a small portion centrifuged or filtered to separate out the salt crystals. Similar to concentrators, BCr primarily use electricity to power mechanical vapor compressors. BCr can concentrate higher salinity brines (up to 300,000 ppm TDS) to ZLD, but also consume more energy than BCo [20]. BCo and BCr are most commonly employed at the end of a composite treatment train, to further concentrate streams that had been initially desalinated by other technologies. Maximizing utilization of the comparatively more energy-efficient technologies lowers the desalination work performed by the energy-intensive BCo and BCr to improve energy-efficiency of the overall process [149–152]. But the benefit may come at the expense of greater capital costs.

Solar evaporation ponds are shallow, artificial ponds where saline water passively evaporates to the point of saturation and mineral solids are precipitated. The salt precipitates can be left in the ponds or taken out for disposal (Fig. 4E) [62,84,92,153]. The technique has been used since antiquity to produce salt but, unlike the previous methods discussed, does not produce freshwater [154]. Evaporation ponds are able to operate across the entire salinity range and can be employed as an alternative to BCr [84].

4.2. Mineral scaling is a critical stumbling block for RO

Reverse osmosis is currently the most energy-efficient technology for desalination of seawater and brackish water (Fig. 3), with state-of-the-art RO facilities operating close to the thermodynamic limit ($\approx$1.9–3.2$\times$ E_{min}) [99,155,156]. However, RO is not suitable for treating high-salinity streams. The hydraulic pressure applied in RO modules scales with the exiting concentrate salinity. High hydraulic pressures are reported to have detrimental, sometimes irreversible, impacts on

membrane permeability and selectivity [157–159]. Hence, RO desalination is traditionally operated below ≈85 bar (1200 psi), which imposes a practical upper bound of 57,000–90,000 ppm TDS on the retentate salinity [99]. High-pressure reverse osmosis (HPRO) operating above 85 bar has been considered, with theoretical analysis showing that 2-stage HPRO can concentrate a hypersaline feed of 70,000 ppm TDS to 250,000 ppm at an SEC of 7.3 kWh$_e$/m^3, substantially below the energy consumptions of current techniques (Fig. 3A) [160,161]. A recent study demonstrated bench-scale HPRO operating up to 150 bar (2180 psi) to desalinate feed concentrations as high as 109,000 ppm TDS [162]. A number of manufacturers offer HPRO membranes in the expensive plate-and-frame configuration that can operate under pressures up to 120–203 bar (1740–2940 psi) [163–167] and, more recently, commercial membrane modules in the more widely applied spiral-wound configuration capable of handling high pressures up to 120–140 bar (1740–2030 psi) have been reported [168,169]. Further, plans for a full-scale HPRO facility treating feed of 130,000 ppm TDS were announced in 2020 [169].

But even if the pressure limit is surmounted, mineral scaling, i.e., inorganic fouling, will still be a critical stumbling block for RO in treating hypersaline streams. Hypersaline feedwaters almost always carry many species that have high potentials to form scales (Table 1), including Ca^{2+}, Mg^{2+}, Ba^{2+}, Sr^{2+}, CO$_3^{2-}$, SO$_4^{2-}$, PO$_4^{3-}$, and silica [170–172]. As water is progressively removed from the feed during RO, the concentrations of sparingly soluble salts eventually exceed solubility limits, and precipitates form on the membrane surface and in bulk solution. Crystallization of minerals on the membrane is exacerbated by the concentration polarization phenomenon, where interfacial solute concentrations are elevated due to the selective permeation of water across the membrane and almost complete rejection of ions [139,173]. Salt crystals formed in the bulk phase can subsequently be deposited onto the membrane by convective water flux [174–176]. Formation and deposition of inorganic minerals on the membrane leads to scaling, blocking the active area for transport and causing deterioration of membrane performance [172,177,178]. Because of the higher solute concentrations in hypersaline desalination, particularly in high recovery yield operations, the membrane inevitably suffers from severe mineral scaling [172,177,178]. In addition, antiscalants, commonly used to suppress scaling, have been reported to be not effective in preventing precipitation at high salinities and even aggravate biofouling of the membrane [138,178]. Furthermore, antiscalant residues in the RO retentate can pose additional management concerns and may necessitate additional posttreatment [178]. Although recent developments in the capability of membrane modules to withstand large pressurizations are promising, mineral scaling remains a persistent issue that is likely to afflict HPRO. To realize the broad implementation of HPRO, research and development of strategies to mitigate the impact of scaling will need to be redoubled [78].

4.3. Evaporative phase-change is inherently energy-intensive

The enthalpy of vaporization of seawater is about 667 kWh/m^3 (with slight variations at different temperatures and salinities) [179,180], which is 1–2 orders of magnitude higher than the specific minimum energy of desalination (Fig. 2). Therefore, desalination techniques based on evaporative phase-change are inherently energy-intensive, with efficiencies governed by a Carnot-like law bound by the boiling point elevation between the saline feed and distilled water [181]. To decrease energy consumption, the enthalpy of vapor condensation needs to be recovered and reused; the more times the latent heat can be reused, the higher the energy efficiency [145,148]. However, even with heat recovery, SECs of facility-scale seawater distillation ranges from 30 to 100 kWh$_{th}$/m^3 (Fig. 3A), which is still ≈30–100 times greater than E_{min}. This is because practical heat recovery is constrained by the operating temperature range and capital cost of additional heat exchange equipment [144,145]. This is reflected in the gain output ratio, defined as the mass

ratio of distillate to input steam, of staged MED and MSF often being limited to <12 and < 10, respectively [148]. Because the operations of BCo and BCr are similar to single-effect evaporators, the portion of latent heat that can be recovered is limited, hence the high energy consumption [4].

Traditional thermal distillation techniques also suffer from other critical limitations that become especially important at high salinities [20,182,183]. Scaling and corrosion are two key factors restricting the application of MED and MSF to salinities beyond seawater. The precipitation of sparingly soluble salts on evaporation surfaces and inside flow channels causes mineral scaling and reduces overall performance by impairing heat transfer and increasing parasitic pressure drop [184,185]. The presence of salts with retrograde solubility, where the saturation concentration decreases with higher temperatures, such as CaSO$_4$, Ca(OH)$_2$, and CaCO$_3$, further exacerbates the problem. Because hypersaline brines almost always contain sparingly soluble salts, including retrograde solubility minerals, and often at concentrations greater than in seawater [186], scaling is a significant operational problem for MED and MSF.

Additionally, hypersaline streams are corrosive due to the high chloride concentration. This is especially problematic for distillation processes as the rate of corrosion increases strongly with temperature [20,186–188]. At the same Cl$^-$ concentration, steel, for example, corrodes >100 times faster at 100 °C than at 60 °C [189]. As such, the common grades of stainless steel typically used in MED and MSF are not able to tolerate the corrosive conditions caused by the concentrated Cl$^-$ environment and high operating temperatures for prolonged operation [20,129]. Although using more corrosion-resistant materials can, in principle, mitigate the problem (as in the discussion of BCo and BCr below), the associated cost swells rapidly because of the multiple effects/stages inherent to MED and MSF, hence, effectively rendering the approach uneconomical. The technical challenges of scaling and corrosion, thus, preclude the application of conventional MED and MSF for hypersaline desalination.

BCo and BCr are able to operate within the technical constraints of scaling and corrosion and treat hypersaline streams, but at significantly higher costs. To prevent scaling in BCo, CaSO$_4$ seed crystals are often added into the recirculating brine. These crystals provide crystallization sites, encouraging precipitation in suspension rather than scaling on surfaces [4,20,84,146]. In BCr, the saline stream is heated under pressure and, therefore, does not vaporize (until depressurization in the crystallization vessel) [4,20,84]. Enhanced hydrodynamic conditions of high velocity and turbulent flows further deter scaling on surfaces [190]. Even with these elaborate features, frequent cleaning and maintenance are needed as mineral scaling cannot be completely avoided. To curb corrosion, BCo and BCr adopt corrosion-resistant but expensive materials, such as super-duplex stainless steel and titanium [4,20]. The exotic material, additional equipment, and operating requirements to handle hypersaline brines drastically elevate the levelized cost for BCo and BCr, thus pricing the technologies out from many markets. The exorbitant material requirement is also a primary reason that BCo and BCr essentially operate as single-effect evaporators and are, hence, considerably more energy-intensive than multi-staged MED and MSF (Fig. 3).

Because of their simplicity of operation, solar evaporation ponds have relatively low operating expenses and are not affected by the deleterious impacts of scaling or corrosion. However, as the rate of evaporation is determined by the solar irradiance [180], the theoretical maximum evaporative productivity of solar ponds is ≈1.6 L h^{-1} m^{-2} (without recovering the enthalpy of condensation) [191]. The slow kinetics necessitate high land investments and constrain solar ponds to arid places where rainfall is low and sunlight is abundant [62,92,144,145,153]. Leaks from ponds also pose environmental risks [3,6,75]. Furthermore, as the water vapor is often not condensed and collected, the method does not produce fresh water [84,92,144].
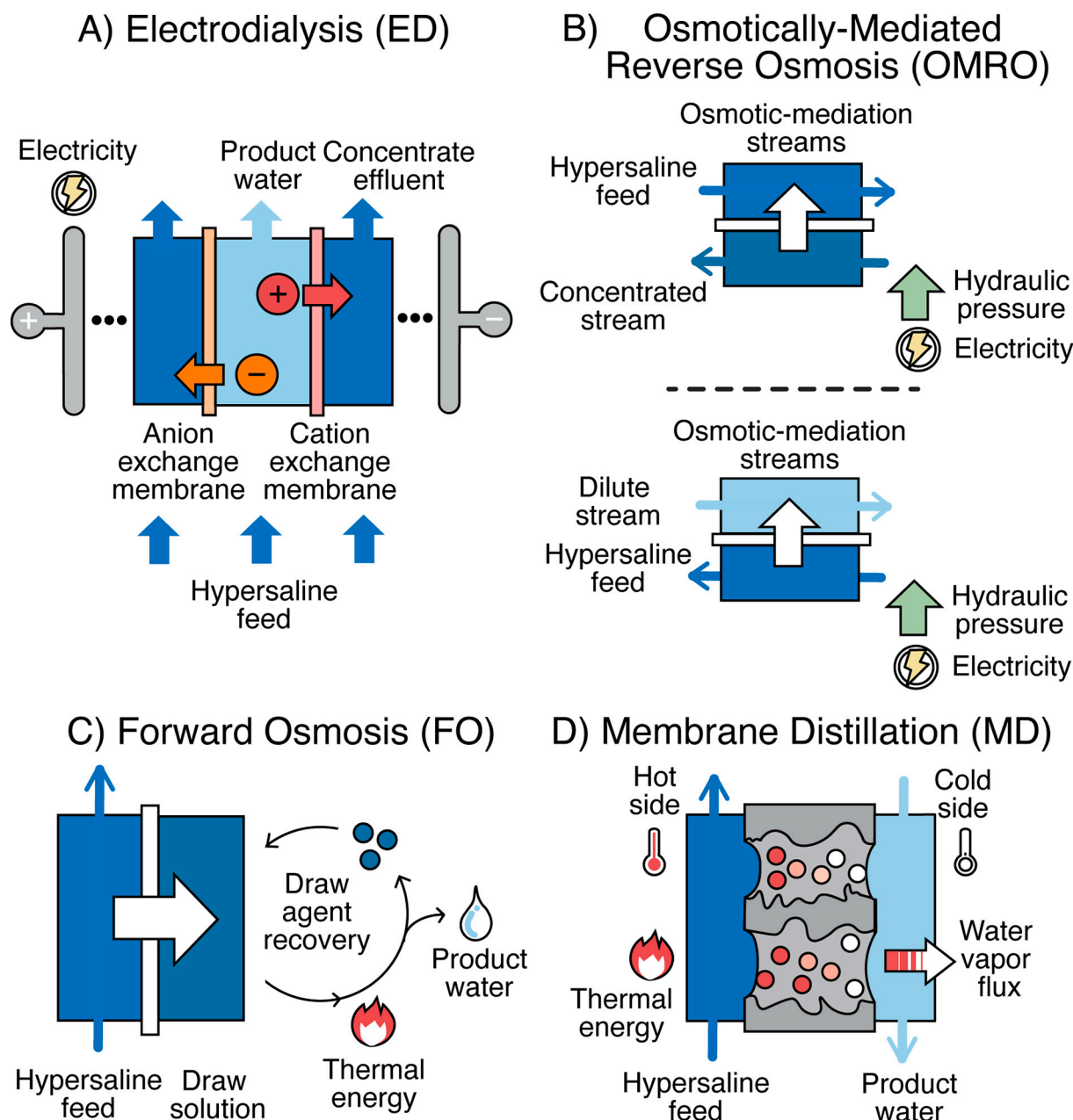
Fig. 5. Schematics illustrating the working principles of alternative and emerging membrane-based technologies for high-salinity desalination: A) electrodialysis (ED) (ellipses represent repeating units), B) osmotically-mediated reverse osmosis (dashed line divides different configurations), C) forward osmosis, and D) membrane distillation. White block arrows denote water flux, whereas colour intensity of blue aqueous streams is representative of the salinity. The primary energy input to ED and OMRO is electricity, whereas FO and MD are based on evaporative phase-change and require thermal energy input. (For interpretation of the references to colour in this figure legend, the reader is referred to the web version of this article.)

5. Alternative and emerging technologies

With the current desalination technologies of membrane-based RO and thermally-driven distillation plagued by scaling, corrosion, and low energy efficiency, the advancement of alternative technologies and development of new approaches can present opportunities for more cost-effective desalination of high-salinity streams. This section reviews alternative and emerging technologies for high-salinity desalination that have the potential to be competitive with existing methods. While some of the technologies discussed are mature within other industries, including brackish and seawater desalination as well as food production, all are nascent in their application to high-salinity desalination. The approaches are broadly categorized into membrane-based techniques of electrodialysis, osmotically-mediated reverse osmosis, forward osmosis,

and membrane distillation, as well as non-membrane-based methods of humidification-dehumidification, solvent extraction desalination, supercritical water desalination, freeze desalination, clathrate hydrate desalination, and solar thermal desalination. All of the non-membrane-based methods as well as membrane distillation and draw agent regeneration in forward osmosis are thermally driven. The working principles are briefly introduced and intrinsic strengths and limitations are discussed. Each technology is critically reviewed along the key dimensions of specific energy consumption, technology development level, capability to achieve zero liquid discharge, salinity of product water (i.e., compatibility with fit-for-purpose applications), and impacts of precipitation and scaling on performance. The list of technologies covered here is not intended to be exhaustive; rather, it focuses on approaches with significant research and development activities. Incipient

techniques and processes that are less studied are, hence, not included here [192–198].

5.1. Electrodialysis

Electrodialysis (ED) utilizes an applied electric potential to drive the transport of salt ions from the saline feed stream across charge-selective ion-exchange membranes (IEMs) to a concentrate stream [199]. An ED stack comprises repeating cells of channels separated by alternating cation and anion exchange membranes, which allow the selective transport of positively- and negatively-charged species, respectively (Fig. 5A depicts a simplified repeating cell). A saline feed stream flows through the channels. An applied voltage sets up opposing fluxes of cations and anions from the product channels across the IEMs to adjacent concentrate channels, thereby lowering the product stream salinity to achieve desalination. ED is widely employed for the desalination of brackish water, i.e., <15,000 ppm TDS [200], but has been recently investigated for hypersaline applications [13].

The primary energetic inefficiency of ED is ohmic losses across the stack, specifically the resistance contributions of the IEMs and aqueous streams to ion flux [199]. Opportunely, since solution conductivity scales almost linearly with salinity, the high ionic conductivity of the streams in hypersaline ED operations favorably reduces the channel resistances, thereby improving overall energy efficiency [13,199]. However, by the same principle, desalinating the product stream to drinking water TDS standards (<1000 ppm TDS) would significantly raise the channel resistance and detrimentally increase ohmic losses. Therefore, ED can be more advantageously employed to partially desalinate hypersaline feeds to lower-salinity streams that can then be desalinated by conventional RO, used in fit-for-purpose applications, or safely discharged [201].

Recent high-salinity ED studies report energy consumptions of 0.1–0.3 kWh$_e$/kg-NaCl (ED energy requirements are sometimes normalized by salt removed) [13,202,203] or, equivalently, 7–22 kWh$_e$/m^3, depending on the feed salinity and stack design [13,14,114,204]. Compared to RO, the increase in kWh$_e$/m^3 SEC of ED with greater recovery yields is relatively small [205]. Because energy consumption is primarily determined by the amount of salt ions separated from the product stream and the stack resistance, increasing Y only alters SEC slightly. This differentiating feature can be potentially leveraged for ED to be competitive in high water recovery operations, e.g., enhanced recovery from inland brackish water RO desalination concentrates [91,206]. Additionally, ED does not require high pressures or temperatures, unlike RO and conventional distillation. By periodically reversing the applied electric voltage, a process known as electrodialysis reversal [207], membrane fouling can be mitigated [84,200,207,208].

Though ED exhibits promise for high-salinity desalination, three major limitations are preventing broader adoption: diminished current efficiency, water transport, and membrane resistance. Compromised current efficiency at high salinity is the primary obstacle: as salinity increases, the ability of IEMs to suppress leakage of like-charged co-ions declines, leading to lower current efficiency and higher energy consumption [209,210]. Osmotic pressure difference across the IEMs and electro-osmosis, the water movement associated with ion fluxes, both cause undesirable water permeation from the product to the concentrate stream, which reduces the product water volume [13,120]. Even though channel resistance is low when the streams are highly saline, ED would still suffer from significant ohmic losses due to the contribution of the membranes to resistance [13,209]. Advancements in membrane technology are needed to fully realize the potential of ED for hypersaline desalination. Specifically, membranes need to maintain adequately high permselectivity in highly saline environments, in addition to having low hydraulic permeability and low ion transport resistance [14,209,210]. However, resistivity and selectivity are intrinsically linked IEM properties, where a reduction in resistivity is almost always accompanied by a drop in permselectivity, i.e., the conductivity-permselectivity tradeoff

[209]. Efforts to develop better membranes for hypersaline ED will need to navigate this constraint. Novel operating strategies, such as multi-stage ED, can be employed to further reduce SEC [120]. Lastly, because of the working principles of the technology, ED by itself is inherently unable to attain ZLD, thus restricting the achievable recovery yields.

5.2. Osmotically-mediated reverse osmosis

To overcome the pressure limitations encountered by conventional RO in high-salinity desalination, an alternative operation of osmotically-mediated reverse osmosis (OMRO) was recently proposed (Fig. 5B) [211–213]. The approach couples a conventional RO stage to osmotically-mediated RO stages, where saline streams are circulated on the permeate side instead of freshwater. These saline receiving streams reduce the transmembrane osmotic pressure difference, enabling water permeation from hypersaline streams to lower salinities using only moderate hydraulic pressures. The diluted receiving stream is then fed to the conventional RO stage to produce freshwater. Therefore, OMRO can desalinate the effluents to concentrations beyond conventional RO limits (57,000–90,000 ppm TDS), while requiring substantially less energy (≈4–29 kWh$_e$/m^3) [11,214] than traditional distillation processes. Various configurations of OMRO include counter-flow/osmotically assisted reverse osmosis (CF/OARO), cascading osmotically mediated reverse osmosis (COMRO), and low salt rejection reverse osmosis (LSRRO) [215,216]; the distinct features and advantages of each configuration were discussed in previous studies [11,212,217,218]. A pilot-scale demonstration of CF/OARO was reported in 2018, and a 5000 m^3/d (1.3 × 10^6 gal/d) CF/OARO plant is currently being built in Saudi Arabia to enhance water recovery from seawater desalination concentrate [219]. In contrast, COMRO has been investigated at bench-scale thus far, and LSRRO has only been modeled [158,213].

Whereas conventional RO is solely a separation process, osmotic mediation intrinsically produces entropy through the mixing of the permeate with a higher salinity stream [103,212]. Therefore, OMRO inevitably has a higher SEC than conventional RO with the same number of stages, implying that high-pressure RO would be energetically more favorably for hypersaline desalination, if the current technical challenges can be adequately addressed. Further advancement of the technology hinges on overcoming three membrane challenges. Firstly, developing membranes with suitable structural and transport properties will be critical. Membrane support layers with low mass transfer resistance (i.e., small structural parameter) are desirable for COMRO and OA/CFRO to mitigate concentration polarization within the membrane, an unavoidable phenomenon that detrimentally elevates the transmembrane osmotic pressure difference [158]. Secondly, the net driving force for water flux, applied hydraulic pressure in excess of transmembrane osmotic pressure, will be relatively low for OMRO, necessitating larger membrane areas compared to HPRO. Membranes with greater water permeabilities will reduce the area requirement, but salt permeation will also correspondingly increase as conventional polymeric membranes are bound by the permeability-selectivity tradeoff [220–222], resulting in compromised separation performance. Thirdly, OMRO is still membrane-based and would inescapably be plagued by mineral scaling and other fouling problems; at present, there are no studies on these issues. Because OA/CFRO employs recirculated working solutions (COMRO and LSRRO do not), the configuration has the added concern of solute loss across the membrane to the product water, which represents a chemical replenishment cost. At the same time, foreign salts and impurities leaked from the feed stream would accumulate in the working solution and pose operational complexities.

5.3. Forward osmosis

Forward osmosis (FO) achieves desalination by two steps. In the first step, a highly concentrated engineered solution draws water from the
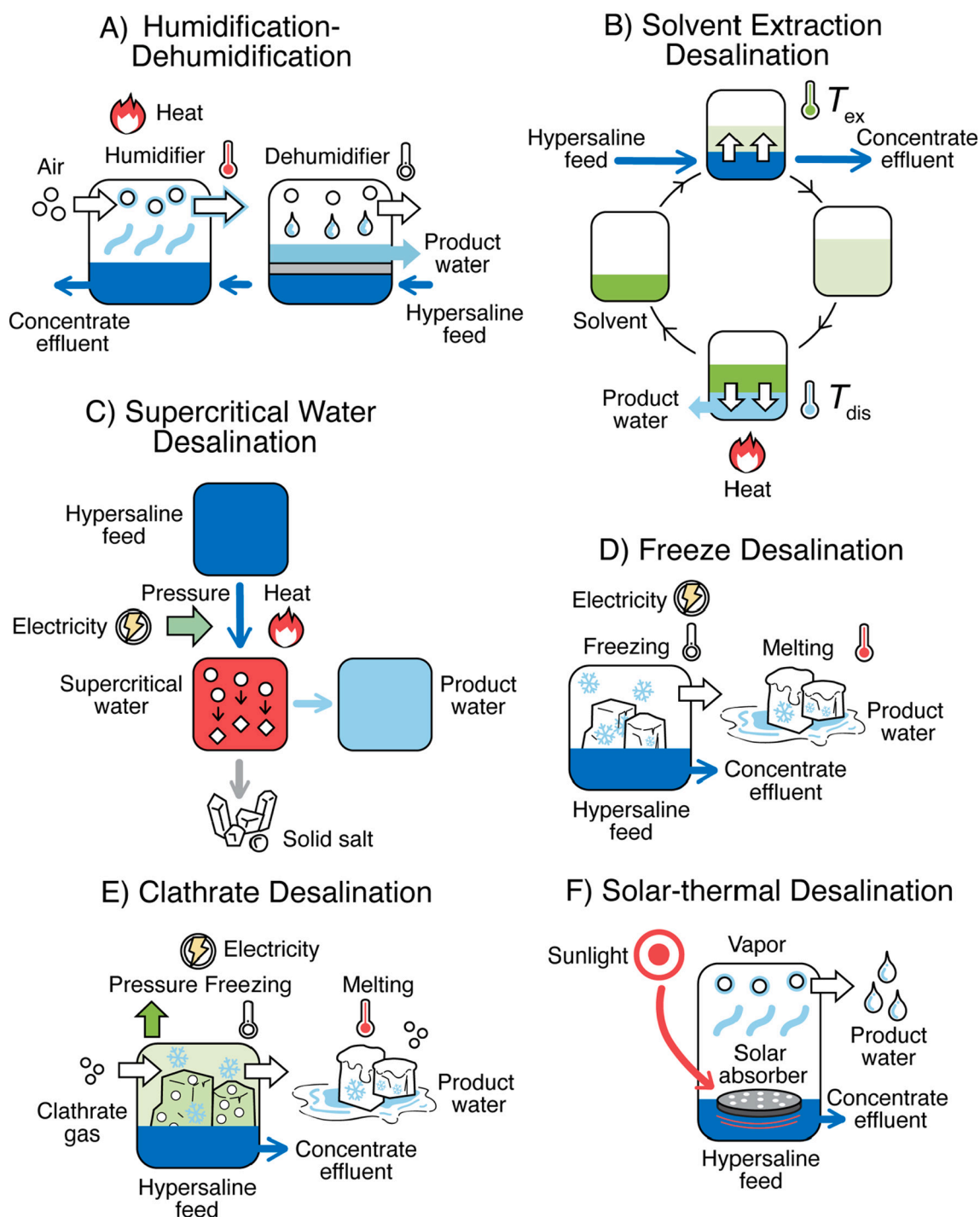
Fig. 6. Schematics illustrating working principles of emerging non-membrane-based technologies for high-salinity desalination: A) humidification-dehumidification (HDH), B) solvent extraction desalination (SED), C) supercritical water desalination (SCWD), D) freeze desalination (FD), E) clathrate hydrate desalination (CHD), and F) solar-thermal desalination (STD). Different colour intensity of blue aqueous streams is representative of the salinity. The major energy input of HDH and SED is heat. SCWD uses both heat and electricity, whereas FD and CHD use electricity and STD uses sunlight. (For interpretation of the references to colour in this figure legend, the reader is referred to the web version of this article.)

saline feed stream across a semipermeable membrane through the action of osmosis. In the second step, freshwater is separated from the diluted draw stream, most commonly by applying heat, yielding product water and regenerating the draw agent to be recycled back to the first step (Fig. 5C) [223–226]. In other words, the first step is actually mixing, and separation only occurs in the second step. The potential of FO for high-salinity desalination has been highlighted in multiple review papers and examined in several experimental studies [2,9,84,227–234]. A bench-

scale investigation demonstrated the capability of FO to desalinate NaCl solutions with salinities as high as 240,000 ppm TDS [230]. An FO unit at a coal-fired power plant treated flue gas desulfurization wastewater of 39,000–52,000 ppm TDS to water recovery yields ranging from 93 to 97%, resulting in an effluent retentate at 220,000 ppm TDS [9]. The reported heat energy input was ≈95 kWh$_{th}$/m^3, supplied by steam.

While water osmosis is spontaneous and auxiliary energy consumption of the first step is very small, reconstitution of the diluted draw

agent back to the initial high concentration requires intensive thermal energy inputs and dominates the overall SEC. Electrolyte salts (e.g., NaCl, $MgSO_4$, and ammonium acetate) have been investigated as draw agents for hypersaline FO desalination, but must be reconcentrated by thermal evaporation (typically using MED, MSF or membrane distillation), inevitably incurring the large enthalpic penalty of water vaporization [84,226]. Volatile solutes (e.g., NH_3-CO_2) have also been explored and, because vaporization enthalpy of the volatile solute is lower than water, studies claim that draw agent regeneration can be comparatively less energy-intensive [9,228–230,234]. But the process still requires phase-change of the draw agent (from aqueous species to vapor) and the concomitant evaporation of water is also unavoidable. FO has yet to make the definitive case that desalinating the diluted draw solution is a better separation than directly desalinating the initial saline feed.

Unlike RO, where the applied hydraulic pressure scales with feed salinity, FO membranes experience pressures very close to ambient regardless of feed concentration. This milder operating pressure has been shown to significantly decrease the deleterious impacts of fouling on FO membranes [84,224]. Fouling that does occur is largely reversible, and foulants can be removed using relatively simple cleaning procedures [2,235,236]. As such, FO shows promise to mitigate one of the critical problems facing membrane-based processes for hypersaline desalination and potentially achieve high water recoveries [9,224,228]. Similar to OMRO, improving membrane selectivity and reducing internal concentration polarization can also improve the cost-effectiveness of FO [223,224,226]. All FO applications experience reverse flux leakage of the draw agent into the feedwater, which imposes a material replenishment cost and can contaminate the dewatered brine stream, complicating subsequent concentrate management [226,235]. The ability of the membrane to reject solutes is reported to decrease at higher draw agent salinities and, therefore, hypersaline FO applications will be more adversely impacted [157,232]. Similarly, salt flux from the saline feed into the draw solution can lead to operational issues for the draw agent regeneration step. While there has been substantial progress in membrane development [235,237,238], to advance the technology to practical application, FO will need to overcome the principal challenge of the high energy demand for draw agent reconstitution and the unavoidable problems due to imperfect membrane selectivity.

5.4. Membrane distillation

Membrane distillation (MD) is a thermally-driven and membrane-based desalination technology that can utilize low-grade heat [239–241]. Detailed working principles can be found in literature and are briefly explained here (Fig. 5D) [239,240,242–244]. A hydrophobic, microporous membrane that is not wetted by water acts as a physical barrier between the saline feed and permeate sides. Low-temperature heat evaporates water from the feed stream. The vapor is driven across membrane pores by a partial vapor pressure gradient and condenses in the permeate side. Nonvolatile solutes, such as ions, are retained in the saline feed stream [239–243]. Most of the high-salinity MD desalination studies are investigations on bench-scale setups and laboratory prototypes [12,245–261]. A recent publication reported a 2 m^3/d (528 gal/d) MD setup in Qatar, desalinating effluent concentrate from a seawater distillation facility at 70,000 ppm TDS to 34% water recovery yield [262]. Full-scale MD desalination plants, hypersaline or otherwise, have not yet been reported [263].

As the partial pressure of water vapor is only weakly sensitive to salt concentration (around 10% decrease for 150,000 ppm TDS NaCl solution, relative to pure water) [264], MD can desalinate across the entire salinity range with only marginal water flux decline [2,239,249,251,265,266]. Because salts are nonvolatile, MD product water is of very low TDS, typically <20 ppm regardless of feed salinity [2,246,249,259,262]. Therefore, MD has the advantages of performance resilience at hypersalinity and high-purity product water. Since MD can

be driven by moderate temperatures, the potential to use low-grade thermal energy instead of high-quality energy inputs is another often-mentioned benefit [77,179,267–272]. In addition, MD has a lower fouling propensity than RO, primarily due to the absence of applied hydraulic pressures [2,239,243,273].

Despite the potential advantages, MD is still a distillation process based on the evaporation of water and is, hence, inherently energy-intensive [2,179,181]. Strategies to reduce energy consumption down from the enthalpy of water vaporization are vitally needed for the technology to be competitive. To this end, capturing and reusing the latent heat released by permeate condensation, either through multi-stage designs or by heat exchange between the influent feed stream and the exiting vapor permeate, have been widely investigated [242,255,274–283]. Although substantial reductions in energy demand were demonstrated, the SEC is still >100 kWh_{th}/m^3 [255,274,278,284–286]. Further analyses are also needed to show that the additional capital cost of the heat recovery equipment is justified by the operational energy savings [255,286].

Volatile components typical to high-salinity streams, such as small organic compounds and dissolved gases, can transport through the membrane with the water vapor flux to contaminate the product water [2,243,287,288]. Surfactants present in some brines (e.g., produced water) and concentrates can cause membrane wetting by lowering the liquid surface tension of the feed stream [2,243,288]. The saline feed can then seep across the membrane through the wetted pores and lower the product water quality [12,247,248,262,265]. Although MD has higher fouling resistance than RO, membrane fouling and also scaling cannot be entirely avoided and will still be problematic due to the frequently high concentrations of foulants and scalants in hypersaline streams. Fouling and scaling will, in turn, trigger flux decline and also pore wetting [246,247,273]. Pretreatments to remove foulants and scalants and posttreatments to remove volatile contaminants from product water have been proposed, but will incur extra costs [2,265,289,290]. MD, being a membrane-based and low-temperature distillation technology, is frequently touted to possess the advantages of both approaches. But the technique unavoidably also suffers from disadvantages afflicting membranes (e.g., scaling, fouling, and pore wetting) and evaporative phase-change (i.e., large enthalpy of vaporization). Realizing MD for high-salinity desalination would require both sets of problems to be surmounted.

5.5. Humidification-dehumidification

Humidification-dehumidification (HDH) is a thermally-driven desalination technology that mimics the natural water cycle (Fig. 6A) [291–293]. In HDH, water is evaporated from the saline feed stream into a dry carrier gas (typically air) at moderate temperatures, usually 50–90 °C, in the humidifier chamber. The moist air is circulated to a cool chamber, the dehumidifier, where water vapor condenses and is collected [293–295]. In a laboratory study, a 66,000 ppm TDS brine was concentrated to 345,000 ppm at an energy cost of 224 kWh_{th}/m^3 [259]. Another study demonstrated ZLD with HDH and modeled the energy cost to be 255–334 kWh_{th}/m^3 [296]. Other studies reported modeled and experimental SEC of hypersaline HDH to be in the range of 92–1480 kWh_{th}/m^3 [297–300]. HDH was only recently commercialized and is not widely considered to be a mainstream desalination approach [297,301].

Though HDH is fundamentally an evaporative process, it differs from conventional distillation in several respects. First, HDH usually operates at ambient pressures and with a top temperature of 50–90 °C, within the range of low-grade heat. HDH is more resistant to scaling and salt crystallization since evaporation typically occurs in the middle of a bubble column, spray tower, or packed bed, away from equipment surfaces, making HDH especially attractive for ZLD operations [301].

However, experimental SECs for HDH are still high (>210 kWh_{th}/m^3) [259,297,302]. Poor energy intensity is a barrier to widespread adoption of the technology. Unlike other evaporative separations that

only heat the feedwater, HDH requires that the carrier gas be heated as well. Because the mass of the carrier gas is more than ten times that of the water vapor it carries, a significant heating and cooling load is additionally imposed [303]. Furthermore, the carrier gas is non-condensable, which presents heat- and mass-transfer resistances that increase the size of humidifiers and dehumidifiers [304,305]. Like other evaporative techniques, dissolved gases and small organic molecules that are volatile will vaporize along with water in HDH and appear in the product water [306]. Innovative reactor designs and features, such as multiple-extraction humidification, bubble column dehumidifiers, and the use of adsorbents, show promise for improving the process efficiency and lowering the SEC [305,307–312]. The tolerance to corrosion and resistance to scaling are significant advantages for HDH in desalinating hypersaline streams. Technological advances to reuse of the enthalpy of condensation without drastically increasing capital cost will improve the competitiveness of HDH.

5.6. Solvent extraction desalination

Solvent extraction desalination (SED) is a thermally-driven technique that does not involve the phase-change of water (Fig. 6B) [10,313,314]. In SED, the saline feed is mixed with a low-polarity solvent at extraction temperature, T_{ex}, at which the two liquids are immiscible and, thus, form a biphasic mixture (i.e., T_{ex} is below the upper consolute temperature or above the lower consolute temperature of the mixture). However, the solvent possesses hydrophilic functional groups and, thus, draws some water from the feed stream into the solvent phase, whereas salts do not favor partitioning into the low dielectric constant environment of the solvent and remain in the aqueous phase. The water-laden solvent phase is then decanted from the concentrated aqueous phase and brought to disengagement temperature, T_{dis}, lowering the solubility limit of water. Consequently, the previously extracted water demixes, or disengages, from the solvent, yielding a desalinated product stream. The product water is physically separated, and the regenerated solvent is recycled back to the process.

SED was first explored for desalination of brackish water and seawater in the 1950s and 1960s [313,315–321] and brackish water desalination was demonstration in a 8 m³/d (2,000 gal/d) pilot-scale plant [322]. Since 2011, there has been renewed interest in this technology for desalination and dewatering of hypersaline streams [10,323–327]. A recent study demonstrated the capability of SED, using amines as solvents, to desalinate brines with salinities up to ≈203,600 ppm TDS (4.0 M NaCl) and with salt removals as high as 98.4% [10]. Water recovery yields >50% were attained for a feed of 83,000 ppm TDS (1.5 M NaCl) in semi-batch experiments with multiple extraction cycles. Preliminary first-order analysis estimates the SEC to be 39–77 kWh$_{th}$/m³ for 50% recovery of a 83,000 ppm TDS feed. Another study achieved ZLD of hypersaline feeds at 247,000 ppm TDS (5.0 M NaCl), again using an amine solvent [324]. So far, hypersaline SED has been reported for different solvent classes of amines, organic acids, and ionic liquids [10,326,327].

Because SED is both membrane-less and non-evaporative, the approach avoids many of the limitations faced by traditional high-salinity desalination technologies. Process top temperatures are typically <80 °C, so corrosion is lessened compared to conventional distillation methods. The extraction of water at the liquid-liquid interface drives precipitation that occurs to take place in the bulk solution, thus reducing the detrimental formation of scales on heat and mass transfer surfaces. Additionally, the temperature swings between T_{ex} and T_{dis} are relatively moderate and, thus, SED can utilize potentially inexpensive low-grade thermal resources for heating and cooling towers, instead of costlier refrigeration, for cooling [313,322].

Although the solvents utilized in SED are of low-polarity, they are not completely insoluble in water. Therefore, a fraction of solvent is lost to both the dewatered raffinate and product water. Recovering the solvent imposes additional costs, and any leaked solvent that is not reclaimed will need to be replenished. Moreover, residual solvent in the concentrate and product streams may necessitate posttreatment, particularly if the solvent poses toxicity concerns. Identification of solvents that minimize loss and are benign to the environment and human health is imperative for advancement of the technology [10,313,314]. At the same time, research on new solvents with high water production capabilities will lower the energy consumption of SED [10,326,328]. Although the technique is not based on vaporization of water, it is still thermally-driven and, therefore, the separation is ultimately bound by the Carnot efficiency [181]. SED applications would have to balance between the operational benefits of a small temperature swing with the lowered theoretical efficiency. Real hypersaline streams have complex water chemistries, beyond single-electrolyte solutions of NaCl typically used in lab studies, and contain other contaminants in addition to inorganic salts. SED performance with actual field samples needs to be investigated, and further studies are necessary to shed light on the fate and transport of pollutants commonly present in real brines, such as organics, heavy metals, oil and grease, particulates, and surfactants. Addressing solvent loss and understanding contaminant impacts and removal will be pivotal to further advancement of the technology.

5.7. Supercritical water desalination

Supercritical water desalination (SCWD) utilizes the switch in solvent polarity from polar to nonpolar at supercritical conditions to precipitate salts from saline feed streams (Fig. 6C) [15,329,330]. Under supercritical conditions, above 374 °C and 221 bar (≈3200 psi), water molecules exhibit much weaker hydrogen bonding than under ambient conditions, and water behaves as a nonpolar solvent [15]. Salts precipitate out from solution as their solubility in the supercritical water is drastically lowered, allowing the convenient separation of solid minerals from the fluid product water stream [331–333]. Because no concentrate waste stream is produced, SCWD is inherently always a ZLD technology. SCWD of hypersaline brines has been experimentally demonstrated in several recent lab- and pilot-scale studies [15,334,335], including treatment of field samples of carbon sequestration and oilfield brines with 121,000 and 224,000 ppm TDS, respectively [334]. To date, there are no reported industrial demonstrations of SCWD using high-salinity streams.

SCWD can advantageously handle different feed stream compositions and treat across the entire salinity range. Furthermore, because the technique precipitates out even sparingly soluble salts, extensive pretreatment is typically not required [330]. Importantly, SCWD precipitation does not occur at an interface but, instead, takes place in the bulk fluid phase. Hence, SCWD can potentially avoid scaling issues on solid surfaces that affect traditional approaches.

SEC of SCWD is determined by the energy required to pressurize and heat the saline feed stream to supercritical conditions. Thus, the technique consumes prime energy sources of both electricity (to power high-pressure pumps) and high-grade heat (due to the requisite high temperature of >374 °C) [330]. The extreme temperatures and pressures needed to achieve supercritical state for water impose very high energy consumption and capital costs for SCWD. Even with energy recovery, SEC to desalinate a 35,000 ppm TDS NaCl feed stream (i.e., approximately seawater salinity) is estimated to be ≈125 kWh/m³ [15]. Materials used in SCWD must be thermally, mechanically, and chemically robust to tolerate the very harsh temperature and pressure. Though durable materials, such as stainless steel and titanium, have been used, the superheated and pressurized high-salinity brine was still shown to cause substantial corrosion to the equipment [336,337]. While most studies have been conducted using simulated NaCl streams, the more complex compositions of real high-salinity brines can create even more oxidative conditions [334,337]. In order for SCWD to be competitive, the two primary challenges of high material durability requirements and large energy costs to attain the intense temperatures and pressures need to be addressed.

5.8. Freeze desalination

In freeze desalination (FD) the saline feed stream is cooled below the freezing point to form ice. Because dissolved solids are excluded from the ice, the pure ice can be physically separated from the salts and melted to yield product water (Fig. 6D) [338–340]. In practice, however, some salt is inevitably trapped within the ice crystals and adhered to the ice surface during freezing. The ice may be further desalinated by washing, pressing, or gentle melting to remove residual salts [16,338,341,342], but because the contamination cannot be completely eliminated, salt rejection is usually poorer than the conventional methods of RO or distillation (as low as ≈40% without ice posttreatment) [343–345]. Detailed working principles of the technique are available in literature [16,346]. The main energy input of FD is electricity for refrigeration [347]. In the 1960s, seawater FD was demonstrated in a 57 m^3/d plant, but the emergence of RO as a more energy-efficient approach sidelined the technique from becoming mainstream [16,338,348]. The technology, though, is used in the food and beverage industry [347,349–351]. More recently, several studies investigated the potential application of FD to hypersaline feeds [341,343,344,352].

Eutectic freeze desalination is FD carried out at the eutectic temperature of the saline feed, where ice and salt hydrates (e.g., NaCl·2H$_2$O$_{(s)}$) form simultaneously [339,353]. At high salinities, the freezing point of water is substantially depressed and approaches the eutectic temperature [354]. As such, hypersaline FD tends to be eutectic by nature. A number of bench-scale studies demonstrated eutectic FD of hypersaline streams [339,345,353,355–364]. The technique is capable of producing solids with very high salt content: NaCl·2H$_2$O$_{(s)}$ is ≈62% salt, by weight [357]. An advantage over conventional operation is that eutectic FD allows for the separation of electrolytes with different eutectic temperatures. Na$_2$SO$_4$·10H$_2$O$_{(s)}$, for example, precipitates at −8 °C, whereas NaCl$_2$·2H$_2$O$_{(s)}$ precipitates at −29 °C [364]. The selective precipitation of ions in eutectic FD offers potential economic benefits through the production of minerals [16,346,353].

FD can desalinate across the whole salinity range, including feed streams saturated in salts [339]. Biofouling of equipment is minimized, since microbial activities are retarded at low temperatures [365]. In addition, metal corrosion rates are orders of magnitude slower at FD operating temperatures than for thermal distillation [338,366]. The significantly reduced requirement for corrosion resistance allows lower-cost materials to be used in FD [16]. Studies suggest that, with diminished scaling, biofouling, and corrosion, the technique can eliminate the need for feed pretreatment altogether [367–369]. Although FD, like distillation, is based on a phase-change of water, the enthalpy of fusion is only ≈1/7 of vaporization [370]. Thus, freeze desalination has an intrinsic enthalpic advantage over evaporative approaches.

However, FD also faces several challenges, with low product water purity being the primary issue. There is an inherent tradeoff between freezing rate and ice purity: fast freezing creates smaller ice crystals with greater specific surface area, which adhere more salts [338]. On the other hand, slow freezing requires the use of large equipment to maintain practically adequate throughput. Further, even with slow freezing, the unavoidable adherence of salts to the ice will still necessitate posttreatment to achieve high-quality product water [338]. Conversely, if a more saline product water is acceptable, FD operation can be simplified and accelerated [344]. A thermodynamic study determined an SEC of 26 kWh$_e$/m^3 to concentrate a 45,000 ppm NaCl feed to 220,000 ppm [371], but experimental energy consumption data for hypersaline FD is sparse. Development of the technology will benefit from more robust SEC reporting. Liquefied natural gas, LNG, has been proposed as a low-cost cooling source for FD [372–377]. However, the opportunity cost of using LNG for desalination instead of electricity generation is not thoroughly examined and, hence, a convincing economic case for the utilization of LNG for FD is yet to emerge.

5.9. Clathrate hydrate desalination

In clathrate hydration desalination (CHD) a saline feed is mixed with clathrate-forming gases at low temperatures and high pressures to form clathrate hydrates: networks of hydrogen-bonded frozen water molecules around the gas molecules (Fig. 6E). Like ice, clathrate hydrates exclude dissolved solids from their structure. The solid hydrates can be removed from the remaining liquid and melted to recover freshwater and liberate the gas [17]. At sufficiently high pressures, clathrate hydrates can form above the freezing point of the saline feed stream [378]. Similar to FD, salts adhere to clathrates, thereby requiring posttreatment (washing, pressing, or gentle melting) to yield low-salinity product water [379,380]. CHD primarily consumes electricity for refrigeration and pressurization. Carbon dioxide, methane, propane, cycloalkanes, hydrofluorocarbons, and their mixtures have been studied for CHD [17,378,379]. Numerous experimental investigations on high-salinity desalination and hydrate formation in hypersaline conditions have been carried out in laboratories [381–392], but the technology has yet to be demonstrated, even at pilot-scale. Detailed reviews on CHD can be found in literature [17,378,379,393].

An analysis modeling seawater CHD estimated energy consumption of ≈65 kWh$_e$/m^3 for 40% water recovery yield [394,395], but there is no data for hypersaline CHD, which is expected to be more energy-intensive. Mixtures of working gases may be employed to raise the operating temperature at the expense of higher pressure; mechanical pressurization is cheaper than refrigeration, suggesting that the tradeoff can lower overall cost [381]. As with freeze desalination, CHD has been proposed to be co-located with liquefied natural gas regasification [394,396,397], but, as discussed previously (Section 5.8), any integration of LNG with desalination would need to justify that the economic benefits outweigh the opportunity costs of using LNG for other applications.

At typical operating temperatures of CHD, corrosion, scale formation, and biofouling, which impair conventional desalination methods, are substantially suppressed [338,365,366]. Because clathrates can form even in saturated solutions, CHD can handle the entire feed salinity range, although higher pressurization or refrigeration to colder temperatures will be required since dissolved solids thermodynamically inhibit clathrate formation [378,398–400]. Commercial application of the technology will, however, be hampered by the slow kinetics of clathrate formation, which worsen with higher salinities [401–404]. For example, a study reported ≈4% water recovery yield from a 450 mL reactor in 30 min using a 70,000 ppm NaCl feed [383]; another study took >3 h to fully enclathrate a 50 mL system of cyclopentane, CO$_2$, and 35,000 ppm NaCl [405]. In addition to removing adhered salts for lower TDS product water, further posttreatment is required to recover the clathrate-forming gas from the product water and concentrate, increasing the cost and complexity of the process [379,380]. Like FD, CHD has poor salt rejection, but further suffers from extremely slow kinetics and more complex operations, particularly the need to recapture clathrate-forming gas. As such, the technology is unlikely to surpass FD.

5.10. Solar thermal desalination

In solar thermal desalination (STD) sunlight is converted into heat to evaporate saltwater (Fig. 6F). Solar evaporation ponds, introduced earlier in the discussion on conventional desalination, are used to concentrate saline streams but do not produce freshwater [154]. Solar stills are engineered STD devices that additionally condense the vapor to recover distilled water [406]. An in-depth analysis of the status, prospects, and challenges of STD can be found in a recent review article [191]. Because solar stills directly utilize solar energy, the technique has the advantages of simple installation and operation, low equipment requirements, and suitability for deployment in remote regions [406]. As STD is based on evaporation, the approach is not limited by feed salinity
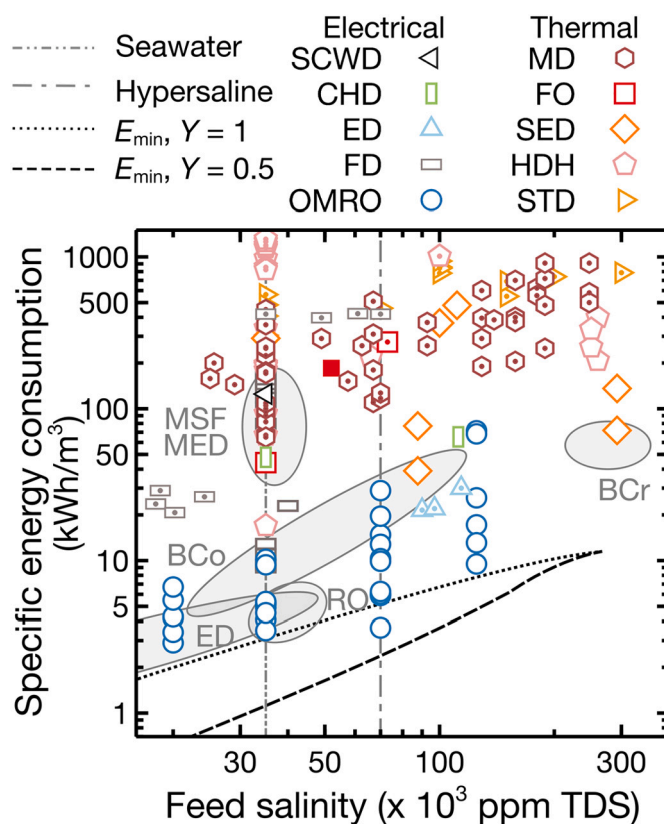
Fig. 7. Specific energy consumption as a function of feed salinity for alternative and emerging methods, where robust data is available [9–11,13–15,218,228,231,245,246,255–257,259,260,268,275,277,278,285,291,296,299,308,311,324,327,330,352,375,377,394,395,414,416,417,419–442]. Filled, dotted, and open symbols denote data from industrial operations, bench- and pilot-scale experiments, and modeling studies, respectively. Ellipses representing the SEC ranges of current conventional desalination technologies are plotted over the same energy and salinity ranges as in Fig. 3. The theoretical specific minimum energy consumption, E_{min}, is plotted as a function of feed salinity for water recovery ratios $Y = 1$ (dotted black line) and $Y = 0.5$ (dashed black line). Typical seawater salinity (35,000 ppm TDS) and our threshold for hypersalinity (70,000 ppm TDS) are plotted as dot-dot-dash and dot-dash gray lines, respectively. The data is also plotted in Supplementary Material (Fig. S4 and S5) along with effluent salinity, illustrating the water recovery associated with each data point. A table of data and sources is available in Supplementary Material (Table S2).

and can, in principle, handle the hypersaline salt concentration range [191]. Where suitable low-cost land is available, STD can potentially serve as a simple ZLD solution.

The sunlight-to-heat conversion efficiency has been enhanced to as high as 99.8% in recent years [407], and further increases are unlikely to meaningfully improve the overall process. On the other hand, heat that is lost to the surroundings and not utilized for evaporation represents an inefficiency. Evaporator designs can address this issue by confining heat to a thin layer of water at the surface, resulting in higher surface temperatures and lower heat loss [18]. In hypersaline STD, the accumulation of salt on the evaporator is especially problematic as the crystals reflect light and can hinder mass transport [18]. Countermeasures investigated include passive washing of the solar evaporator [407–409], developing evaporators with clog-resistant water transport channels [410–412], and precipitating salts outside of the evaporator [413–415].

Regardless of the advancements in solar absorption, heat localization, and salt buildup mitigation, STD remains energy-intensive. Unless the latent heat released by the condensing vapor is recovered, the SEC is, at best, the enthalpy of water vaporization (≈ 667 kWh$_{th}$/m^3) [180]. Additionally, water productivity of STD is limited by the solar irradiance: with no heat recovery, the area-normalized water production rate is ≈ 1.6 L m^{-2} h^{-1} [191]. Thus, an operationally feasible water production output would require considerable land area. Reusing the latent heat of condensation is, therefore, crucial to improving both SEC and water productivity [191]. A few studies have investigated multi-stage designs for STD [416–420], but only one is focused on hypersaline streams or high water recoveries [419]. Furthermore, most research

employs synthetic NaCl solutions as feeds; investigating STD with saline feeds that contain foulants (e.g., scalants, organics, and microbes) will be key to realizing the technique for treating recalcitrant hypersaline streams [18]. Overall, STD will have to demonstrate cost-competitiveness against hypersaline desalination approaches that use solar energy indirectly, such as photovoltaic-powered mechanical vapor compression [191].

6. Challenges and outlook

Environmental, regulatory, economic, and water scarcity drivers are anticipated to stimulate demand for hypersaline desalination. In order to meet the challenges of high-salinity desalination in a more sustainable manner, existing methods need to be advanced and new techniques developed. Specifically, the technologies must be competitive in energy consumption while simultaneously coping with corrosion, scaling, and other fouling complications. Our survey of the current technological landscape along the dimension of energy consumption, summarized in Fig. 7, suggests that electrodialysis, osmotically-mediated reverse osmosis, and solvent extraction desalination are the alternative and emerging techniques with energy costs that can rival traditional approaches. Data used in Fig. 7 is detailed in Table S2 of the Supplementary Material, and Figs. S4 and S5 present the concentrate salinities (when reported) to illustrate the recovery yields achieved by the emerging technologies. However, the majority of the SECs are from model analyses and bench-scale setups, and almost all of the experimental studies used sodium chloride solutions to simulate hypersaline streams. For these technologies,

Criteria	ED	OMRO	FO	MD	HDH	SED	SCWD	FD	CHD	STD
Primary energy input	⚡	⚡	🔥/🔥	🔥	🔥/🔥	🔥	⚡+🔥	⚡	⚡	🔥
Product water salinity	FFP	FFP	FFP	DW	DW	FFP	DW	FFP	FFP	DW
Industrial-scale demonstration	✓[1]		✓		✓			✓[1]		
ZLD demonstrated					✓	✓	✓			✓
Precipitation in bulk solution					✓[2]	✓	✓			

⚡ = electricity   🔥 = steam   🔥 = low grade heat   ✓ = demonstrated performance

FFP = fit-for-purpose   DW = drinking water

[1] ED demonstrated in brackish water desalination; FD demonstrated in food and beverage industry
[2] Precipitation occurs at solution-air interface, away from solid surfaces

Fig. 8. Graphical summary of the emerging hypersaline desalination technologies along the evaluation metrics of primary energy input, product water salinity, industrial-scale demonstration, ZLD demonstration, and capability to precipitate salts in the bulk solution. Green check marks indicate the technology demonstrated performance of the metric. (For interpretation of the references to colour in this figure legend, the reader is referred to the web version of this article.)

the next steps of advancement would be to validate actual energy requirements in prototype- and pilot-scale systems, and demonstrate the desalination of technically-complex real brines. Other methods that are presently more energy-intensive will benefit from charting out fundamentals-based pathways to achieve lower energy demands. Because the enthalpies of vaporization and fusion are invariable thermodynamic determinants, recovery of the enthalpic energy for multiple reuses is, therefore, pivotal for phase-change approaches.

Fig. 8 presents a graphical summary for the evaluated metrics of energy grade, product water salinity (i.e., compatibility with fit-for-purpose applications), technology demonstration status, zero liquid discharge capability, and ability to precipitate solids in bulk aqueous phase. ED and FD are mature technologies with industrial-scale demonstrations in brackish water desalination and the food and beverage industries, respectively. The operational knowledge these technologies can draw upon will, therefore, place them in a more advantageous position when extending into high-salinity desalination. While industrial-scale demonstrations have been reported for FO, MD, and HDH in high-salinity desalination, know-how accrued from the limited field operations is likely to be not as extensive. As such, these technologies, along with the rest, will face steep learning curves in initial scale-up.

High-salinity streams have highly diverse compositions and constituent impurities. Here, certain desalination technologies can be uniquely suited to treat specific brines or address particular contaminants, even though the techniques may not be the most energy-efficient in general. Approaches that precipitate mineral solids in the bulk aqueous phase, away from heat and mass transfer surfaces (for example, solvent extraction desalination, supercritical water desalination, and humidification-dehumidification), will have an advantage in the desalination of high-scaling propensity feeds, high water recovery yield applications, and zero-liquid discharge operations.

Development of more comprehensive energy metrics will enable greater insights when comparing between different desalination approaches. The industry standard of SEC reports the energy to produce a unit volume of product water. But SEC does not indicate the grade of energy used or reflect factors that determine the inherent difficulties of separation, e.g. feed stream salinity, water recovery yield, and salt rejection. Alternative energy metrics have been proposed, including 1st-law efficiency, 2nd-law efficiency, exergy destruction, and the standard primary energy used for Fig. 3B [103,439,443–446], and efforts should continue to introduce additional complementing standards. Metrics that incorporate the grade and carbon intensity of energy utilized will become increasingly essential as renewable sources continue to replace

fossil fuels in electricity generation [447–456]. Practically all the desalination technologies evaluated in this review exhibit a tradeoff between capital and operating expenditures. Because energy consumption is a major contributor to operating cost, efforts to lower SEC will have to be weighed against the associated increase in capital expense. Technologies that do not utilize high temperatures can potentially sidestep problems caused by the acute corrosiveness of hypersaline brines and allow equipment to be made from lower-cost materials [189,301]. Techno-economic analyses and life cycle impact assessments can provide more inclusive quantification of the balance between overall costs and benefits [94,457–459], to inform the development and implementation of nascent hypersaline technologies.

Almost all existing desalination operations produce potable water (from seawater and brackish groundwater). In contrast, the alternative and emerging technologies operate in different salinity ranges, and the market for fit-for-purpose applications that do not require drinking water quality is budding [7,460,461]. Hence, some of the approaches, particularly those not based on vaporization, can be advantageously more cost-effective for such treatment goals. Conversely, evaporative techniques inherently produce practically salt-free water, but at generally greater costs. Further, the best performing desalination technology is likely to be different at different brine salinities and chemistries. Therefore, overall efficiency and effectiveness can potentially be improved by pairing a technique that is most appropriate for hypersaline desalination but has low salt rejection with another method that works better at relatively lower salinities (such as reverse osmosis, the state-of-the-art for desalination of seawater salinities). Fit-for-purpose water reuse and composite treatment trains may allow greater flexibility in design by bypassing the traditional prerequisite of very high salt rejections to access other advantages, such as scaling- and fouling-resistance, high energy efficiencies at hypersalinity, and compatibility with lower energy grades. On the other hand, evaporative techniques, the prevailing approach for hypersaline desalination, lack this degree of freedom, producing practically salt-free water but at high costs. Lastly, the frequent presence of valuable components at significant concentrations in hypersaline streams, such as lithium [462,463], cesium [464,465], and rubidium [465–467], offers opportunities for valorization [464–466,468,469]. The development of selective recovery techniques can realize the co-production of such resources and enhance the net economics of high-salinity desalination. Mineral recovery and brine valorization have been rigorously analyzed in other review papers and should continue to be a point of strategic research and development efforts [19,78].

Declaration of competing interest

The authors declare the following financial interests/personal relationships which may be considered as potential competing interests: N.Y.Y., K.M.S., I.H.B., and R.K.W. have patent pending to Assignee.

Acknowledgements

Appendix A. Supplementary Material

Supplementary Material to this article can be found online at https://doi.org/10.1016/j.desal.2022.115827.

References

[1] N. Ahmad, R.E. Baddour, A review of sources, effects, disposal methods, and regulations of brine into marine environments, Ocean Coast. Manag. 87 (2014) 1–7, https://doi.org/10.1016/j.ocecoaman.2013.10.020.

[2] D.L. Shaffer, L.H. Arias Chavez, M. Ben-Sasson, S. Romero-Vargas Castrillón, N.Y. Yip, M. Elimelech, Desalination and reuse of high-salinity shale gas produced water: drivers, technologies, and future directions, Environ. Sci. Technol. 47 (2013) 9569–9583, https://doi.org/10.1021/es401966e.

[3] P.V. Brady, R.J. Kottenstette, T.M. Mayer, M.M. Hightower, Inland desalination: challenges and research needs, J. Contemp. WaterRes. Educ. 132 (2005), https://doi.org/10.1111/j.1936-704X.2005.mp132001007.x.

[4] M. Mickley, Membrane Concentrate Disposal: Practices and Regulation, Final Report, U.S. Department of the Interior, Bureau of Reclamation, Technical Service Center, Water Treatment Engineering and Research Group, 2001.

[5] National Research Council, D. on E. and L. Studies, W.S. and T. Board, C. on A.D. Technology, Desalination: A National Perspective, National Academies Press, 2008.

[6] J.M. Estrada, R. Bhamidimarri, A review of the issues and treatment options for wastewater from shale gas extraction by hydraulic fracturing, Fuel 182 (2016) 292–303, https://doi.org/10.1016/j.fuel.2016.05.051.

[7] M.S. Mauter, P.S. Fiske, Desalination for a circular water economy, Energy Environ. Sci. 13 (2020) 3180–3184, https://doi.org/10.1039/D0EE01653E.

[8] M. Mickley, WateReuse Foundation, Survey of High-recovery and Zero Liquid Discharge Technologies for Water Utilities, WateReuse Foundation, Alexandria, Va, 2008.

[9] M.M. Pendergast, M.S. Nowosielski-Slepowron, J. Tracy, Going big with forward osmosis, Desalin. Water Treat. 57 (2016) 26529–26538, https://doi.org/10.1080/19443994.2016.1168581.

[10] C. Boo, R.K. Winton, K.M. Conway, N.Y. Yip, Membrane-less and non-evaporative desalination of hypersaline brines by temperature swing solvent extraction, Environ. Sci. Technol. Lett. 6 (2019) 359–364, https://doi.org/10.1021/acs.estlett.9b00182.

[11] A.A. Atia, N.Y. Yip, V. Fthenakis, Pathways for minimal and zero liquid discharge with enhanced reverse osmosis technologies: module-scale modeling and techno-economic assessment, Desalination 509 (2021), 115069, https://doi.org/10.1016/j.desal.2021.115069.

[12] J. Kim, H. Kwon, S. Lee, S. Lee, S. Hong, Membrane distillation (MD) integrated with crystallization (MDC) for shale gas produced water (SGPW) treatment, Desalination 403 (2017) 172–178, https://doi.org/10.1016/j.desal.2016.07.045.

[13] R.K. McGovern, A.M. Weiner, L. Sun, C.G. Chambers, S.M. Zubair, J.H. Lienhard V, On the cost of electrodialysis for the desalination of high salinity feeds, Appl. Energy 136 (2014) 649–661, https://doi.org/10.1016/j.apenergy.2014.09.050.

[14] H. Yan, Y. Wang, L. Wu, M.A. Shehzad, C. Jiang, R. Fu, Z. Liu, T. Xu, Multistage-batch electrodialysis to concentrate high-salinity solutions: process optimisation, water transport, and energy consumption, J. Membr. Sci. 570–571 (2019) 245–257, https://doi.org/10.1016/j.memsci.2018.10.008.

[15] S.O. Odu, A.G.J. van der Ham, S. Metz, S.R.A. Kersten, Design of a Process for supercritical water desalination with zero liquid discharge, Ind. Eng. Chem. Res. 54 (2015) 5527–5535, https://doi.org/10.1021/acs.iecr.5b00826.

[16] P.M. Williams, M. Ahmad, B.S. Connolly, D.L. Oatley-Radcliffe, Technology for freeze concentration in the desalination industry, Desalination 356 (2015) 314–327, https://doi.org/10.1016/j.desal.2014.10.023.

[17] A. Hassanpouryouzband, E. Joonaki, M.V. Farahani, S. Takeya, C. Ruppel, J. Yang, N.J. English, J.M. Schicks, K. Edlmann, H. Mehrabian, Z.M. Aman, B. Tohidi, Gas hydrates in sustainable chemistry, Chem. Soc. Rev. (2020) https://doi.org/10.1039/C8CS00989A.

[18] L. Zang, C. Finnerty, S. Zheng, K. Conway, L. Sun, J. Ma, B. Mi, Interfacial solar vapor generation for desalination and brine treatment: evaluating current strategies of solving scaling, Water Res. 198 (2021), 117135, https://doi.org/10.1016/j.watres.2021.117135.

[19] A.S. Bello, N. Zouari, D.A. Da'ana, J.N. Hahladakis, M.A. Al-Ghouti, An overview of brine management: emerging desalination technologies, life cycle assessment, and metal recovery methodologies, J. Environ. Manag. 288 (2021), 112358, https://doi.org/10.1016/j.jenvman.2021.112358.

[20] A. Panagopoulos, K.-J. Haralambous, M. Loizidou, Desalination brine disposal methods and treatment technologies - a review, Sci. Total Environ. 693 (2019) 133545, https://doi.org/10.1016/j.scitotenv.2019.07.351.

[21] L.M. Vane, Water recovery from brines and salt-saturated solutions: operability and thermodynamic efficiency considerations for desalination technologies, J. Chem. Technol. 92 (2017) 2506–2518, https://doi.org/10.1002/jctb.5225.

[22] F.E. Ahmed, R. Hashaikeh, N. Hilal, Hybrid technologies: the future of energy efficient desalination – a review, Desalination 495 (2020), 114659, https://doi.org/10.1016/j.desal.2020.114659.

[23] N.A. Ahmad, P.S. Goh, L.T. Yogarathinam, A.K. Zulhairun, A.F. Ismail, Current advances in membrane technologies for produced water desalination, Desalination 493 (2020), 114643, https://doi.org/10.1016/j.desal.2020.114643.

[24] E. Jones, M. Qadir, M.T.H. van Vliet, V. Smakhtin, S. Kang, The state of desalination and brine production: a global outlook, Sci. Total Environ. 657 (2019) 1343–1356, https://doi.org/10.1016/j.scitotenv.2018.12.076.

[25] C.E. Clark, J.A. Veil, Produced Water Volumes and Management Practices in the United States, Argonne National Lab. (ANL), Argonne, IL (United States), 2009, https://doi.org/10.2172/1007397.

[26] C.L. Conrad, Y. Ben Yin, T. Hanna, A.J. Atkinson, P.J.J. Alvarez, T.N. Tekavec, M.A. Reynolds, M.S. Wong, Fit-for-purpose treatment goals for produced waters in shale oil and gas fields, Water Res. 173 (2020), 115467, https://doi.org/10.1016/j.watres.2020.115467.

[27] A. Fakhru'l-Razi, A. Pendashteh, L.C. Abdullah, D.R.A. Biak, S.S. Madaeni, Z.Z. Abidin, Review of technologies for oil and gas produced water treatment, J. Hazard. Mater. 170 (2009) 530–551, https://doi.org/10.1016/j.jhazmat.2009.05.044.

[28] G.E. Ericksen, J.D. Vine, Chemical composition and distribution of lithium-rich brines in Salar de Uyuni and nearby salars in Southwestern Bolivia, in: S.S. Penner (Ed.), Lithium Needs and Resources, Pergamon, 1978, pp. 355–363, https://doi.org/10.1016/B978-0-08-022733-7.50020-4.

[29] B. Ericsson, B. Hallmans, Treatment and disposal of saline wastewater from coal mines in Poland, Desalination 98 (1994) 239–248, https://doi.org/10.1016/0011-9164(94)00148-0.

[30] Q. Feng, T. Li, B. Qian, L. Zhou, B. Gao, T. Yuan, Chemical characteristics and utilization of coal mine drainage in China, Mine Water Environ. 33 (2014) 276–286, https://doi.org/10.1007/s10230-014-0271-y.

[31] H.E. Ben Ali, C.M. Neculita, J.W. Molson, A. Maqsoud, G.J. Zagury, Performance of passive systems for mine drainage treatment at low temperature and high salinity: a review, Miner. Eng. 134 (2019) 325–344, https://doi.org/10.1016/j.mineng.2019.02.010.

[32] J. Lin, W. Ye, H. Zeng, H. Yang, J. Shen, S. Darvishmanesh, P. Luis, A. Sotto, B. Van der Bruggen, Fractionation of direct dyes and salts in aqueous solution using loose nanofiltration membranes, J. Membr. Sci. 477 (2015) 183–193, https://doi.org/10.1016/j.memsci.2014.12.008.

[33] T. Stephenson, Characterisation of textile wastewaters - a review, Environ. Technol. 15 (1994) 917–929, https://doi.org/10.1080/09593339409385500.

[34] Y. He, G.-M. Li, H. Wang, Z.-W. Jiang, J.-F. Zhao, H.-X. Su, Q.-Y. Huang, Experimental study on the rejection of salt and dye with cellulose acetate nanofiltration membrane, J. Taiwan Inst. Chem. Eng. 40 (2009) 289–295, https://doi.org/10.1016/j.jtice.2008.08.008.

[35] M.C. Kannaujiya, T. Mandal, D.D. Mandal, M.K. Mondal, Treatment of leather industry wastewater and recovery of valuable substances to solve waste management problem in environment, in: R.N. Bharagava (Ed.), Environmental Contaminants: Ecological Implications and Management, Springer, Singapore, 2019, pp. 311–340, https://doi.org/10.1007/978-981-13-7904-8_14.

[36] S. Sundarapandiyan, R. Chandrasekar, B. Ramanaiah, S. Krishnan, P. Saravanan, Electrochemical oxidation and reuse of tannery saline wastewater, J. Hazard. Mater. 180 (2010) 197–203, https://doi.org/10.1016/j.jhazmat.2010.04.013.

[37] V. Sivakumar, V. John Sundar, T. Rangasamy, C. Muralidharan, G. Swaminathan, Management of total dissolved solids in tanning process through improved techniques, J. Clean. Prod. 13 (2005) 699–703, https://doi.org/10.1016/j.jclepro.2004.01.006.

[38] W.L. Bourcier, T.J. Wolery, T. Wolfe, C. Haussmann, T.A. Buscheck, R.D. Aines, A preliminary cost and engineering estimate for desalinating produced formation water associated with carbon dioxide capture and storage, Int. J. Greenh. Gas Control. 5 (2011) 1319–1328, https://doi.org/10.1016/j.ijggc.2011.06.001.

[39] H. Wang, L. Zhang, H. Lei, Y. Wang, H. Liu, X. Li, X. Su, Potential for uranium release under geologic CO2 storage conditions: the impact of Fe(III), Int. J. Greenhouse Gas Control 107 (2021), 103266, https://doi.org/10.1016/j.ijggc.2021.103266.

[40] D. Zarzo, 11 - Beneficial uses and valorization of reverse osmosis brines, in: V.G. Gude (Ed.), Emerging Technologies for Sustainable Desalination Handbook, Butterworth-Heinemann, 2018, pp. 365–397, https://doi.org/10.1016/B978-0-12-815818-0.00011-4 (accessed May 19, 2020).

[41] S. Klas, Y. Peretz, Fish survival in groundwater-desalination concentrate, Aquac. Eng. 88 (2020), https://doi.org/10.1016/j.aquaeng.2019.102037.

[42] R. Xiong, C. Wei, Current status and technology trends of zero liquid discharge at coal chemical industry in China, J. Water Process Eng. 19 (2017) 346–351, https://doi.org/10.1016/j.jwpe.2017.09.005.

[43] J. Shi, W. Huang, H. Han, C. Xu, Review on treatment technology of salt wastewater in coal chemical industry of China, Desalination 493 (2020), 114640, https://doi.org/10.1016/j.desal.2020.114640.

[44] B. Chen, S. Yang, Q. Cao, Y. Qian, Life cycle economic assessment of coal chemical wastewater treatment facing the 'zero liquid discharge' industrial water policies in China: discharge or reuse? Energy Policy 137 (2020), 111107 https://doi.org/10.1016/j.enpol.2019.111107.

[45] Steam Electric Power Generating Point Source Category: Final Detailed Study Report, United States Environmental Protection Agency, 2009.

[46] D.B. Gingerich, M.S. Mauter, Flue gas desulfurization wastewater composition and implications for regulatory and treatment train design, Environ. Sci. Technol. 54 (2020) 3783–3792, https://doi.org/10.1021/acs.est.9b07433.

[47] R.B. Brennan, M.G. Healy, L. Morrison, S. Hynes, D. Norton, E. Clifford, Management of landfill leachate: the legacy of European Union Directives, Waste Manag. 55 (2016) 355–363, https://doi.org/10.1016/j.wasman.2015.10.010.

[48] C.M. Moody, T.G. Townsend, A comparison of landfill leachates based on waste composition, Waste Manag. 63 (2017) 267–274, https://doi.org/10.1016/j.wasman.2016.09.020.

[49] C. Pavelka, R.C. Loehr, B. Haikola, Hazardous waste landfill leachate characteristics, Waste Manag. 13 (1993) 573–580, https://doi.org/10.1016/0956-053X(93)90017-Q.

[50] E. Chapman, R. Capo, B. Stewart, C. Kirby, R. Hammack, K. Schroeder, H. Edenborn, Geochemical and strontium isotope characterization of produced waters from Marcellus Shale natural gas extraction, Environ. Sci. Technol. 46 (2012) 3545–3553, https://doi.org/10.1021/es204005g.

[51] G.A. Kahrilas, J. Blotevogel, P.S. Stewart, T. Borch, Biocides in hydraulic fracturing fluids: a critical review of their usage, mobility, degradation, and toxicity, Environ. Sci. Technol. 49 (2015) 16–32, https://doi.org/10.1021/es503724k.

[52] S.J. Maguire-Boyle, A.R. Barron, Organic compounds in produced waters from shale gas wells, Environ. Sci.: Processes Impacts 16 (2014) 2237–2248, https://doi.org/10.1039/C4EM00376D.

[53] D.E. Garrett, Borates: Handbook of Deposits, Processing, Properties, and Use, Elsevier, 1998.

[54] E.L. Bray, Magnesium, U.S. Geological Survey, 2020. https://pubs.usgs.gov/periodicals/mcs2020/mcs2020.pdf. (Accessed 7 January 2020).

[55] W.H. Eatock, Advances in potassium mining and refining, in: Potassium in Agriculture, John Wiley & Sons, Ltd, 1985, pp. 29–48, https://doi.org/10.2134/1985.potassium.c2.

[56] V. Flexer, C.F. Baspineiro, C.I. Galli, Lithium recovery from brines: a vital raw material for green energies with a potential environmental impact in its mining and processing, Sci. Total Environ. 639 (2018) 1188–1204, https://doi.org/10.1016/j.scitotenv.2018.05.223.

[57] J. Lin, F. Lin, X. Chen, W. Ye, X. Li, H. Zeng, B. Van der Bruggen, Sustainable management of textile wastewater: a hybrid tight ultrafiltration/bipolar-membrane electrodialysis process for resource recovery and zero liquid discharge, Ind. Eng. Chem. Res. 58 (2019) 11003–11012, https://doi.org/10.1021/acs.iecr.9b01353.

[58] T.V. Bartholomew, M.S. Mauter, Energy and CO2 emissions penalty ranges for geologic carbon storage brine management, Environ. Sci. Technol. 55 (2021) 4305–4313, https://doi.org/10.1021/acs.est.0c06017.

[59] X. Li, D. Hasson, R. Semiat, H. Shemer, Intermediate concentrate demineralization techniques for enhanced brackish water reverse osmosis water recovery – a review, Desalination 466 (2019) 24–35, https://doi.org/10.1016/j.desal.2019.05.004.

[60] A. He, G.Wetterau Subramani, V. Veerapaneni, 2. Water quality and planning strategies (accessed January 8, 2021), in: Inland Desalination & Concentrate Management, American Water Works Association, 2019.

[61] M. Ahmed, W.H. Shayya, D. Hoey, J. Al-Handaly, Brine disposal from reverse osmosis desalination plants in Oman and the United Arab Emirates, Desalination 133 (2001) 135–147, https://doi.org/10.1016/S0011-9164(01)80004-7.

[62] J. Morillo, J. Usero, D. Rosado, H. El Bakouri, A. Riaza, F.-J. Bernaola, Comparative study of brine management technologies for desalination plants, Desalination 336 (2014) 32–49, https://doi.org/10.1016/j.desal.2013.12.038.

[63] A. Giwa, V. Dufour, F. Al Marzooqi, M. Al Kaabi, S.W. Hasan, Brine management methods: recent innovations and current status, Desalination 407 (2017) 1–23, https://doi.org/10.1016/j.desal.2016.12.008.

[64] P.C. Singer, F.K. Pfaender, J. Chinchilli, A.F. Maciorowski, I.I.I. Lamb, Assessment of coal conversion wastewaters: characterization and preliminary biotreatability. Report for November 1976-May 1978, North Carolina Univ., Chapel Hill (USA). Dept. of Environmental Sciences and Engineering, 1978 (accessed January 8, 2021), https://www.osti.gov/biblio/5701670.

[65] D.B. Gingerich, E. Grol, M.S. Mauter, Fundamental challenges and engineering opportunities in flue gas desulfurization wastewater treatment at coal fired power plants, Environ. Sci.: Water Res. Technol. 4 (2018) 909–925, https://doi.org/10.1039/C8EW00264A.

[66] S.K. Maiti, S. De, T. Hazra, A. Debsarkar, A. Dutta, Characterization of leachate and its impact on surface and groundwater quality of a closed dumpsite – a case study at Dhapa, Kolkata, India, Procedia Environ. Sci. 35 (2016) 391–399, https://doi.org/10.1016/j.proenv.2016.07.019.

[67] D.E. Meeroff, J. Lakner, B. Shaha, E. Walecki, A. Harris, L. Meyer, in: Futuristic On-Site Leachate Management, 2016, pp. 1–10, https://doi.org/10.1061/9780784479865.001.

[68] Y. Abu-Rukah, O. Al-Kofahi, The assessment of the effect of landfill leachate on ground-water quality—a case study. El-Akader landfill site—north Jordan, J. Arid Environ. 49 (2001) 615–630, https://doi.org/10.1006/jare.2001.0796.

[69] B. Bhalla, M.S. Saini, M.K. Jha, Effect of age and seasonal variations on leachate characteristics of municipal solid waste landfill, Int. J. Res. Eng. 2 (2013) 223–232, https://doi.org/10.15623/ijret.2013.0208037.

[70] L.R. Scharfstein, W.F. Brindley, Chloride stress corrosion cracking of austenitic stainless steel—effect of temperature and pH, Corrosion 14 (1958) 60–64, https://doi.org/10.5006/0010-9312-14.12.60.

[71] J.A. Bush, J. Vanneste, T.Y. Cath, Membrane distillation for concentration of hypersaline brines from the Great Salt Lake: effects of scaling and fouling on performance, efficiency, and salt rejection, Sep. Purif. Technol. 170 (2016) 78–91, https://doi.org/10.1016/j.seppur.2016.06.028.

[72] M. Herzberg, M. Elimelech, Biofouling of reverse osmosis membranes: role of biofilm-enhanced osmotic pressure, J. Membr. Sci. 295 (2007) 11–20, https://doi.org/10.1016/j.memsci.2007.02.024.

[73] A.H. Taheri, L.N. Sim, C.T. Haur, E. Akhondi, A.G. Fane, The fouling potential of colloidal silica and humic acid and their mixtures, J. Membr. Sci. 433 (2013) 112–120, https://doi.org/10.1016/j.memsci.2013.01.034.

[74] A. Burbano, P. Brandhuber, Demonstration of Membrane Zero Liquid Discharge for Drinking Water System: Literature Review, Water Resource Foundation, 2012.

[75] S.J. Khan, D. Murchland, M. Rhodes, T.D. Waite, Management of concentrated waste streams from high-pressure membrane water treatment systems, Crit. Rev. Environ. Sci. Technol. 39 (2009) 367–415, https://doi.org/10.1080/10643380701635904.

[76] Z. Salem, K. Hamouri, R. Djemaa, K. Allia, Evaluation of landfill leachate pollution and treatment, Desalination 220 (2008) 108–114, https://doi.org/10.1016/j.desal.2007.01.026.

[77] B.K. Pramanik, L. Shu, V. Jegatheesan, A review of the management and treatment of brine solutions, Environ. Sci.: Water Res. Technol. 3 (2017) 625–658, https://doi.org/10.1039/c6ew00339g.

[78] O. Ogunbiyi, J. Saththasivam, D. Al-Masri, Y. Manawi, J. Lawler, X. Zhang, Z. Liu, Sustainable brine management from the perspectives of water, energy and mineral recovery: a comprehensive review, Desalination 513 (2021), 115055, https://doi.org/10.1016/j.desal.2021.115055.

[79] A. Vengosh, R.B. Jackson, N. Warner, T.H. Darrah, A. Kondash, A critical review of the risks to water resources from unconventional shale gas development and hydraulic fracturing in the United States, Environ. Sci. Technol. 48 (2014) 8334–8348, https://doi.org/10.1021/es405118y.

[80] T. Zhang, R.W. Hammack, R.D. Vidic, Fate of Radium in Marcellus Shale Flowback Water Impoundments and Assessment of Associated Health Risks, Environ. Sci. Technol. 49 (2015) 9347–9354, https://doi.org/10.1021/acs.est.5b01393.

[81] Evaporator treats landfill leachate, Water Desalin. Rep. 57 (2021) 1.

[82] B.D. Lutz, A.N. Lewis, M.W. Doyle, Generation, transport, and disposal of wastewater associated with Marcellus Shale gas development, Water Resour. Res. 49 (2013) 647–656, https://doi.org/10.1002/wrcr.20096.

[83] S. Bolyard, State of Practice of Landfill Leachate Management and Treatment in the US, 2018.

[84] T. Tong, M. Elimelech, The global rise of zero liquid discharge for wastewater management: drivers, technologies, and future directions, Environ. Sci. Technol. 50 (2016) 6846–6855, https://doi.org/10.1021/acs.est.6b01000.

[85] A. Echchelh, T. Hess, R. Sakrabani, Reusing oil and gas produced water for irrigation of food crops in drylands, Agric. Water Manag. 206 (2018) 124–134, https://doi.org/10.1016/j.agwat.2018.05.006.

[86] B. Durham, M. Mierzejewski, Water reuse and zero liquid discharge: a sustainable water resource solution, Water Supply 3 (2003) 97–103, https://doi.org/10.2166/ws.2003.0050.

[87] Muhammad Yaqub, W. Lee, Zero-liquid discharge (ZLD) technology for resource recovery from wastewater: a review, Sci. Total Environ. 681 (2019) 551–563, https://doi.org/10.1016/j.scitotenv.2019.05.062.

[88] R. Bond, Zeroing in on ZLD technologies for inland desalination, J. AWWA 100 (2008) 76–89, https://doi.org/10.1002/j.1551-8833.2008.tb09722.x.

[89] X. Han, D. Zhang, J. Yan, S. Zhao, J. Liu, Process development of flue gas desulphurization wastewater treatment in coal-fired power plants towards zero liquid discharge: energetic, economic and environmental analyses, J. Clean. Prod. 261 (2020), 121144, https://doi.org/10.1016/j.jclepro.2020.121144.

[90] V.C. Onishi, E.S. Fraga, J.A. Reyes-Labarta, J.A. Caballero, 12 - Desalination of shale gas wastewater: thermal and membrane applications for zero-liquid discharge, in: V.G. Gude (Ed.), Emerging Technologies for Sustainable Desalination Handbook, Butterworth-Heinemann, 2018, pp. 399–431, https://doi.org/10.1016/B978-0-12-815818-0.00012-6 (accessed February 11, 2021).

[91] Y. Oren, E. Korngold, N. Daltrophe, R. Messalem, Y. Volkman, L. Aronov, M. Weismann, N. Bouriakov, P. Glueckstern, J. Gilron, Pilot studies on high recovery BWRO-EDR for near zero liquid discharge approach, Desalination 261 (2010) 321–330, https://doi.org/10.1016/j.desal.2010.06.010.

[92] A. Pérez-González, A.M. Urtiaga, R. Ibáñez, I. Ortiz, State of the art and review on the treatment technologies of water reverse osmosis concentrates, Water Res. 46 (2012) 267–283, https://doi.org/10.1016/j.watres.2011.10.046.

[93] A. Subramani, M. Badruzzaman, J. Oppenheimer, J.G. Jacangelo, Energy minimization strategies and renewable energy utilization for desalination: a review, Water Res. 45 (2011) 1907–1920, https://doi.org/10.1016/j.watres.2010.12.032.

[94] T. Mezher, H. Fath, Z. Abbas, A. Khaled, Techno-economic assessment and environmental impacts of desalination technologies, Desalination 266 (2011) 263–273, https://doi.org/10.1016/j.desal.2010.08.035.

[95] A. Panagiotopoulos, Essential Thermodynamics, Drios Press, 2014.

[96] K.S. Pitzer, Thermodynamics of electrolytes. I. Theoretical basis and general equations, J. Phys. Chem. 77 (1873) 268–277, https://doi.org/10.1021/j100621a026.

[97] K.S. Pitzer, G. Mayorga, Thermodynamics of electrolytes. II. Activity and osmotic coefficients for strong electrolytes with one or both ions univalent, J. Phys. Chem. 77 (1973) 2300–2308, https://doi.org/10.1021/j100638a009.

[98] K.S. Pitzer, J.C. Peiper, R.H. Busey, Thermodynamic properties of aqueous sodium chloride solutions, J. Phys. Chem. Ref. Data 13 (1984) 1–102, https://doi.org/10.1063/1.555709.

[99] J. Kim, K. Park, D.R. Yang, S. Hong, A comprehensive review of energy consumption of seawater reverse osmosis desalination plants, Appl. Energy 254 (2019), 113652, https://doi.org/10.1016/j.apenergy.2019.113652.

[100] M. Elimelech, W.A. Phillip, The future of seawater desalination: energy, technology, and the environment, Science 333 (2011) 712–717, https://doi.org/10.1126/science.1200488.

[101] J.H. Perry, Chemical Engineers' Handbook, 8th ed., McGraw-Hill, 2008.

[102] S.I. Sandler, Chemical, Biochemical, and Engineering Thermodynamics, John Wiley & Sons, 2017.

[103] K.H. Mistry, R.K. McGovern, G.P. Thiel, E.K. Summers, S.M. Zubair, J. H. Lienhard, Entropy generation analysis of desalination technologies, Entropy 13 (2011) 1829–1864, https://doi.org/10.3390/e13101829.

[104] A. Panagopoulos, A comparative study on minimum and actual energy consumption for the treatment of desalination brine, Energy 212 (2020) 118733, https://doi.org/10.1016/j.energy.2020.118733.

[105] Frequently Asked Questions (FAQs) - U.S. Energy Information Administration (EIA), (n.d.). /tools/faqs/index.php (accessed May 9, 2021).

[106] K.C. Ng, M. Burhan, Q. Chen, D. Ybyraiymkul, F.H. Akhtar, M. Kumja, R.W. Field, M.W. Shahzad, A thermodynamic platform for evaluating the energy efficiency of combined power generation and desalination plants, Npj Clean Water 4 (2021) 1–10, https://doi.org/10.1038/s41545-021-00114-5.

[107] H. Dahmardeh, H.A. Akhlaghi Amiri, S.M. Nowee, Evaluation of mechanical vapor recompression crystallization process for treatment of high salinity wastewater, Chem. Eng. Process. Process Intensif. 145 (2019), 107682, https://doi.org/10.1016/j.cep.2019.107682.

[108] Z. Zimerman, Development of large capacity high efficiency mechanical vapor compression (MVC) units, Desalination 96 (1994) 51–58, https://doi.org/10.1016/0011-9164(94)85156-5.

[109] L. Liang, D. Han, R. Ma, T. Peng, Treatment of high-concentration wastewater using double-effect mechanical vapor recompression, Desalination 314 (2013) 139–146, https://doi.org/10.1016/j.desal.2013.01.016.

[110] H. Ettouney, Design of single-effect mechanical vapor compression, Desalination 190 (2006) 1–15, https://doi.org/10.1016/j.desal.2005.08.003.

[111] R. Matz, U. Fisher, A comparison of the relative economics of sea water desalination by vapour compression and reverse osmosis for small to medium capacity plants, Desalination 36 (1981) 137–151, https://doi.org/10.1016/S0011-9164(00)88637-3.

[112] G. Kronenberg, F. Lokiec, Low-temperature distillation processes in single- and dual-purpose plants, Desalination 136 (2001) 189–197, https://doi.org/10.1016/S0011-9164(01)00181-3.

[113] N.H. Aly, A.K. El-Figi, Mechanical vapor compression desalination systems — a case study, Desalination 158 (2003) 143–150, https://doi.org/10.1016/S0011-9164(03)00444-2.

[114] M. Turek, P. Dydo, R. Klimek, Salt production from coal-mine brine in ED–evaporation–crystallization system, Desalination 184 (2005) 439–446, https://doi.org/10.1016/j.desal.2005.03.047.

[115] B. Ericsson, B. Hallmans, Treatment of saline wastewater for zero discharge at the Debiensko coal mines in Poland, Desalination 105 (1996) 115–123, https://doi.org/10.1016/0011-9164(96)00065-3.

[116] M. Lucas, B. Tabourier, The mechanical vapour compression process applied to seawater desalination: a 1,500 ton/day unit installed in the nuclear power plant of Flamanville, France, Desalination 52 (1985) 123–133, https://doi.org/10.1016/0011-9164(85)85003-7.

[117] P. Malek, J.M. Ortiz, H.M.A. Schulte-Herbrüggen, Decentralized desalination of brackish water using an electrodialysis system directly powered by wind energy, Desalination 377 (2015) 54–64, https://doi.org/10.1016/j.desal.2015.08.023.

[118] M. Demircioglu, N. Kabay, I. Kurucaovali, E. Ersoz, Demineralization by electrodialysis (ED) — separation performance and cost comparison for monovalent salts, Desalination 153 (2003) 329–333, https://doi.org/10.1016/S0011-9164(02)01119-0.

[119] K. Walha, R.B. Amar, L. Firdaous, F. Quéméneur, P. Jaouen, Brackish groundwater treatment by nanofiltration, reverse osmosis and electrodialysis in Tunisia: performance and cost comparison, Desalination 207 (2007) 95–106, https://doi.org/10.1016/j.desal.2006.03.583.

[120] G.J. Doornbusch, M. Tedesco, J.W. Post, Z. Borneman, K. Nijmeijer, Experimental investigation of multistage electrodialysis for seawater desalination, Desalination 464 (2019) 105–114, https://doi.org/10.1016/j.desal.2019.04.025.

[121] J.M. Ortiz, E. Expósito, F. Gallud, V. García-García, V. Montiel, A. Aldaz, Desalination of underground brackish waters using an electrodialysis system powered directly by photovoltaic energy, Sol. Energy Mater. Sol. Cells 92 (2008) 1677–1688, https://doi.org/10.1016/j.solmat.2008.07.020.

[122] W.P. Harkare, S.K. Adhikary, P.K. Narayanan, V.B. Bhayani, N.J. Dave, K. P. Govindan, Desalination of brackish water by electrodialysis, Desalination 42 (1982) 97–105, https://doi.org/10.1016/S0011-9164(00)88745-7.

[123] C.C.N. Kunrath, D.C. Patrocínio, M.A. Siqueira Rodrigues, T. Benvenuti, F.D. R. Amado, Electrodialysis reversal as an alternative treatment for producing drinking water from brackish river water: a case study in the dry season, northeastern Brazil, J. Environ Chem. Eng. 8 (2020), 103719, https://doi.org/10.1016/j.jece.2020.103719.

[124] G. Doornbusch, M. van der Wal, M. Tedesco, J. Post, K. Nijmeijer, Z. Borneman, Multistage electrodialysis for desalination of natural seawater, Desalination 505 (2021), 114973, https://doi.org/10.1016/j.desal.2021.114973.

[125] M. Turek, Cost effective electrodialytic seawater desalination, Desalination 153 (2003) 371–376, https://doi.org/10.1016/S0011-9164(02)01130-X.

[126] P. Fernández-Izquierdo, L. García-Rodríguez, D.-C. Alarcón-Padilla, P. Palenzuela, I. Martín-Mateos, Experimental analysis of a multi-effect distillation unit operated out of nominal conditions, Desalination 284 (2012) 233–237, https://doi.org/10.1016/j.desal.2011.09.004.

[127] A. Chorak, P. Palenzuela, D.-C. Alarcón-Padilla, A. Ben Abdellah, Experimental characterization of a multi-effect distillation system coupled to a flat plate solar collector field: empirical correlations, Appl. Therm. Eng. 120 (2017) 298–313, https://doi.org/10.1016/j.applthermaleng.2017.03.115.

[128] A.M. El-Nashar, Predicting part load performance of small MED evaporators - a simple simulation program and its experimental verification, Desalination 130 (2000) 217–234, https://doi.org/10.1016/S0011-9164(00)00088-6.

[129] M. Al-Shammiri, M. Safar, Multi-effect distillation plants: state of the art, Desalination 126 (1999) 45–59, https://doi.org/10.1016/S0011-9164(99)00154-X.

[130] D.M.K. Al-Gobaisi, A quarter-century of seawater desalination by large multistage flash plants in Abu Dhabi (plant performance analysis, assessment, present efforts toward enhancement and future hopes), Desalination 99 (1994) 509–512, https://doi.org/10.1016/0011-9164(94)00196-0.

[131] A.M.K. El-Ghonemy, Performance test of a sea water multi-stage flash distillation plant: case study, Alex. Eng. J. 57 (2018) 2401–2413, https://doi.org/10.1016/j.aej.2017.08.019.

[132] O.A. Hamed, M.A.K. Al-Sofi, M. Imam, G.M. Mustafa, K. Ba Mardouf, H. Al-Washmi, Thermal performance of multi-stage flash distillation plants in Saudi Arabia, Desalination 128 (2000) 281–292, https://doi.org/10.1016/S0011-9164(00)00043-6.

[133] M.A.-K. Al-Sofi, M.A. Al-Hussain, A.A.-A. Al-Omran, K.M. Farran, A full decade of operating experience on Al-Khobar-II multi-stage flash (MSF) evaporators (1982–1992), Desalination 96 (1994) 313–323, https://doi.org/10.1016/0011-9164(94)85182-4.

[134] S. Al-Hengari, M. El-Bousiffi, W. El-Mudir, Performance analysis of a MSF desalination unit, Desalination 182 (2005) 73–85, https://doi.org/10.1016/j.desal.2005.03.010.

[135] M.W. Shahzad, M. Burhan, K.C. Ng, A standard primary energy approach for comparing desalination processes, Npj Clean Water 2 (2019) 1–7.

[136] M.W. Shahzad, M. Burhan, D. Ybyraiymkul, K.C. Ng, Desalination processes'' efficiency and future roadmap, Entropy 21 (2019) 84, https://doi.org/10.3390/e21010084.

[137] C. Fritzmann, J. Löwenberg, T. Wintgens, T. Melin, State-of-the-art of reverse osmosis desalination, Desalination 216 (2007) 1–76, https://doi.org/10.1016/j.desal.2006.12.009.

[138] L.F. Greenlee, D.F. Lawler, B.D. Freeman, B. Marrot, P. Moulin, Reverse osmosis desalination: water sources, technology, and today's challenges, J. Water Res. 43 (2009) 2317–2348, https://doi.org/10.1016/j.watres.2009.03.010.

[139] R.W. Baker, Membrane Technology and Applications, John Wiley & Sons, 2012.

[140] M. Qasim, M. Badrelzaman, N.N. Darwish, N.A. Darwish, N. Hilal, Reverse osmosis desalination: a state-of-the-art review, Desalination 459 (2019) 59–104, https://doi.org/10.1016/j.desal.2019.02.008.

[141] Y. Cohen, R. Semiat, A. Rahardianto, A perspective on reverse osmosis water desalination: quest for sustainability, AIChE J. 63 (2017) 1771–1784.

[142] J.D. Seader, E.J. Henley, Separation Process Principles, 2nd ed., Wiley, Hoboken, N.J, 2006.

[143] K.S. Spiegler, A.D.K. Laird, Principles of Desalination, Academic Press, 1980.

[144] M. Shatat, S.B. Riffat, Water desalination technologies utilizing conventional and renewable energy sources, Int. J. Low Carbon Technol. 9 (2014) 1–19, https://doi.org/10.1093/ijlct/cts025.

[145] A.D. Khawaji, I.K. Kutubkhanah, J.-M. Wie, Advances in seawater desalination technologies, Desalination 221 (2008) 47–69, https://doi.org/10.1016/j.desal.2007.01.067.

[146] A. Subramani, J.G. Jacangelo, Treatment technologies for reverse osmosis concentrate volume minimization: a review, Sep. Purif. Technol. 122 (2014) 472–489, https://doi.org/10.1016/j.seppur.2013.12.004.

[147] H.T. El-Dessouky, H.M. Ettouney, Y. Al-Roumi, Multi-stage flash desalination: present and future outlook, Chem. Eng. J. 73 (1999) 173–190, https://doi.org/10.1016/S1385-8947(99)00035-2.

[148] A. Al-Karaghouli, L.L. Kazmerski, Energy consumption and water production cost of conventional and renewable-energy-powered desalination processes, Renew. Sust. Energ. Rev. 24 (2013) 343–356, https://doi.org/10.1016/j.rser.2012.12.064.

[149] H. Guo, H.M. Ali, A. Hassanzadeh, Simulation study of flat-sheet air gap membrane distillation modules coupled with an evaporative crystallizer for zero liquid discharge water desalination, Appl. Therm. Eng. 108 (2016) 486–501, https://doi.org/10.1016/j.applthermaleng.2016.07.131.

[150] Q. Chen, M. Burhan, M.W. Shahzad, D. Ybyraiymkul, F.H. Akhtar, Y. Li, K.C. Ng, A zero liquid discharge system integrating multi-effect distillation and evaporative crystallization for desalination brine treatment, Desalination 502 (2021), 114928, https://doi.org/10.1016/j.desal.2020.114928.

[151] A. Panagopoulos, Energetic, economic and environmental assessment of zero liquid discharge (ZLD) brackish water and seawater desalination systems, Energy

Convers. Manag. 235 (2021), 113957, https://doi.org/10.1016/j.enconman.2021.113957.

[152] R. Wang, S. Lin, Thermodynamics and energy efficiency of zero liquid discharge, ACS EST Eng. (2022), https://doi.org/10.1021/acsestengg.2c00013.

[153] M. Ahmed, W.H. Shayya, D. Hoey, A. Mahendran, R. Morris, J. Al-Handaly, Use of evaporation ponds for brine disposal in desalination plants, Desalination 130 (2000) 155–168, https://doi.org/10.1016/S0011-9164(00)00083-7.

[154] S. Hughes, N. Payne, P. Rainbird, M. Allen, M. Corney, in: Salt of the Hearth: Understanding the Briquetage From a Later Romano-British Saltern at Pyde Drove, Near Woolavington, Somerset, Britannia 48, 2017, pp. 117–133, https://doi.org/10.1017/S0068113X17000228.

[155] J. Kim, S. Hong, A novel single-pass reverse osmosis configuration for high-purity water production and low energy consumption in seawater desalination, Desalination 429 (2018) 142–154, https://doi.org/10.1016/j.desal.2017.12.026.

[156] N. Voutchkov, Energy use for membrane seawater desalination–current status and trends, Desalination 431 (2018) 2–14, https://doi.org/10.1016/j.desal.2017.10.033.

[157] A.P. Straub, C.O. Osuji, T.Y. Cath, M. Elimelech, Selectivity and mass transfer limitations in pressure-retarded osmosis at high concentrations and increased operating pressures, Environ. Sci. Technol. 49 (2015) 12551–12559, https://doi.org/10.1021/acs.est.5b01317.

[158] X. Chen, C. Boo, N.Y. Yip, Transport and structural properties of osmotic membranes in high-salinity desalination using cascading osmotically mediated reverse osmosis, Desalination 479 (2020), 114335, https://doi.org/10.1016/j.desal.2020.114335.

[159] R. Rautenbach, T. Linn, L. Eilers, Treatment of severely contaminated waste water by a combination of RO, high-pressure RO and NF — potential and limits of the process, J. Membr. Sci. 174 (2000) 231–241, https://doi.org/10.1016/S0376-7388(00)00388-4.

[160] A.B. Schantz, B. Xiong, E. Dees, D.R. Moore, X. Yang, M. Kumar, Emerging investigators series: prospects and challenges for high-pressure reverse osmosis in minimizing concentrated waste streams, Environ. Sci.: Water Res. Technol. 4 (2018) 894–908, https://doi.org/10.1039/C8EW00137E.

[161] D.M. Davenport, A. Deshmukh, J.R. Werber, M. Elimelech, High-pressure reverse osmosis for energy-efficient hypersaline brine desalination: current status, design considerations, and research needs, Environ. Sci. Technol. Lett. 5 (2018) 467–475, https://doi.org/10.1021/acs.estlett.8b00274.

[162] D.M. Davenport, L. Wang, E. Shalusky, M. Elimelech, Design principles and challenges of bench-scale high-pressure reverse osmosis up to 150 bar, Desalination 517 (2021), 115237, https://doi.org/10.1016/j.desal.2021.115237.

[163] K. Cook, Rochem Separation Systems, Inc. Disc Tube {trademark} Module Technology: Innovative Technology Evaluation Report, Science Applications International Corp, San Diego, CA (United States, 1998.

[164] Pall Corporation, Pall Disc TubeTM Module System, (n.d.). https://shop.pall.com/us/en/oil-gas/midstream/midstream-process-water-/pall-disc-tube-module-system-zidgri78l7k.

[165] ROTREAT, Radial Channel Disc Tube Module. http://rcdt-module.com/, 2017.

[166] RisingSun Membrane, DTRO High Pressure Disc Tubu RO Membrane Element, (n.d.). https://www.risingsunmembranes.com/uploads/201811540/DTRO-high-pressure.pdf?rnd=534.

[167] Aquatech, Integrated, Ultra-High Recovery Membrane Process, (n.d.). https://www.aquatech.com/innovations/reverse-osmosis-process/.

[168] DuPont, Specialty Membranes XUS180808 Ultra-High Pressure RO Element. https://www.dupont.com/products/dupontspecialtymembranesxus180808ultrahighpressureroelement.html#:~:text=The%20Specialty%20Membranes%20XUS180808%20Reverse,wide%20distinct%20combination%20of%20features.&text=The%20products%20are%20ideal%20for,waste%20streams%20in%20various%20industries, 2015.

[169] Saltworks Technologies, Next Generation Ultra High-Pressure Reverse Osmosis (UHP RO), 2020. https://www.saltworkstech.com/news/first-commercial-order-of-a-next-generation-ultra-high-pressure-reverse-osmosis-uhp-ro-industrial-system/.

[170] A. Rahardianto, B.C. McCool, Y. Cohen, Reverse osmosis desalting of inland brackish water of high gypsum scaling propensity: kinetics and mitigation of membrane mineral scaling, Environ. Sci. Technol. 42 (2008) 4292–4297, https://doi.org/10.1021/es702463a.

[171] A. Antony, J.H. Low, S. Gray, A.E. Childress, P. Le-Clech, G. Leslie, Scale formation and control in high pressure membrane water treatment systems: a review, J. Membr. Sci. 383 (2011) 1–16, https://doi.org/10.1016/j.memsci.2011.08.054.

[172] T. Tong, A.F. Wallace, S. Zhao, Z. Wang, Mineral scaling in membrane desalination: mechanisms, mitigation strategies, and feasibility of scaling-resistant membranes, J. Membr. Sci. 579 (2019) 52–69, https://doi.org/10.1016/j.memsci.2019.02.049.

[173] M. Mulder, J. Mulder, Basic Principles of Membrane Technology, Springer, Netherlands, 1996.

[174] S. Shirazi, C.-J. Lin, D. Chen, Inorganic fouling of pressure-driven membrane processes — a critical review, Desalination 250 (2010) 236–248, https://doi.org/10.1016/j.desal.2009.02.056.

[175] H.-J. Oh, Y.-K. Choung, S. Lee, J.-S. Choi, T.-M. Hwang, J.H. Kim, Scale formation in reverse osmosis desalination: model development, Desalination 238 (2009) 333–346, https://doi.org/10.1016/j.desal.2008.10.005.

[176] A. Matin, F. Rahman, H.Z. Shafi, S.M. Zubair, Scaling of reverse osmosis membranes used in water desalination: phenomena, impact, and control; future directions, Desalination 455 (2019) 135–157, https://doi.org/10.1016/j.desal.2018.12.009.

[177] S. Jiang, Y. Li, B.P. Ladewig, A review of reverse osmosis membrane fouling and control strategies, Sci. Total Environ. 595 (2017) 567–583, https://doi.org/10.1016/j.scitotenv.2017.03.235.

[178] W. Yu, D. Song, W. Chen, H. Yang, Antiscalants in RO membrane scaling control, Water Res. 115985 (2020), https://doi.org/10.1016/j.watres.2020.115985.

[179] A. Deshmukh, C. Boo, V. Karanikola, S. Lin, A.P. Straub, T. Tong, D.M. Warsinger, M. Elimelech, Membrane distillation at the water-energy nexus: limits, opportunities, and challenges, Energy Environ. Sci. 11 (2018) 1177–1196, https://doi.org/10.1039/C8EE00291F.

[180] M.H. Sharqawy, S.M. Zubair, J.H.L. V, M.H. Sharqawy, S.M. Zubair, Thermophysical properties of seawater: a review of existing correlations and data, Desalin. Water Treat. 16 (2010) 354–380, https://doi.org/10.5004/dwt.2010.1079.

[181] D. Brogioli, F. La Mantia, N.Y. Yip, Thermodynamic analysis and energy efficiency of thermal desalination processes, Desalination 428 (2018) 29–39, https://doi.org/10.1016/j.desal.2017.11.010.

[182] O.A. Hamed Evolutionary Developments of Thermal Desalination Plants in the Arab Gulf Region, in: 2004 Beirut Conference. 2004.

[183] H. El-Dessouky, I. Alatiqi, H. Ettouney, Process synthesis: The multi-stage flash desalination system, Desalination 115 (1998) 155–179, https://doi.org/10.1016/S0011-9164(98)00035-6.

[184] A.M. Shams El Din, M.E. El-Dahshan, R.A. Mohammed, Scale formation in flash chambers of high-temperature MSF distillers, Desalination 177 (2005) 241–258, https://doi.org/10.1016/j.desal.2004.09.030.

[185] J. Zhao, M. Wang, H.M.S. Lababidi, H. Al-Adwani, K.K. Gleason, A review of heterogeneous nucleation of calcium carbonate and control strategies for scale formation in multi-stage flash (MSF) desalination plants, Desalination 442 (2018) 75–88, https://doi.org/10.1016/j.desal.2018.05.008.

[186] A. Panagopoulos, M. Loizidou, K.-J. Haralambous, Stainless steel in thermal desalination and brine treatment: current status and prospects, Met. Mater. Int. (2019), https://doi.org/10.1007/s12540-019-00398-w.

[187] S. Liyanaarachchi, L. Shu, S. Muthukumaran, V. Jegatheesan, K. Baskaran, Problems in seawater industrial desalination processes and potential sustainable solutions: a review, Rev. Environ. Sci. Biotechnol. 13 (2014) 203–214, https://doi.org/10.1007/s11157-013-9326-y.

[188] M.A. Deyab, Enhancement of corrosion resistance in MSF desalination plants during acid cleaning operation by cationic surfactant, Desalination 456 (2019) 32–37, https://doi.org/10.1016/j.desal.2019.01.018.

[189] J.E. Truman, The influence of chloride content, pH and temperature of test solution on the occurrence of stress corrosion cracking with austenitic stainless steel, Corros. Sci. 17 (1977) 737–746, https://doi.org/10.1016/0010-938X(77)90069-5.

[190] F. Farahbod, Experimental evaluation of forced circulation crystallizer performance in production of sugar crystals, J. Food Process Eng. 42 (2019), e13017, https://doi.org/10.1111/jfpe.13017.

[191] Z. Wang, T. Horseman, A.P. Straub, N.Y. Yip, D. Li, M. Elimelech, S. Lin, Pathways and challenges for efficient solar-thermal desalination, Sci. Adv. 5 (2019) eaax0763, https://doi.org/10.1126/sciadv.aax0763.

[192] E. Huth, S. Muthu, L. Ruff, J.A. Brant, Feasibility assessment of pervaporation for desalinating high-salinity brines, J. Water Reuse Desalin. 4 (2014) 109–124, https://doi.org/10.2166/wrd.2014.038.

[193] S. Choi, B. Kim, K.G. Nayar, J. Yoon, S. Al-Hammadi, J. Han, B. Al-Anzi, Techno-economic analysis of ion concentration polarization desalination for high salinity desalination applications, Water Res. 155 (2019) 162–174, https://doi.org/10.1016/j.watres.2019.02.023.

[194] B. Kim, R. Kwak, H.J. Kwon, V.S. Pham, M. Kim, B. Al-Anzi, G. Lim, J. Han, Purification of high salinity brine by multi-stage ion concentration polarization desalination, Sci. Rep. 6 (2016) 31850, https://doi.org/10.1038/srep31850.

[195] Y.-D. Kim, K. Thu, M.E. Masry, K.C. Ng, Water quality assessment of solar-assisted adsorption desalination cycle, Desalination 344 (2014) 144–151, https://doi.org/10.1016/j.desal.2014.03.021.

[196] A. Rommerskirchen, C.J. Linnartz, F. Egidi, S. Kendir, M. Wessling, Flow-electrode capacitive deionization enables continuous and energy-efficient brine concentration, Desalination 490 (2020), 114453, https://doi.org/10.1016/j.desal.2020.114453.

[197] S.-Y. Woo, H.-S. Lee, H. Ji, D.-S. Moon, Y.-D. Kim, Silica gel-based adsorption cooling cum desalination system: focus on brine salinity, operating pressure, and its effect on performance, Desalination 467 (2019) 136–146, https://doi.org/10.1016/j.desal.2019.06.016.

[198] Q. Chen, R. Alrowais, M. Burhan, D. Ybyraiymkul, M.W. Shahzad, Y. Li, K.C. Ng, A self-sustainable solar desalination system using direct spray technology, Energy 205 (2020) 118037, https://doi.org/10.1016/j.energy.2020.118037.

[199] H. Strathmann, Ion-Exchange Membrane Separation Processes, Elsevier, 2004.

[200] H. Strathmann, Electrodialysis, a mature technology with a multitude of new applications, Desalination 264 (2010) 268–288, https://doi.org/10.1016/j.desal.2010.04.069.

[201] R.K. McGovern, S.M. Zubair, J.H.L. V, Hybrid electrodialysis reverse osmosis system design and its optimization for treatment of highly saline brines, IDA J. Desalin. Water Reuse 6 (2014) 15–23, https://doi.org/10.1179/2051645214Y.0000000016.

[202] M. Reig, S. Casas, C. Aladjem, C. Valderrama, O. Gibert, F. Valero, C.M. Centeno, E. Larrotcha, J.L. Cortina, Concentration of NaCl from seawater reverse osmosis brines for the chlor-alkali industry by electrodialysis, Desalination 342 (2014) 107–117, https://doi.org/10.1016/j.desal.2013.12.021.

[203] Y. Tanaka, R. Ehara, S. Itoi, T. Goto, Ion-exchange membrane electrodialytic salt production using brine discharged from a reverse osmosis seawater desalination

plant, J. Membr. Sci. 222 (2003) 71–86, https://doi.org/10.1016/S0376-7388 (03)00217-5.

[204] M. Turek, Electrodialytic desalination and concentration of coal-mine brine, Desalination 162 (2004) 355–359, https://doi.org/10.1016/S0011-9164(04) 00069-4.

[205] S. Lin, Energy Efficiency of Desalination: Fundamental Insights from Intuitive Interpretation, Environ. Sci. Technol. 54 (2020) 76–84, https://doi.org/10.1021/ acs.est.9b04788.

[206] E. Korngold, L. Aronov, N. Belayev, K. Kock, Electrodialysis with brine solutions oversaturated with calcium sulfate, Desalination 172 (2005) 63–75, https://doi. org/10.1016/j.desal.2004.06.197.

[207] W.E. Katz, The electrodialysis reversal (EDR) process, Desalination 28 (1979) 31–40, https://doi.org/10.1016/S0011-9164(00)88124-2.

[208] M.A.C.K. Hansima, M. Makehelwala, K.B.S.N. Jinadasa, Y. Wei, K.G. N. Nanayakkara, A.C. Herath, R. Weerasooriya, Fouling of ion exchange membranes used in the electrodialysis reversal advanced water treatment: a review, Chemosphere 263 (2021), 127951, https://doi.org/10.1016/j. chemosphere.2020.127951.

[209] H. Fan, N.Y. Yip, Elucidating conductivity-permselectivity tradeoffs in electrodialysis and reverse electrodialysis by structure-property analysis of ion-exchange membranes, J. Membr. Sci. 573 (2019) 668–681, https://doi.org/ 10.1016/j.memsci.2018.11.045.

[210] B. Sun, M. Zhang, S. Huang, J. Wang, X. Zhang, Limiting concentration during batch electrodialysis process for concentrating high salinity solutions: a theoretical and experimental study, Desalination 498 (2021), 114793, https:// doi.org/10.1016/j.desal.2020.114793.

[211] T.V. Bartholomew, L. Mey, J.T. Arena, N.S. Siefert, M.S. Mauter, Osmotically assisted reverse osmosis for high salinity brine treatment, Desalination 421 (2017) 3–11, https://doi.org/10.1016/j.desal.2017.04.012.

[212] X. Chen, N.Y. Yip, Unlocking high-salinity desalination with cascading osmotically mediated reverse osmosis: energy and operating pressure analysis, Environ. Sci. Technol. 52 (2018) 2242–2250, https://doi.org/10.1021/acs. est.7b05774.

[213] Z. Wang, A. Deshmukh, Y. Du, M. Elimelech, Minimal and zero liquid discharge with reverse osmosis using low-salt-rejection membranes, Water Res. 170 (2020), 115317, https://doi.org/10.1016/j.watres.2019.115317.

[214] C.D. Peters, N.P. Hankins, Osmotically assisted reverse osmosis (OARO): five approaches to dewatering saline brines using pressure-driven membrane processes, Desalination 458 (2019) 1–13, https://doi.org/10.1016/j. desal.2019.01.025.

[215] RO Technology Concentrates Brine, Water Desalination Report, 53 (2021) 1–3.

[216] L.T. Choong, P.N. Govindan, M.G. St John, S. Lam, J.R. Andrews, K.M. Chehayeb, Osmotic desalination methods and associated systems, WO2017019944A8, 2017.

[217] T.V. Bartholomew, N.S. Siefert, M.S. Mauter, Cost optimization of osmotically assisted reverse osmosis, Environ. Sci. Technol. 52 (2018) 11813–11821, https:// doi.org/10.1021/acs.est.8b02771.

[218] Z. Wang, D. Feng, Y. Chen, D. He, M. Elimelech, Comparison of energy consumption of osmotically assisted reverse osmosis and low-salt-rejection reverse osmosis for brine management, Environ. Sci. Technol. (2021), https://doi. org/10.1021/acs.est.1c01638.

[219] Gradiant Corporation Gradiant and SAWACO Deploy Environmentally Friendly High Recovery Desalination Technology, Gradiant Corporation, (n.d.). https:// gradiant.com/gradiant-and-sawaco-deploy-environmentally-friendly-high-recovery-desalination-technology/ (accessed April 12, 2021).

[220] X. Chen, C. Boo, N.Y. Yip, Influence of solute molecular diameter on permeability-selectivity tradeoff of thin-film composite polyamide membranes in aqueous separations, Water Res. 201 (2021), 117311, https://doi.org/10.1016/j. watres.2021.117311.

[221] G.M. Geise, H.B. Park, A.C. Sagle, B.D. Freeman, J.E. McGrath, Water permeability and water/salt selectivity tradeoff in polymers for desalination, J. Membr. Sci. 369 (2011) 130–138, https://doi.org/10.1016/j. memsci.2010.11.054.

[222] Z. Yang, H. Guo, C.Y. Tang, The upper bound of thin-film composite (TFC) polyamide membranes for desalination, J. Membr. Sci. 590 (2019), 117297, https://doi.org/10.1016/j.memsci.2019.117297.

[223] T.Y. Cath, A.E. Childress, M. Elimelech, Forward osmosis: principles, applications, and recent developments, J. Membr. Sci. 281 (2006) 70–87, https://doi.org/ 10.1016/j.memsci.2006.05.048.

[224] B.D. Coday, P. Xu, E.G. Beaudry, J. Herron, K. Lampi, N.T. Hancock, T.Y. Cath, The sweet spot of forward osmosis: treatment of produced water, drilling wastewater, and other complex and difficult liquid streams, Desalination 333 (2014) 23–35, https://doi.org/10.1016/j.desal.2013.11.014.

[225] H.K. Shon, S. Phuntsho, T.C. Zhang, R.Y. Surampalli, Forward Osmosis: Fundamentals and Applications, American Society of Civil Engineers, 2015.

[226] C. Klaysom, T.Y. Cath, T. Depuydt, I.F.J. Vankelecom, Forward and pressure retarded osmosis: potential solutions for global challenges in energy and water supply, Chem. Soc. Rev. 42 (2013) 6959–6989, https://doi.org/10.1039/ C3CS60051C.

[227] Y. Zhou, M. Huang, Q. Deng, T. Cai, Combination and performance of forward osmosis and membrane distillation (FO-MD) for treatment of high salinity landfill leachate, Desalination 420 (2017) 99–105, https://doi.org/10.1016/j. desal.2017.06.027.

[228] R.L. McGinnis, N.T. Hancock, M.S. Nowosielski-Slepowron, G.D. McGurgan, Pilot demonstration of the NH3/CO2 forward osmosis desalination process on high salinity brines, Desalination 312 (2013) 67–74, https://doi.org/10.1016/j. desal.2012.11.032.

[229] Md.S. Islam, S. Sultana, J.R. McCutcheon, Md.S. Rahaman, Treatment of fracking wastewaters via forward osmosis: evaluation of suitable organic draw solutions, Desalination 452 (2019) 149–158, https://doi.org/10.1016/j.desal.2018.11.010.

[230] M. Al-Furaiji, N. Benes, A. Nijmeijer, J.R. McCutcheon, Use of a forward osmosis-membrane distillation integrated process in the treatment of high-salinity oily wastewater, Ind. Eng. Chem. Res. 58 (2019) 956–962, https://doi.org/10.1021/ acs.iecr.8b04875.

[231] Y. Zhong, X. Feng, W. Chen, X. Wang, K.-W. Huang, Y. Gnanou, Z. Lai, Using UCST ionic liquid as a draw solute in forward osmosis to treat high-salinity water, Environ. Sci. Technol. 50 (2016) 1039–1045, https://doi.org/10.1021/acs. est.5b03747.

[232] G. Chen, R. Liu, H.K. Shon, Y. Wang, J. Song, X.-M. Li, T. He, Open porous hydrophilic supported thin-film composite forward osmosis membrane via co-casting for treatment of high-salinity wastewater, Desalination 405 (2017) 76–84, https://doi.org/10.1016/j.desal.2016.12.004.

[233] P. Zhao, B. Gao, Q. Yue, S. Liu, H.K. Shon, Effect of high salinity on the performance of forward osmosis: water flux, membrane scaling and removal efficiency, Desalination 378 (2016) 67–73, https://doi.org/10.1016/j. desal.2015.09.028.

[234] J.R. McCutcheon, R.L. McGinnis, M. Elimelech, Desalination by ammonia–carbon dioxide forward osmosis: influence of draw and feed solution concentrations on process performance, J. Membr. Sci. 278 (2006) 114–123, https://doi.org/ 10.1016/j.memsci.2005.10.048.

[235] D.L. Shaffer, J.R. Werber, H. Jaramillo, S. Lin, M. Elimelech, Forward osmosis: where are we now? Desalination 356 (2015) 271–284, https://doi.org/10.1016/j. desal.2014.10.031.

[236] A.M. Awad, R. Jalab, J. Minier-Matar, S. Adham, M.S. Nasser, S.J. Judd, The status of forward osmosis technology implementation, Desalination 461 (2019) 10–21, https://doi.org/10.1016/j.desal.2019.03.013.

[237] N. Akther, A. Sodiq, A. Giwa, S. Daer, H.A. Arafat, S.W. Hasan, Recent advancements in forward osmosis desalination: a review, Chem. Eng. J. 281 (2015) 502–522, https://doi.org/10.1016/j.cej.2015.05.080.

[238] S. Zhao, L. Zou, C.Y. Tang, D. Mulcahy, Recent developments in forward osmosis: opportunities and challenges, J. Membr. Sci. 396 (2012) 1–21, https://doi.org/ 10.1016/j.memsci.2011.12.023.

[239] A. Alkhudhiri, N. Darwish, N. Hilal, Membrane distillation: a comprehensive review, Desalination 287 (2012) 2–18, https://doi.org/10.1016/j. desal.2011.08.027.

[240] D. González, J. Amigo, F. Suárez, Membrane distillation: perspectives for sustainable and improved desalination, Renew. Sust. Energ. Rev. 80 (2017) 238–259, https://doi.org/10.1016/j.rser.2017.05.078.

[241] M. Khayet, T. Matsuura, Membrane distillation: principles and applications, in: Membrane Distillation: Principles and Applications, Elsevier, Oxford, 2011, https://doi.org/10.1016/b978-0-444-53126-1.10017-x.

[242] P. Wang, T.-S. Chung, Recent advances in membrane distillation processes: membrane development, configuration design and application exploring, J. Membr. Sci. 474 (2015) 39–56, https://doi.org/10.1016/j. memsci.2014.09.016.

[243] K.W. Lawson, D.R. Lloyd, Membrane distillation, J. Membr. Sci. 124 (1997) 1–25.

[244] E. Drioli, A. Ali, F. Macedonio, Membrane distillation: recent developments and perspectives, Desalination 356 (2015) 56–84, https://doi.org/10.1016/j. desal.2014.10.028.

[245] H. Geng, Q. He, H. Wu, P. Li, C. Zhang, H. Chang, Experimental study of hollow fiber AGMD modules with energy recovery for high saline water desalination, Desalination 344 (2014) 55–63, https://doi.org/10.1016/j.desal.2014.03.016.

[246] O.R. Lokare, S. Tavakkoli, S. Wadekar, V. Khanna, R.D. Vidic, Fouling in direct contact membrane distillation of produced water from unconventional gas extraction, J. Membr. Sci. 524 (2017) 493–501, https://doi.org/10.1016/j. memsci.2016.11.072.

[247] K. Sardari, P. Fyfe, D. Lincicome, S.Ranil Wickramasinghe, Combined electrocoagulation and membrane distillation for treating high salinity produced waters, J. Membr. Sci. 564 (2018) 82–96, https://doi.org/10.1016/j. memsci.2018.06.041.

[248] C. Boo, J. Lee, M. Elimelech, Omniphobic polyvinylidene fluoride (PVDF) membrane for desalination of shale gas produced water by membrane distillation, Environ. Sci. Technol. 50 (2016) 12275–12282, https://doi.org/10.1021/acs. est.6b03882.

[249] S. Adham, A. Hussain, J.M. Matar, R. Dores, A. Janson, Application of membrane distillation for desalting brines from thermal desalination plants, Desalination 314 (2013) 101–108, https://doi.org/10.1016/j.desal.2013.01.003.

[250] T.Y. Cath, V.D. Adams, A.E. Childress, Experimental study of desalination using direct contact membrane distillation: a new approach to flux enhancement, J. Membr. Sci. 228 (2004) 5–16, https://doi.org/10.1016/j.memsci.2003.09.006.

[251] M. Safavi, T. Mohammadi, High-salinity water desalination using VMD, Chem. Eng. J. 149 (2009) 191–195, https://doi.org/10.1016/j.cej.2008.10.021.

[252] A. Alkhudhiri, N. Darwish, N. Hilal, Produced water treatment: application of air gap membrane distillation, Desalination 309 (2013) 46–51, https://doi.org/ 10.1016/j.desal.2012.09.017.

[253] J. Li, Y. Guan, F. Cheng, Y. Liu, Treatment of high salinity brines by direct contact membrane distillation: effect of membrane characteristics and salinity, Chemosphere 140 (2015) 143–149, https://doi.org/10.1016/j. chemosphere.2014.12.006.

[254] Y. Chul Woo, Y. Chen, L.D. Tijing, S. Phuntsho, T. He, J.-S. Choi, S.-H. Kim, H. Kyong Shon, CF4 plasma-modified omniphobic electrospun nanofiber membrane for produced water brine treatment by membrane distillation,

J. Membr. Sci. 529 (2017) 234–242, https://doi.org/10.1016/j.memsci.2017.01.063.

[255] J.A. Andrés-Mañas, A. Ruiz-Aguirre, F.G. Acién, G. Zaragoza, Performance increase of membrane distillation pilot scale modules operating in vacuum-enhanced air-gap configuration, Desalination 475 (2020), https://doi.org/10.1016/j.desal.2019.114202.

[256] S. Mansour, A. Giwa, S.W. Hasan, Novel graphene nanoplatelets-coated polyethylene membrane for the treatment of reject brine by pilot-scale direct contact membrane distillation: an optimization study, Desalination 441 (2018) 9–20, https://doi.org/10.1016/j.desal.2018.04.026.

[257] L. Eykens, I. Hitsov, K. De Sitter, C. Dotremont, L. Pinoy, B. Van der Bruggen, Direct contact and air gap membrane distillation: differences and similarities between lab and pilot scale, Desalination 422 (2017) 91–100, https://doi.org/10.1016/j.desal.2017.08.018.

[258] L. Song, Z. Ma, X. Liao, P.B. Kosaraju, J.R. Irish, K.K. Sirkar, Pilot plant studies of novel membranes and devices for direct contact membrane distillation-based desalination, J. Membr. Sci. 323 (2008) 257–270, https://doi.org/10.1016/j.memsci.2008.05.079.

[259] J. Minier-Matar, R. Sharma, A. Hussain, A. Janson, S. Adham, Field evaluation of membrane distillation followed by humidification/dehumidification crystallizer for inland desalination of saline groundwater, Desalination 398 (2016) 12–21, https://doi.org/10.1016/j.desal.2016.07.006.

[260] R. Schwantes, L. Bauer, K. Chavan, D. Dücker, C. Felsmann, J. Pfafferott, Air gap membrane distillation for hypersaline brine concentration: operational analysis of a full-scale module–new strategies for wetting mitigation, Desalination 444 (2018) 13–25, https://doi.org/10.1016/j.desal.2018.06.012.

[261] A. Ruiz-Aguirre, J.A. Andrés-Mañas, G. Zaragoza, Evaluation of permeate quality in pilot scale membrane distillation systems, Membranes 9 (2019) 69, https://doi.org/10.3390/membranes9060069.

[262] J. Minier-Matar, A. Hussain, A. Janson, F. Benyahia, S. Adham, Field evaluation of membrane distillation technologies for desalination of highly saline brines, Desalination 351 (2014) 101–108, https://doi.org/10.1016/j.desal.2014.07.027.

[263] N. Thomas, M.O. Mavukkandy, S. Loutatidou, H.A. Arafat, Membrane distillation research & implementation: lessons from the past five decades, Sep. Purif. Technol. 189 (2017) 108–127, https://doi.org/10.1016/j.seppur.2017.07.069.

[264] P. Olynyk, A.R. Gordon, The Vapor Pressure of Aqueous Solutions of Sodium Chloride at 20, 25 and 30° for Concentrations from 2 Molal to Saturation, J. Am. Chem. Soc. 65 (1943) 224–226, https://doi.org/10.1021/ja01242a023.

[265] H. Chang, T. Li, B. Liu, R.D. Vidic, M. Elimelech, J.C. Crittenden, Potential and implemented membrane-based technologies for the treatment and reuse of flowback and produced water from shale gas and oil plays: A review, Desalination 455 (2019) 34–57, https://doi.org/10.1016/j.desal.2019.01.001.

[266] L. Zou, X. Zhang, P. Gusnawan, G. Zhang, J. Yu, Crosslinked PVDF based hydrophilic-hydrophobic dual-layer hollow fiber membranes for direct contact membrane distillation desalination: from the seawater to oilfield produced water, J. Membr. Sci. (2020), 118802, https://doi.org/10.1016/j.memsci.2020.118802.

[267] K. Bourouni, M.T. Chaibi, Application of Geothermal Energy for Brackish Water Desalination in the South of Tunisia, 2005 Antalya, Turkey.

[268] A.E. Jansen, J.W. Assink, J.H. Hanemaaijer, J. van Medevoort, E. van Sonsbeek, Development and pilot testing of full-scale membrane distillation modules for deployment of waste heat, Desalination 323 (2013) 55–65, https://doi.org/10.1016/j.desal.2012.11.030.

[269] P.D. Dongare, A. Alabastri, S. Pedersen, K.R. Zodrow, N.J. Hogan, O. Neumann, J. Wu, T. Wang, A. Deshmukh, M. Elimelech, Q. Li, P. Nordlander, N.J. Halas, Nanophotonics-enabled solar membrane distillation for off-grid water purification, Proc. Natl. Acad. Sci. U. S. A. 114 (2017) 6936–6941, https://doi.org/10.1073/pnas.1701835114.

[270] D.B. Gingerich, M.S. Mauter, Quantity, Quality, and Availability of Waste Heat from United States Thermal Power Generation, Environ Sci Technol. 49 (2015) 8297–8306, https://doi.org/10.1021/es5060989.

[271] W. Wang, Y. Shi, C. Zhang, S. Hong, L. Shi, J. Chang, R. Li, Y. Jin, C. Ong, S. Zhuo, P. Wang, Simultaneous production of fresh water and electricity via multistage solar photovoltaic membrane distillation, Nat. Commun. 10 (2019) 3012, https://doi.org/10.1038/s41467-019-10817-6.

[272] C. Zhang, Y. Shi, L. Shi, H. Li, R. Li, S. Hong, S. Zhuo, T. Zhang, P. Wang, Designing a next generation solar crystallizer for real seawater brine treatment with zero liquid discharge, Nat. Commun. 12 (2021) 998, https://doi.org/10.1038/s41467-021-21124-4.

[273] T. Horseman, Y. Yin, K.S. Christie, Z. Wang, T. Tong, S. Lin, Wetting, scaling, and fouling in membrane distillation: state-of-the-art insights on fundamental mechanisms and mitigation strategies, ACS EST Eng. 1 (2021) 117–140, https://doi.org/10.1021/acsestengg.0c00025.

[274] H. Geng, J. Wang, C. Zhang, P. Li, H. Chang, High water recovery of RO brine using multi-stage air gap membrane distillation, Desalination 355 (2015) 178–185, https://doi.org/10.1016/j.desal.2014.10.038.

[275] R. Schwantes, A. Cipollina, F. Gross, J. Koschikowski, D. Pfeifle, M. Rolletschek, V. Subiela, Membrane distillation: solar and waste heat driven demonstration plants for desalination, Desalination 323 (2013) 93–106, https://doi.org/10.1016/j.desal.2013.04.011.

[276] E.K. Summers, H.A. Arafat, J.H. Lienhard, Energy efficiency comparison of single-stage membrane distillation (MD) desalination cycles in different configurations, Desalination 290 (2012) 54–66, https://doi.org/10.1016/j.desal.2012.01.004.

[277] H.C. Duong, P. Cooper, B. Nelemans, T.Y. Cath, L.D. Nghiem, Evaluating energy consumption of air gap membrane distillation for seawater desalination at pilot scale level, Sep. Purif. Technol. 166 (2016) 55–62, https://doi.org/10.1016/j.seppur.2016.04.014.

[278] A. Ruiz-Aguirre, J.A. Andrés-Mañas, J.M. Fernández-Sevilla, G. Zaragoza, Experimental characterization and optimization of multi-channel spiral wound air gap membrane distillation modules for seawater desalination, Sep. Purif. Technol. 205 (2018) 212–222, https://doi.org/10.1016/j.seppur.2018.05.044.

[279] X. Li, Y. Qin, R. Liu, Y. Zhang, K. Yao, Study on concentration of aqueous sulfuric acid solution by multiple-effect membrane distillation, Desalination 307 (2012) 34–41, https://doi.org/10.1016/j.desal.2012.08.023.

[280] A. Ruiz-Aguirre, J.A. Andrés-Mañas, J.M. Fernández-Sevilla, G. Zaragoza, Modeling and optimization of a commercial permeate gap spiral wound membrane distillation module for seawater desalination, Desalination 419 (2017) 160–168, https://doi.org/10.1016/j.desal.2017.06.019.

[281] K. Zhao, W. Heinzl, M. Wenzel, S. Büttner, F. Bollen, G. Lange, S. Heinzl, N. Sarda, Experimental study of the memsys vacuum-multi-effect-membrane-distillation (V-MEMD) module, Desalination 323 (2013) 150–160, https://doi.org/10.1016/j.desal.2012.12.003.

[282] J.-G. Lee, W.-S. Kim, Numerical study on multi-stage vacuum membrane distillation with economic evaluation, Desalination 339 (2014) 54–67, https://doi.org/10.1016/j.desal.2014.02.003.

[283] H.W. Chung, J. Swaminathan, D.M. Warsinger, J.H. Lienhard V, Multistage vacuum membrane distillation (MSVMD) systems for high salinity applications, J. Membr. Sci. 497 (2016) 128–141, https://doi.org/10.1016/j.memsci.2015.09.009.

[284] F. Banat, N. Jwaied, M. Rommel, J. Koschikowski, M. Wieghaus, Performance evaluation of the "large SMADES" autonomous desalination solar-driven membrane distillation plant in Aqaba, Jordan, Desalination 217 (2007) 17–28, https://doi.org/10.1016/j.desal.2006.11.027.

[285] H.C. Duong, A.R. Chivas, B. Nelemans, M. Duke, S. Gray, T.Y. Cath, L.D. Nghiem, Treatment of RO brine from CSG produced water by spiral-wound air gap membrane distillation — a pilot study, Desalination 366 (2015) 121–129, https://doi.org/10.1016/j.desal.2014.10.026.

[286] A. Hussain, A. Janson, J.M. Matar, S. Adham, Membrane distillation: recent technological developments and advancements in membrane materials, Emerg. Mater. (2021), https://doi.org/10.1007/s42247-020-00152-8.

[287] E. Curcio, E. Drioli, Membrane distillation and related operations—a review, Sep. Purif. Rev. 34 (2005) 35–86, https://doi.org/10.1081/SPM-200054951.

[288] M.S. El-Bourawi, Z. Ding, R. Ma, M. Khayet, A framework for better understanding membrane distillation separation process, J. Membr. Sci. 285 (2006) 4–29, https://doi.org/10.1016/j.memsci.2006.08.002.

[289] G. Viader, O. Casal, B. Lefèvre, N. de Arespacochaga, C. Echevarría, J. López, C. Valderrama, J.L. Cortina, Integration of membrane distillation as volume reduction technology for in-land desalination brines management: pre-treatments and scaling limitations, J. Environ. Manag. 289 (2021), 112549, https://doi.org/10.1016/j.jenvman.2021.112549.

[290] I.-M. Hsieh, A.K. Thakur, M. Malmali, Comparative analysis of various pretreatments to mitigate fouling and scaling in membrane distillation, Desalination 509 (2021), 115046, https://doi.org/10.1016/j.desal.2021.115046.

[291] K.H. Mistry, J.H. Lienhard, S.M. Zubair, Effect of entropy generation on the performance of humidification-dehumidification desalination cycles, Int. J. Therm. Sci. 49 (2010) 1837–1847, https://doi.org/10.1016/j.ijthermalsci.2010.05.002.

[292] Z. Rahimi-Ahar, M.S. Hatamipour, L.R. Ahar, Air humidification-dehumidification process for desalination: a review, Prog. Energy Combust. Sci. 80 (2020), 100850, https://doi.org/10.1016/j.pecs.2020.100850.

[293] G.P. Thiel, J.H. Lienhard, Treating produced water from hydraulic fracturing: composition effects on scale formation and desalination system selection, Desalination 346 (2014) 54–69, https://doi.org/10.1016/j.desal.2014.05.001.

[294] G.P. Narayan, M.H. Sharqawy, E.K. Summers, J.H. Lienhard, S.M. Zubair, M.A. Antar, The potential of solar-driven humidification–dehumidification desalination for small-scale decentralized water production, Renew. Sust. Energ. Rev. 14 (2010) 1187–1201, https://doi.org/10.1016/j.rser.2009.11.014.

[295] D.U. Lawal, N.A.A. Qasem, Humidification-dehumidification desalination systems driven by thermal-based renewable and low-grade energy sources: a critical review, Renew. Sust. Energ. Rev. 125 (2020), 109817, https://doi.org/10.1016/j.rser.2020.109817.

[296] Q. Chen, F.H. Akhtar, M. Burhan, K.C. Ng, K. M, A novel zero-liquid discharge desalination system based on the humidification-dehumidification process: a preliminary study, Water Res. 207 (2021), 117794, https://doi.org/10.1016/j.watres.2021.117794.

[297] Saltworks Technologies, SaltMaker-MultiEffect Closed Evaporator Crystallizer, (n.d.). https://cdn.saltworkstech.com/wp-content/uploads/2018/10/Saltmaker-Spec-Sheet-RQ.pdf (accessed July 13, 2020).

[298] X. Huang, H. Wang, W. Liu, X. Ling, Y. Li, Y. Wang, J. Li, Performance analysis of a multi-stage humidification–dehumidification desalination system with different salinity levels, Energy Convers. Manag. 215 (2020), 112928, https://doi.org/10.1016/j.enconman.2020.112928.

[299] S. Dehghani, A. Date, A. Akbarzadeh, An experimental study of brine recirculation in humidification-dehumidification desalination of seawater, Case Stud. Therm. Eng. 14 (2019), 100463, https://doi.org/10.1016/j.csite.2019.100463.

[300] I. Ghofrani, A. Moosavi, Energy, exergy, exergoeconomics, and exergoenvironmental assessment of three brine recycle humidification-dehumidification desalination systems applicable for industrial wastewater treatment, Energy Convers. Manag. 205 (2020), 112349, https://doi.org/10.1016/j.enconman.2019.112349.

[301] Gradiant Corporation, Carrier Gas Extraction. https://gradiant.com/wp-content/uploads/2020/08/CGE-Brochure_2020.pdf, 2020.

[302] X. Huang, X. Ling, Y. Li, W. Liu, T. Ke, A graphical method for the determination of optimum operating parameters in a humidification-dehumidification desalination system, Desalination 455 (2019) 19–33, https://doi.org/10.1016/j.desal.2018.12.013.

[303] ASHRAE, ASHRAE Psychrometric Chart No. 1, 1992 (accessed August 4, 2020), https://www.ashrae.org/File%20Library/Technical%20Resources/Bookstore/UP3/IP-1.pdf.

[304] M. Capocelli, L. Di Paola, M. De Falco, V. Piemonte, D. Barba, A novel process of humidification-dehumidification with brine recirculation for desalination in remote areas of the world, Desalin.Water Treat. 69 (2017) 244–251, https://doi.org/10.5004/dwt.2017.20297.

[305] G.P. Narayan, M.H. Sharqawy, S. Lam, S.K. Das, J.H. Lienhard, Bubble columns for condensation at high concentrations of noncondensable gas: heat-transfer model and experiments, AIChE J. 59 (2013) 1780–1790, https://doi.org/10.1002/aic.13944.

[306] P. Wang, X. Zhang, S.G. Gouda, Q. Yuan, Humidification-dehumidification process used for the concentration and nutrient recovery of biogas slurry, J. Clean. Prod. 247 (2020), 119142, https://doi.org/10.1016/j.jclepro.2019.119142.

[307] H. Müller-Holst, Solar thermal desalination method using the multiple effect humidification (MEH) method, in: L. Rizzuti, H.M. Ettouney, A. Cipollina (Eds.), Solar Desalination for the 21st Century, Springer Netherlands, Dordrecht, 2007, pp. 215–225, https://doi.org/10.1007/978-1-4020-5508-9_16.

[308] R.K. McGovern, G.P. Thiel, G. Prakash Narayan, S.M. Zubair, J.H. Lienhard, Performance limits of zero and single extraction humidification-dehumidification desalination systems, Appl. Energy 102 (2013) 1081–1090, https://doi.org/10.1016/j.apenergy.2012.06.025.

[309] G.P. Narayan, M.H. Sharqawy, S.M. Zubair, Thermodynamic analysis of humidification dehumidification desalination cycles, Desalin. Water Treat. 16 (2010) 339–353, https://doi.org/10.5004/dwt.2010.1078.

[310] K.M. Chehayeb, J.H. Lienhard V, Effect of Feed Salinity on the Performance of Humidification Dehumidification Desalination, San Diego. (n.d.) 16.

[311] M. Capocelli, M. Balsamo, A. Lancia, D. Barba, Process analysis of a novel humidification-dehumidification-adsorption (HDHA) desalination method, Desalination 429 (2018) 155–166, https://doi.org/10.1016/j.desal.2017.12.020.

[312] E.W. Tow, J.H. Lienhard, Experiments and modeling of bubble column dehumidifier performance, Int. J. Therm. Sci. 80 (2014) 65–75, https://doi.org/10.1016/j.ijthermalsci.2014.01.018.

[313] D.W. Hood, R.R. Davison, The place of solvent extraction in saline water conversion, in: Saline Water Conversion, American Chemical Society, 1960, pp. 40–49, https://doi.org/10.1021/ba-1960-0027.ch006.

[314] A. Bajpayee, T. Luo, A. Muto, G. Chen, Very low temperature membrane-free desalination by directional solvent extraction, Energy Environ. Sci. 4 (2011) 1672, https://doi.org/10.1039/c1ee01027a.

[315] R.R. Davison, W.B. Harris, W.H. Smith, A solvent extraction desalination pilot plant, Desalination 3 (1967) 17–26, https://doi.org/10.1016/S0011-9164(00)84020-5.

[316] J.C.N. Kimberlin, R.W. Richardson, Desalination by solvent extraction, US3177139A (accessed May 19, 2020), https://patents.google.com/patent/US3177139A/en, 1965.

[317] R.R. Davison, W.H. Smith, D.W. Hood, Phase equilibria of desalination solvents: water-NaCl-amines, J. Chem. Eng. Data 11 (1966) 304–309, https://doi.org/10.1021/je60030a005.

[318] R.R. Davidson, W.H. Smith, D.W. Hood, Structure and amine-water solubility in desalination by solvent extraction, J. Chem. Eng. Data 5 (1960) 420–423, https://doi.org/10.1021/je60008a005.

[319] A.F. Isbell, D.W. Hood, Synthesis of solvents for water desalination: amines and ethers, J. Chem. Eng. Data 7 (1962) 575–580, https://doi.org/10.1021/je60015a044.

[320] R.R. Davison, D.W. Hood, Thermodynamic cycles for recovery of water by solvent extraction, Ind. Eng. Chem. Proc. Des. Dev. 3 (1964) 399–404, https://doi.org/10.1021/i260012a023.

[321] R.R. Davison, D.W. Hood, Vapor compression solvent extractor desalination, US3424675A (accessed May 19, 2020), https://patents.google.com/patent/US3424675A/en, 1969.

[322] R.R. Davison, W.B. Harris, W.H. Smith, A solvent extraction desalination pilot plant, Desalination 3 (1967) 17–26, https://doi.org/10.1016/S0011-9164(00)84020-5.

[323] M. Milosevic, K.J.J. Staal, B. Schuur, A.B. de Haan, Extractive concentration of aqueous salt solutions in aqueous two phase systems, Desalination 324 (2013) 99–110, https://doi.org/10.1016/j.desal.2013.06.008.

[324] C. Boo, I.H. Billinge, X. Chen, K.M. Shah, N.Y. Yip, Zero liquid discharge of ultrahigh-salinity brines with temperature swing solvent extraction, Environ. Sci. Technol. (2020), https://doi.org/10.1021/acs.est.0c02555.

[325] M.M. Milosevic, Extraction Based Strategies for Energy Efficient Salt Concentration, 2013, https://doi.org/10.6100/IR760488.

[326] J. Guo, Z.D. Tucker, Y. Wang, B.L. Ashfeld, T. Luo, Task-Specific Ionic Liquid Enables Highly Efficient Low Temperature Desalination by Directional Solvent Extraction, 2020, https://doi.org/10.26434/chemrxiv.11840025.v1.

[327] A. Bajpayee, S.J.P. Kress, K. Kleinguetl, G. Chen, M. Fowler, Water extraction using a directional solvent, US9428404B2 (2016).

[328] S. Alotaibi, O.M. Ibrahim, S. Luo, T. Luo, Modeling of a continuous water desalination process using directional solvent extraction, Desalination 420 (2017) 114–124, https://doi.org/10.1016/j.desal.2017.07.004.

[329] Y. Marcus, Supercritical Water: A Green Solvent: Properties and Uses, John Wiley & Sons (2012).

[330] S. van Wyk, A.G.J. van der Ham, S.R.A. Kersten, Analysis of the energy consumption of supercritical water desalination (SCWD), Desalination 474 (2020), https://doi.org/10.1016/j.desal.2019.114189.

[331] I. Leusbrock, S.J. Metz, G. Rexwinkel, G.F. Versteeg, Solubility of 1: 1 alkali nitrates and chlorides in near-critical and supercritical water, J. Chem. Eng. Data 54 (2009) 3215–3223, https://doi.org/10.1021/je900175b.

[332] S.J. Metz, I. Leusbrock, Method and system for supercritical removal of an inorganic compound, US20110180384A1 (2009).

[333] M. Hodes, P.A. Marrone, G.T. Hong, K.A. Smith, J.W. Tester, Salt precipitation and scale control in supercritical water oxidation—part A: fundamentals and research, J. Supercrit. Fluids 29 (2004) 265–288, https://doi.org/10.1016/S0896-8446(03)00093-7.

[334] S.A. Dastgheib, H.H. Salih, Treatment of highly saline brines by supercritical precipitation followed by supercritical membrane separation, Ind. Eng. Chem. Res. 58 (2019) 3370–3376, https://doi.org/10.1021/acs.iecr.8b06298.

[335] D.E. López, J.P. Trembly, Desalination of hypersaline brines with joule-heating and chemical pre-treatment: conceptual design and economics, Desalination 415 (2017) 49–57, https://doi.org/10.1016/j.desal.2017.04.003.

[336] P.A. Marrone, G.T. Hong, Corrosion control methods in supercritical water oxidation and gasification processes, J. Supercrit. Fluids 51 (2009) 83–103, https://doi.org/10.1016/j.supflu.2009.08.001.

[337] P. Kritzer, Corrosion in high-temperature and supercritical water and aqueous solutions: a review, J. Supercrit. Fluids 29 (2004) 1–29, https://doi.org/10.1016/S0896-8446(03)00031-7.

[338] W.E. Johnson, State-of-the-art of freezing processes, their potential and future, Desalination 19 (1976) 349–358, https://doi.org/10.1016/S0011-9164(00)88043-1.

[339] G.L. Stepakoff, D. Siegelman, R. Johnson, W. Gibson, Development of a eutectic freezing process for brine disposal, Desalination 15 (1974) 25–38, https://doi.org/10.1016/S0011-9164(00)82061-5.

[340] I. Tsironi, D. Schlesinger, A. Späh, L. Eriksson, M. Segad, F. Perakis, Brine rejection and hydrate formation upon freezing of NaCl aqueous solutions, Phys. Chem. Chem. Phys. 22 (2020) 7625–7632, https://doi.org/10.1039/C9CP05436G.

[341] B. Habib, M. Farid, Heat transfer and operating conditions for freeze concentration in a liquid–solid fluidized bed heat exchanger, Chem. Eng. Process. Process Intensif. 45 (2006) 698–710, https://doi.org/10.1016/j.cep.2006.02.006.

[342] L. Erlbeck, M. Rädle, R. Nessel, F. Illner, W. Müller, K. Rudolph, T. Kunz, F.-J. Methner, Investigation of the depletion of ions through freeze desalination, Desalination 407 (2017) 93–102, https://doi.org/10.1016/j.desal.2016.12.009.

[343] S. Samsuri, N.A.N. Rizan, S.H. Hung, N.A. Amran, N.S. Sambudi, Progressive freeze concentration for volume reduction of produced water and biodiesel wastewater, Chem. Eng. Technol. 42 (2019) 1764–1770, https://doi.org/10.1002/ceat.201800505.

[344] M. Ahmed, D. Oatley-Radcliffe, P.M. Williams, Reverse osmosis brine concentration using falling film freeze crystallisation technology: a pilot-scale study, Desalin.Water Treat. 203 (2020) 11–34, https://doi.org/10.5004/dwt.2020.26210.

[345] D.G. Randall, C. Zinn, A.E. Lewis, Treatment of textile wastewaters using Eutectic Freeze Crystallization, Water Sci. Technol. 70 (2014) 736–741, https://doi.org/10.2166/wst.2014.289.

[346] D.G. Randall, J. Nathoo, A succinct review of the treatment of reverse osmosis brines using freeze crystallization, J. Water Process Eng. 8 (2015) 186–194, https://doi.org/10.1016/j.jwpe.2015.10.005.

[347] P. Englezos, The freeze concentration process and its applications, Dev. Chem. Eng. Miner. Process. 2 (1994) 3–15, https://doi.org/10.1002/apj.5500020102.

[348] N. Ganiaris, J. Lambiris, R. Glasser, J.A. Hunter, W.W. Rinne, S.C. Verikios, Secondary Refrigerant Freezing Desalting Process: Operation of a 15,000 GPD Pilot Plant (accessed July 21, 2020), UNT Digital Library, 1969, https://digital.library.unt.edu/ark:/67531/metadc38804/m1/1/.

[349] M.S. Rahman, M. Ahmed, X.D. Chen, Freezing melting process and desalination: review of present status and future prospects, Int. J. Nucl. Desalin. 2 (2007) 253, https://doi.org/10.1504/IJND.2007.013549.

[350] J. Sánchez Machado, E. Hernandez, J. Auleda, M. Raventós, Review: freeze concentration technology applied to dairy products, Food Sci. Technol. Int. 17 (2011) 5–13, https://doi.org/10.1177/1082013210382479.

[351] D. Rusev, D. Diamantidou, F. Vassallo, H. Rastegarian, I. Gkoutzamani, J. Novakovic, J.A. van der Dijs, M. Avramidi, N. Brown, S. Ebrahimi, Report on the operation and optimization process of the pilot plants at Botlek (accessed April 12, 2022), The Zero Brine Project, 2021, https://zerobrine.eu/wp-content/uploads/2021/10/D2.6-Report-on-the-operation-and-optimization-process-of-the-pilot-plants-at-Botlek.pdf.

[352] P.M. Williams, M. Ahmad, B.S. Connolly, Freeze desalination: an assessment of an ice maker machine for desalting brines, Desalination 308 (2013) 219–224, https://doi.org/10.1016/j.desal.2012.07.037.

[353] D.G. Randall, J. Nathoo, A.E. Lewis, A case study for treating a reverse osmosis brine using Eutectic Freeze Crystallization—approaching a zero waste process, Desalination 266 (2011) 256–262, https://doi.org/10.1016/j.desal.2010.08.034.

[354] P.W. Atkins, Physical Chemistry, First Edition, W. H. Freeman and Company, 1978.

[355] G. Apsey, A.E. Lewis, Selenium Impurity in Sodium Sulphate Decahydrate Formed by Eutectic Freeze Crystallization of Industrial Waste Brine, 113 (2013) 7.

[356] A. Lewis, Novel Technology for Recovery of Water and Solid Salts from Hypersaline Brines: Eutectic Freeze Crystallization, Water Research Commission, Gezina, South Africa (2008).

[357] A.E. Lewis, J. Nathoo, K. Thomsen, H.J. Kramer, G.J. Witkamp, S.T. Reddy, D. G. Randall, Design of a Eutectic Freeze Crystallization process for multicomponent waste water stream, Chem. Eng. Res. Des. 88 (2010) 1290–1296, https://doi.org/10.1016/j.cherd.2010.01.023.

[358] J. Nathoo, R. Jivanji, A.E. Lewis, Freezing your brines off: Eutectic Freeze Crystallization for brine treatment, in: Tshwane, South Africa, 2009.

[359] D.G. Randall, A. Lewis, M. Rodriguez-Pascual, J. Nathoo, T. Reddy, G. Apsey, M. Kapembwa, T. Egan, C. Jemitias, Extended Investigations into Recovery of Water and Salts from Multi-component Hypersaline Brines using Eutectic Freeze Crystallization, Crystallization and Precipitation Research Unit, Department of Chemical Engineering, University of Cape Town, 2013.

[360] S.T. Reddy, A.E. Lewis, G.J. Witkamp, H.J.M. Kramer, J. van Spronsen, Recovery of Na2SO4·10H2O from a reverse osmosis retentate by eutectic freeze crystallisation technology, Chem. Eng. Res. Des. 88 (2010) 1153–1157, https://doi.org/10.1016/j.cherd.2010.01.010.

[361] R.J.C. Vaessen, B.J.H. Janse, M.M. Seckler, G.J. Witkamp, Evaluation of the performance of a newly developed eutectic freeze crystallizer: scraped cooled wall crystallizer, Chem. Eng. Res. Des. 81 (2003) 1363–1372, https://doi.org/10.1205/026387603771339573.

[362] F. van der Ham, G.J. Witkamp, J. de Graauw, G.M. van Rosmalen, Eutectic freeze crystallization: application to process streams and waste water purification, Chem. Eng. Process. Process Intensif. 37 (1998) 207–213, https://doi.org/10.1016/S0255-2701(97)00055-X.

[363] F. van der Ham, G.J. Witkamp, J. de Graauw, G.M. van Rosmalen, Eutectic freeze crystallization simultaneous formation and separation of two solid phases, J. Cryst. Growth 198–199 (1999) 744–748, https://doi.org/10.1016/S0022-0248(98)01003-3.

[364] K.H. Nelson, T.G. Thompson, Deposition of Salts From Sea Water by Frigid Concentration, Defense Technical Information Center, Fort Belvoir, VA, 1954, https://doi.org/10.21236/AD0030051.

[365] G. Tchobanoglous, F. Burton, H.D. Stensel, Wastewater Engineering Treatment and Reuse, 4th ed., McGraw-Hill Companies, Inc., 2003, pp. 585–586.

[366] V.V. Gerasimov, I.L. Rozenfeld, Effect of temperature on the rate of corrosion of metals, in: Bulletin of the Academy of Sciences of the USSR 6, Division of Chemical Science, 1957, pp. 1192–1197, https://doi.org/10.1007/BF01167386.

[367] D.S. Jean, D.J. Lee, J.C.S. Wu, Separation of oil from oily sludge by freezing and thawing, Water Res. 33 (1999) 1756–1759, https://doi.org/10.1016/S0043-1354(99)00005-6.

[368] M. John, T. Choudhury, R. Filimonov, E. Kurvinen, M. Saeed, A. Mikkola, M. Mänttäri, M. Louhi-Kultanen, Impurity separation efficiency of multi-component wastewater in a pilot-scale freeze crystallizer, Sep. Purif. Technol. 236 (2020), 116271, https://doi.org/10.1016/j.seppur.2019.116271.

[369] M. John, A. Häkkinen, M. Louhi-Kultanen, Purification efficiency of natural freeze crystallization for urban wastewaters, Cold Reg. Sci. Technol. 170 (2020), 102953, https://doi.org/10.1016/j.coldregions.2019.102953.

[370] W.M. Haynes, D.R. Lide, T.J. Bruno, eds., CRC Handbook of Chemistry and Physics, 97th ed., CRC Press, New York, 2016.

[371] M.A. Abd Elrahman, S. Abdo, E. Hussein, A.A. Altohamy, A.A.A. Attia, Exergy and parametric analysis of freeze desalination with reversed vapor compression cycle, Therm. Sci. Eng. Prog. 19 (2020), 100583, https://doi.org/10.1016/j.tsep.2020.100583.

[372] A. Antonelli, Desalinated water production at LNG-terminals, Desalination 45 (1983) 383–390, https://doi.org/10.1016/0011-9164(83)87052-0.

[373] W. Cao, C. Beggs, I.M. Mujtaba, Theoretical approach of freeze seawater desalination on flake ice maker utilizing LNG cold energy, Desalination 355 (2015) 22–32, https://doi.org/10.1016/j.desal.2014.09.034.

[374] J. Chang, J. Zuo, K.-J. Lu, T.-S. Chung, Freeze desalination of seawater using LNG cold energy, Water Res. 102 (2016) 282–293, https://doi.org/10.1016/j.watres.2016.06.046.

[375] J. Chang, J. Zuo, K.-J. Lu, T.-S. Chung, Membrane development and energy analysis of freeze desalination-vacuum membrane distillation hybrid systems powered by LNG regasification and solar energy, Desalination 449 (2019) 16–25, https://doi.org/10.1016/j.desal.2018.10.008.

[376] P. Wang, T.-S. Chung, A conceptual demonstration of freeze desalination–membrane distillation (FD–MD) hybrid desalination process utilizing liquefied natural gas (LNG) cold energy, Water Res. 46 (2012) 4037–4052, https://doi.org/10.1016/j.watres.2012.04.042.

[377] K.J. Lu, Z.L. Cheng, J. Chang, L. Luo, T.-S. Chung, Design of zero liquid discharge desalination (ZLDD) systems consisting of freeze desalination, membrane distillation, and crystallization powered by green energies, Desalination 458 (2019) 66–75, https://doi.org/10.1016/j.desal.2019.02.001.

[378] S. Ho-Van, B. Bouillot, J. Douzet, S.M. Babakhani, J.M. Herri, Cyclopentane hydrates – a candidate for desalination? J. Environ. Chem. Eng. 7 (2019) 103359 https://doi.org/10.1016/j.jece.2019.103359.

[379] P. Babu, A. Nambiar, T. He, I.A. Karimi, J.D. Lee, P. Englezos, P. Linga, A review of clathrate hydrate based desalination to strengthen energy-water nexus, ACS Sustain. Chem. Eng. 6 (2018) 8093–8107, https://doi.org/10.1021/acssuschemeng.8b01616.

[380] M. Usman, Z. Rehman, K. Seong, M.H. Song, Vacuum degassing of aqueous tetrafluroethane (R134a) solution during seawater desalination utilizing gas hydrate, Desalination 498 (2021), 114754, https://doi.org/10.1016/j.desal.2020.114754.

[381] J.-H. Cha, Y. Seol, Increasing gas hydrate formation temperature for desalination of high salinity produced water with secondary guests, ACS Sustain. Chem. Eng. 1 (2013) 1218–1224, https://doi.org/10.1021/sc400160u.

[382] J. Mok, W. Choi, Y. Seo, Evaluation of kinetic salt-enrichment behavior and separation performance of HFC-152a hydrate-based desalination using an experimental measurement and a thermodynamic correlation, Water Res. 193 (2021), 116882, https://doi.org/10.1016/j.watres.2021.116882.

[383] L. Cai, B.A. Pethica, P.G. Debenedetti, S. Sundaresan, Formation of cyclopentane methane binary clathrate hydrate in brine solutions, Chem. Eng. Sci. 141 (2016) 125–132, https://doi.org/10.1016/j.ces.2015.11.001.

[384] K.C. Kang, P. Linga, K. Park, S.-J. Choi, J.D. Lee, Seawater desalination by gas hydrate process and removal characteristics of dissolved ions (Na+, K+, Mg2+, Ca2+, B3+, Cl−, SO42−), Desalination 353 (2014) 84–90, https://doi.org/10.1016/j.desal.2014.09.007.

[385] P. Mekala, P. Babu, J.S. Sangwai, P. Linga, Formation and dissociation kinetics of methane hydrates in seawater and silica sand, Energy Fuel 28 (2014) 2708–2716, https://doi.org/10.1021/ef402445k.

[386] D. Lee, Y. Lee, S. Lee, Y. Seo, Accurate measurement of phase equilibria and dissociation enthalpies of HFC-134a hydrates in the presence of NaCl for potential application in desalination, Korean J. Chem. Eng. 33 (2016) 1425–1430, https://doi.org/10.1007/s11814-015-0268-7.

[387] P.T. Ngema, P. Naidoo, A.H. Mohammadi, D. Richon, D. Ramjugernath, Thermodynamic stability conditions of clathrate hydrates for refrigerant (R134a or R410a or R507) with MgCl2 aqueous solution, Fluid Phase Equilib. 413 (2016) 92–98, https://doi.org/10.1016/j.fluid.2015.11.002.

[388] P.T. Ngema, P. Naidoo, A.H. Mohammadi, D. Ramjugernath, Phase stability conditions for clathrate hydrates formation in CO2 + (NaCl or CaCl2 or MgCl2) + cyclopentane + water systems: experimental measurements and thermodynamic modeling, J. Chem. Eng. Data 64 (2019) 4638–4646, https://doi.org/10.1021/acs.jced.8b00872.

[389] P.T. Ngema, P. Naidoo, A.H. Mohammadi, D. Richon, D. Ramjugernath, Experimental clathrate hydrate dissociation data for systems comprising refrigerant + CaCl2 aqueous solutions, J. Chem. Eng. Data 61 (2016) 827–836, https://doi.org/10.1021/acs.jced.5b00675.

[390] H. Fakharian, H. Ganji, A. Naderifar, Desalination of high salinity produced water using natural gas hydrate, J. Taiwan Inst. Chem. Eng. 72 (2017) 157–162, https://doi.org/10.1016/j.jtice.2017.01.025.

[391] H. Fakharian, H. Ganji, A. Naderifar, Saline produced water treatment using gas hydrates, J. Environ. Chem. Eng. 5 (2017) 4269–4273, https://doi.org/10.1016/j.jece.2017.08.008.

[392] H. Fakharian, H. Ganji, A. Naderifar, H.R. Mofrad, M. Kakavand, Effect of gas type and salinity on performance of produced water desalination using gas hydrates, J. Water Reuse Desalin. 9 (2019) 396–404, https://doi.org/10.2166/wrd.2019.013.

[393] S. Nallakukkala, B. Lal, Seawater and produced water treatment via gas hydrate: review, J. Environ. Chem. Eng. 9 (2021) 105053, https://doi.org/10.1016/j.jece.2021.105053.

[394] T. He, S.K. Nair, P. Babu, P. Linga, I.A. Karimi, A novel conceptual design of hydrate based desalination (HyDesal) process by utilizing LNG cold energy, Appl. Energy 222 (2018) 13–24, https://doi.org/10.1016/j.apenergy.2018.04.006.

[395] J. Javanmardi, M. Moshfeghian, Energy consumption and economic evaluation of water desalination by hydrate phenomenon, Appl. Therm. Eng. 23 (2003) 845–857, https://doi.org/10.1016/S1359-4311(03)00023-1.

[396] T. He, Z.R. Chong, P. Babu, P. Linga, Techno-economic evaluation of cyclopentane hydrate-based desalination with liquefied natural gas cold energy utilization, Energy Technol. 8 (2020) 1900212, https://doi.org/10.1002/ente.201900212.

[397] Z.R. Chong, T. He, P. Babu, J. Zheng, P. Linga, Economic evaluation of energy efficient hydrate based desalination utilizing cold energy from liquefied natural gas (LNG), Desalination 463 (2019) 69–80, https://doi.org/10.1016/j.desal.2019.04.015.

[398] H.D. Nagashima, T. Miyagi, K. Yasuda, R. Ohmura, Clathrate hydrates at temperatures below the freezing point of water: a review, Fluid Phase Equilib. 517 (2020), 112610, https://doi.org/10.1016/j.fluid.2020.112610.

[399] G. Zylyftari, J.W. Lee, J.F. Morris, Salt effects on thermodynamic and rheological properties of hydrate forming emulsions, Chem. Eng. Sci. 95 (2013) 148–160, https://doi.org/10.1016/j.ces.2013.02.056.

[400] P.D. Dholabhai, N. Kalogerakis, P.R. Bishnoi, Equilibrium conditions for carbon dioxide hydrate formation in aqueous electrolyte solutions, J. Chem. Eng. Data 38 (1993) 650–654, https://doi.org/10.1021/je00012a045.

[401] H. Pahlavanzadeh, A.M. Javidani, H. Ganji, A. Mohammadi, Investigation of the effect of NaCl on the kinetics of R410a hydrate formation in the presence and absence of cyclopentane with potential application in hydrate-based desalination, Ind. Eng. Chem. Res. 59 (2020) 14115–14125, https://doi.org/10.1021/acs.iecr.0c02504.

[402] M. Kishimoto, S. Iijima, R. Ohmura, Crystal growth of clathrate hydrate at the interface between seawater and hydrophobic-guest liquid: effect of elevated salt concentration, Ind. Eng. Chem. Res. 51 (2012) 5224–5229, https://doi.org/10.1021/ie202785z.

[403] W. Choi, Y. Lee, J. Mok, S. Lee, J.D. Lee, Y. Seo, Thermodynamic and kinetic influences of NaCl on HFC-125a hydrates and their significance in gas hydrate-based desalination, Chem. Eng. J. 358 (2019) 598–605, https://doi.org/10.1016/j.cej.2018.10.032.

[404] H.P. Veluswamy, P. Linga, Natural gas hydrate formation using saline/seawater for gas storage application, Energy Fuel 35 (2021) 5988–6002, https://doi.org/10.1021/acs.energyfuels.1c00399.

[405] J. Lee, K.-S. Kim, Y. Seo, Thermodynamic, structural, and kinetic studies of cyclopentane + CO2 hydrates: applications for desalination and CO2 capture, Chem. Eng. J. 375 (2019), 121974, https://doi.org/10.1016/j.cej.2019.121974.

[406] A.A. Delyannis, E. Delyannis, Solar desalination, Desalination 50 (1984) 71–81.

[407] N. Cao, S. Lu, R. Yao, C. Liu, Q. Xiong, W. Qin, X. Wu, A self-regenerating air-laid paper wrapped ASA 3D cone-shaped Janus evaporator for efficient and stable solar desalination, Chem. Eng. J. 397 (2020), 125522, https://doi.org/10.1016/j.cej.2020.125522.

[408] Y. Xia, Y. Li, S. Yuan, Y. Kang, M. Jian, Q. Hou, L. Gao, H. Wang, X. Zhang, A self-rotating solar evaporator for continuous and efficient desalination of hypersaline brine, J. Mater. Chem. A 8 (2020) 16212–16217, https://doi.org/10.1039/D0TA04677A.

[409] J. Lee, K. Kim, S.H. Park, G.Y. Yoon, J. Kim, S.J. Lee, Macroporous photothermal bilayer evaporator for highly efficient and self-cleaning solar desalination, Nano Energy 77 (2020), 105130, https://doi.org/10.1016/j.nanoen.2020.105130.

[410] Q. Huang, C. Du, C. Guo, C. Huang, X. Wang, A high-efficiency salt-rejecting solar evaporator with optimized porous structure for continuous solar desalination, Appl. Therm. Eng. 187 (2021), 116515, https://doi.org/10.1016/j.applthermaleng.2020.116515.

[411] S. He, C. Chen, Y. Kuang, R. Mi, Y. Liu, Y. Pei, W. Kong, W. Gan, H. Xie, E. Hitz, C. Jia, X. Chen, A. Gong, J. Liao, J. Li, Z.J. Ren, B. Yang, S. Das, L. Hu, Nature-inspired salt resistant bimodal porous solar evaporator for efficient and stable water desalination, Energy Environ. Sci. 12 (2019) 1558–1567, https://doi.org/10.1039/C9EE00945K.

[412] Y. Kuang, C. Chen, S. He, E.M. Hitz, Y. Wang, W. Gan, R. Mi, L. Hu, A high-performance self-regenerating solar evaporator for continuous water desalination, Adv. Mater. 31 (2019) 1900498, https://doi.org/10.1002/adma.201900498.

[413] C. Liu, Y. Peng, X. Zhao, Continuous solar desalination based on restricted salt crystallization zone, Desalination 501 (2021), 114911, https://doi.org/10.1016/j.desal.2020.114911.

[414] J. Xu, Z. Wang, C. Chang, B. Fu, P. Tao, C. Song, W. Shang, T. Deng, Solar-driven interfacial desalination for simultaneous freshwater and salt generation, Desalination 484 (2020), 114423, https://doi.org/10.1016/j.desal.2020.114423.

[415] Y. Shi, R. Li, Y. Jin, S. Zhuo, L. Shi, J. Chang, S. Hong, K.-C. Ng, P. Wang, A 3D photothermal structure toward improved energy efficiency in solar steam generation, Joule 2 (2018) 1171–1186, https://doi.org/10.1016/j.joule.2018.03.013.

[416] L. Huang, H. Jiang, Y. Wang, Z. Ouyang, W. Wang, B. Yang, H. Liu, X. Hu, Enhanced water yield of solar desalination by thermal concentrated multistage distiller, Desalination 477 (2020), 114260, https://doi.org/10.1016/j.desal.2019.114260.

[417] Z. Xu, L. Zhang, L. Zhao, B. Li, B. Bhatia, C. Wang, K.L. Wilke, Y. Song, O. Labban, J.H. Lienhard, R. Wang, E.N. Wang, Ultrahigh-efficiency desalination via a thermally-localized multistage solar still, Energy Environ. Sci. 13 (2020) 830–839, https://doi.org/10.1039/C9EE04122B.

[418] G. Xie, W. Chen, T. Yan, J. Tang, H. Liu, S. Cao, Three-effect tubular solar desalination system with vacuum operation under actual weather conditions, Energy Convers. Manag. 205 (2020) 112371, https://doi.org/10.1016/j.enconman.2019.112371.

[419] W. Wang, S. Aleid, Y. Shi, C. Zhang, R. Li, M. Wu, S. Zhuo, P. Wang, Integrated solar-driven PV cooling and seawater desalination with zero liquid discharge, Joule (2021), https://doi.org/10.1016/j.joule.2021.05.010.

[420] E. Chiavazzo, M. Morciano, F. Viglino, M. Fasano, P. Asinari, Passive solar high-yield seawater desalination by modular and low-cost distillation, Nat. Sustain. 1 (2018) 763–772, https://doi.org/10.1038/s41893-018-0186-x.

[421] H.T.A. El-Dessouky, Humidification-dehumidification desalination process using waste heat from a gas turbine, Desalination 71 (1989) 19–33, https://doi.org/10.1016/0011-9164(89)87055-9.

[422] N. Xu, J. Li, Y. Wang, C. Fang, X. Li, Y. Wang, L. Zhou, B. Zhu, Z. Wu, S. Zhu, J. Zhu, A water lily–inspired hierarchical design for stable and efficient solar evaporation of high-salinity brine, Sci. Adv. 5 (2019), eaaw7013, https://doi.org/10.1126/sciadv.aaw7013.

[423] F. Zhu, L. Wang, B. Demir, M. An, Z. Liang Wu, J. Yin, R. Xiao, Q. Zheng, J. Qian, Accelerating solar desalination in brine through ion activated hierarchically porous polyion complex hydrogels, Mater. Horiz. 7 (2020) 3187–3195, https://doi.org/10.1039/D0MH01259A.

[424] T. Mtombeni, J.P. Maree, C.M. Zvinowanda, J.K.O. Asante, F.S. Oosthuizen, W. J. Louw, Evaluation of the performance of a new freeze desalination technology, Int. J. Environ. Sci. Technol. 10 (2013) 545–550, https://doi.org/10.1007/s13762-013-0182-7.

[425] C.Y. Cheng, W.C. Cheng, M.D. Yang, The vacuum freezing multiple phase transformation process, Desalination 67 (1987) 139–153, https://doi.org/10.1016/0011-9164(87)90239-6.

[426] A.A. Madani, Zero-discharge direct-contact freezing/solar evaporator desalination complex, Desalination 85 (1992) 179–195, https://doi.org/10.1016/0011-9164(92)80004-S.

[427] M.V. Rane, Y.S. Padiya, Heat pump operated freeze concentration system with tubular heat exchanger for seawater desalination, Energ. Sust. Dev. 15 (2011) 184–191, https://doi.org/10.1016/j.esd.2011.03.001.

[428] M.J. Fernández-Torres, D.G. Randall, R. Melamu, H. von Blottnitz, A comparative life cycle assessment of eutectic freeze crystallisation and evaporative crystallisation for the treatment of saline wastewater, Desalination 306 (2012) 17–23, https://doi.org/10.1016/j.desal.2012.08.022.

[429] Z. Chang, H. Zheng, Y. Yang, Y. Su, Z. Duan, Experimental investigation of a novel multi-effect solar desalination system based on humidification–dehumidification process, Renew. Energy 69 (2014) 253–259, https://doi.org/10.1016/j.renene.2014.03.048.

[430] T. Rajaseenivasan, K. Srithar, Potential of a dual purpose solar collector on humidification dehumidification desalination system, Desalination 404 (2017) 35–40, https://doi.org/10.1016/j.desal.2016.10.015.

[431] R. Santosh, G. Kumaresan, S. Selvaraj, T. Arunkumar, R. Velraj, Investigation of humidification-dehumidification desalination system through waste heat recovery from household air conditioning unit, Desalination 467 (2019) 1–11, https://doi.org/10.1016/j.desal.2019.05.016.

[432] R. Santosh, G. Kumaresan, G.K. Kumar, R. Velraj, Experimental parametric investigation of waste heat powered humidification dehumidification system for production of freshwater from wastewater, Desalination 484 (2020), 114422, https://doi.org/10.1016/j.desal.2020.114422.

[433] G. Narayan, M.G. St, S.M. John, J.H.Lienhard Zubair, Thermal design of the humidification dehumidification desalination system: an experimental investigation, Int. J. Heat Mass Transf. 58 (2013) 740–748, https://doi.org/10.1016/j.ijheatmasstransfer.2012.11.035.

[434] S. Dehghani, F. Mahmoudi, A. Date, A. Akbarzadeh, Experimental performance evaluation of humidification-dehumidification system with direct-contact dehumidifier, J. Energy. Resourc. Technol. 142 (2019), https://doi.org/10.1115/1.4044551.

[435] H. Abbady, A.S.A. Mohamed, M. Salem Ahmed, H. Hassan, Performance enhancement of a humidification–dehumidification seawater desalination system, Environ. Sci.: Water Res. Technol. 6 (2020) 3276–3292, https://doi.org/10.1039/D0EW00558D.

[436] S.A. Nada, H.F. Elattar, A. Fouda, Experimental study for hybrid humidification–dehumidification water desalination and air conditioning system, Desalination 363 (2015) 112–125, https://doi.org/10.1016/j.desal.2015.01.032.

[437] W.F. He, L.N. Xu, D. Han, Parametric analysis of an air-heated humidification-dehumidification (HDH) desalination system with waste heat recovery, Desalination 398 (2016) 30–38, https://doi.org/10.1016/j.desal.2016.07.016.

[438] W.F. He, L.N. Xu, D. Han, L. Gao, C. Yue, W.H. Pu, Thermodynamic investigation of waste heat driven desalination unit based on humidification dehumidification (HDH) processes, Appl. Therm. Eng. 100 (2016) 315–324, https://doi.org/10.1016/j.applthermaleng.2016.02.047.

[439] G.P. Thiel, E.W. Tow, L.D. Banchik, H.W. Chung, J.H. Lienhard, Energy consumption in desalinating produced water from shale oil and gas extraction, Desalination 366 (2015) 94–112, https://doi.org/10.1016/j.desal.2014.12.038.

[440] E.Sh. Mohamed, P. Boutikos, E. Mathioulakis, V. Belessiotis, Experimental evaluation of the performance and energy efficiency of a Vacuum Multi-Effect Membrane Distillation system, Desalination 408 (2017) 70–80, https://doi.org/10.1016/j.desal.2016.12.020.

[441] A. Hagedorn, G. Fieg, D. Winter, J. Koschikowski, T. Mann, Methodical design and operation of membrane distillation plants for desalination, Chem. Eng. Res. Des. 125 (2017) 265–281, https://doi.org/10.1016/j.cherd.2017.07.024.

[442] Y.-Q. Luo, F. Song, J.-M. Wu, F. Wang, X.-L. Wang, Y.-Z. Wang, A nature-inspired suspended solar evaporator for water desalination of high-salinity brines, Chem. Eng. J. 421 (2021), 129824, https://doi.org/10.1016/j.cej.2021.129824.

[443] A.T. Bouma, J. Swaminathan, J.H. Lienhard, Metrics matter: accurately defining energy efficiency in desalination, J. Heat Transf. 142 (2020), 122101, https://doi.org/10.1115/1.4048250.

[444] K. Spiegler, Y. El-Sayed, The energetics of desalination processes, Desalination 134 (2001) 109–128, https://doi.org/10.1016/S0011-9164(01)00121-7.

[445] H. Mehdizadeh, Membrane desalination plants from an energy–exergy viewpoint, Desalination 191 (2006) 200–209, https://doi.org/10.1016/j.desal.2005.06.037.

[446] V.G. Gude, Exergy evaluation of desalination processes, ChemEngineering 2 (2018) 28, https://doi.org/10.3390/chemengineering2020028.

[447] Soteris A. Kalogirou, Seawater desalination using renewable energy sources, Prog. Energy Combust. Sci. 31 (3) (2005) 242–281, https://doi.org/10.1016/j.pecs.2005.03.001.

[448] Mohamed A. Eltawil, Zhao Zhengming, Liqiang Yuan, A review of renewable energy technologies integrated with desalination systems, Renew. Energ. Rev. 13 (9) (2009) 2245–2262, https://doi.org/10.1016/j.rser.2009.06.011.

[449] Eftihia Tzen, Richard Morris, Renewable energy sources for desalination, Sol. Energy 75 (5) (2003) 375–379, https://doi.org/10.1016/j.solener.2003.07.010.

[450] Ali Al-Karaghouli, Lawrence L. Kazmerski, Energy consumption and water production cost of conventional and renewable-energy-powered desalination processes, Renew. Sust. Energ. Rev. 24 (2013) 343–356, https://doi.org/10.1016/j.rser.2012.12.064.

[451] N. Ghaffour, S. Lattemann, T. Missimer, K.C. Ng, S. Sinha, G. Amy, Renewable energy-driven innovative energy-efficient desalination technologies, Appl. Energy 136 (2014) 1155–1165, https://doi.org/10.1016/j.apenergy.2014.03.033.

[452] Catherine Charcosset, A review of membrane processes and renewable energies for desalination, Desalination 245 (1-3) (2009) 214–231, https://doi.org/10.1016/j.desal.2008.06.020.

[453] Lourdes García-Rodríguez, Renewable energy applications in desalination: state of the art, Sol. Energy 75 (5) (2003) 381–393, https://doi.org/10.1016/j.solener.2003.08.005.

[454] A. Subramani, M. Badruzzaman, J. Oppenheimer, J.G. Jacangelo, Energy minimization strategies and renewable energy utilization for desalination: a review, Water Res. 45 (5) (2011) 1907–1920, https://doi.org/10.1016/j.watres.2010.12.032.

[455] A. Alkaisi, R. Mossad, A. Sharifian-Barforoush, A review of the water desalination systems integrated with renewable energy, Energy Procedia 110 (2017) 268–274, https://doi.org/10.1016/j.egypro.2017.03.138.

[456] Veera Gnaneswar Gude, Nagamany Nirmalakhandan, Shuguang Deng, Renewable and sustainable approaches for desalination, Renew. Sust. Energ. Rev. 14 (9) (2010) 2641–2654, https://doi.org/10.1016/j.rser.2010.06.008.

[457] P. Kobos, T. Drennen, A. Outkin, E. Webb, S. Paap, S. Wiryadinata, Techno-Economic Analysis: Best Practices and Assessment Tools, Sandia National Laboratory, Albuquerque, New Mexico, 2020, https://doi.org/10.2172/1738878.

[458] M. Hauschild, R.K. Rosenbaum, S. Olsen (Eds.), Life Cycle Assessment: Theory and Practice, Springer International Publishing, 2018, https://doi.org/10.1007/978-3-319-56475-3 (accessed January 8, 2021).

[459] J. Zhou, V.W.-C. Chang, A.G. Fane, Life Cycle Assessment for desalination: A review on methodology feasibility and reliability, Water Res. 61 (2014) 210–223, https://doi.org/10.1016/j.watres.2014.05.017.

[460] C.L. Conrad, Y. Ben Yin, T. Hanna, A.J. Atkinson, P.J.J. Alvarez, T.N. Tekavec, M. A. Reynolds, M.S. Wong, Fit-for-purpose treatment goals for produced waters in shale oil and gas fields, Water Res. 173 (2020), 115467, https://doi.org/10.1016/j.watres.2020.115467.

[461] C.-Y. Chen, S.-W. Wang, H. Kim, S.-Y. Pan, C. Fan, Y.J. Lin, Non-conventional water reuse in agriculture: A circular water economy, Water Res. 199 (2021), 117193, https://doi.org/10.1016/j.watres.2021.117193.

[462] Y. Zhao, H. Wang, Y. Li, M. Wang, X. Xiang, An integrated membrane process for preparation of lithium hydroxide from high Mg/Li ratio salt lake brine, Desalination 493 (2020), 114620, https://doi.org/10.1016/j.desal.2020.114620.

[463] M. Peterská, C. Valderrama, O. Gibert, J.L. Cortina, Extraction of valuable metal ions (Cs, Rb, Li, U) from reverse osmosis concentrate using selective sorbents, Desalination 286 (2012) 316–323, https://doi.org/10.1016/j.desal.2011.11.042.

[464] J. Morillo, J. Usero, D. Rosado, H. El Bakouri, A. Riaza, F.-J. Bernaola, Comparative study of brine management technologies for desalination plants, Desalination 336 (2014) 32–49, https://doi.org/10.1016/j.desal.2013.12.038.

[465] M. Peterská, C. Valderrama, O. Gibert, J.L. Cortina, Extraction of valuable metal ions (Cs, Rb, Li, U) from reverse osmosis concentrate using selective sorbents, Desalination 286 (2012) 316–323, https://doi.org/10.1016/j.desal.2011.11.042.

[466] T. Jeppesen, L. Shu, G. Keir, V. Jegatheesan, Metal recovery from reverse osmosis concentrate, J. Clean. Prod. 17 (2009) 703–707, https://doi.org/10.1016/j.jclepro.2008.11.013.

[467] J. Morillo, J. Usero, D. Rosado, H. El Bakouri, A. Riaza, F.-J. Bernaola, Comparative study of brine management technologies for desalination plants, Desalination 336 (2014) 32–49, https://doi.org/10.1016/j.desal.2013.12.038.

[468] D. Randall, A. Lewis, M. Rodriguez-Pascual, J. Nathoo, T. Reddy, G. Apsey, M. Kapembwa, T. Egan, J. Chivavava, Extended Investigations into Recovery of Water and Salts from Multi-component Hypersaline Brines using Eutectic Freeze Crystallization, Water Research Commission, 2013.

[469] D.G. Randall, R. Mohamed, J. Nathoo, H. Rossenrode, A.E. Lewis, Improved calcium sulfate recovery from a reverse osmosis retentate using eutectic freeze crystallization, Water Sci. Technol. 67 (2013) 139–146, https://doi.org/10.2166/wst.2012.540.